The Synaptic Basis of Binocular Alignment and its Development in Ferret Primary Visual Cortex

Dissertation

zur

Erlangung des Doktorgrades (Dr. rer. nat.)

der

Mathematisch-Naturwissenschaftlichen Fakultät

der

Rheinischen Friedrich-Wilhelms-Universität Bonn

vorgelegt von

Clara Tepohl

aus

Starnberg, Deutschland

Bonn, Juli 2023

Angefertigt mit Genehmigung der Mathematisch-Naturwissenschaftlichen Fakultät
der Rheinischen Friedrich-Wilhelms-Universität Bonn

Gutachter und Betreuer:	David Fitzpatrick, Ph.D.
Gutachter und Mitbetreuer:	Prof. Walter Witke
Gutachter:	Robert Stackman, Ph.D.
Gutachter:	Rodney Murphey, Ph.D.

Tag der Promotion:	6. Oktober 2023
Erscheinungsjahr:	2023

Abstract

The brain integrates information from a myriad of external stimuli to generate a rich but consistent representation of the world and instruct behavior. For coherent binocular vision, signals from both eyes need to be combined to generate a unified percept. In visually experienced animals, neurons in primary visual cortex (V1) display highly similar responses to right and left eye stimulation, referred to as binocular alignment [1, 2, 3, 4, 5, 6, 7]. Yet, in visually naïve animals, neurons exhibit more diverse responses for each eye and visual experience is required for improving binocular alignment and thereby refining binocular vision [4, 5, 8]. While studies have addressed the alignment process of neurons or networks, we still lack an understanding about the synaptic basis of binocular alignment. Two hypotheses ascribe contrasting importance to 1) feedforward driven convergence of monocular signals from each eye and 2) a binocular (driven by stimuli through either eye), recurrent, intracortical network in the alignment process.

We used *in-vivo* two-photon functional imaging of dendritic spines of layer 2/3 (L2/3) neurons in ferret V1 to disentangle the contribution of monocular and binocular inputs. We probed the functional properties of dendritic spines and somata during right and left eye stimulation in ferrets with and without prior visual experience to uncover how somatic binocular responses are supported by excitatory synaptic inputs over development.

We find that individual neurons receive a mixture of monocular and binocular synaptic inputs at both developmental stages. Amongst this diversity of inputs, we find a unique role for binocular congruent inputs. These spines exhibit strong tuning correlation between right and left eye responses and therefore convey input that is aligned between both eyes. Consistently across development, the more binocular congruent inputs a neuron receives, the more congruent its somatic output. Higher levels of somatic congruency after visual experience are attributed to a greater proportion of binocular congruent inputs relative to naïve animals. The critical relevance of numbers of synapses is further highlighted by the fact that binocular congruent spines in experienced animals do not exhibit greater synaptic strength than noncongruent and monocular inputs. Lastly, it seems that the increase in numbers of binocular congruent inputs after eye opening transforms the dominant source of ipsilateral eye inputs.

We conclude that binocular alignment in L2/3 of ferret V1 arises from biases in the synaptic interactions within a binocular, intracortical (recurrent) network, rather than the classic feedforward model in which monocular inputs become aligned. Over development, a numerically growing binocular congruent network overrides other sources of inputs from the ipsilateral eye inducing changes in somatic responses to the ipsilateral eye that are better aligned with the contralateral eye.

Acknowledgements

First of all, I have to thank Benjamin Scholl. Without him, I would not have done my doctoral work on the ferret visual cortex. He gave a talk in Göttingen where I was pursuing my master's degree at the time. Had it not have been for his honed skill of giving talks and the exciting work he was conducting at the time, I would have stayed in Göttingen for my Ph.D.. Thanks to him and his captivating talk, I learnt about functional spine imaging and quickly realized how it allows answering numerous questions about signal integration in individual neurons. Intrigued by the technique and my passion for the visual system, I moved to Florida. Ben introduced me to the technique and also became my mentor with whom I conducted my master's thesis work, the first half of my doctoral work, and went through the process of publishing a paper for the first time. I deeply appreciate him for the scientist he is and have learnt a lot through him.

But honestly, nothing of what I did the last years would have been possible without David Fitzpatrick. Not only because he owns and runs the lab, but also because he has been continuously supporting me throughout my time in his lab. He took me on as a Ph.D. student and watched me struggle and grow as a scientist and as a person over the years. I am beyond thankful for having David as my supervisor, mentor, and supporter. Moreover, I am continuously impressed by his scientific and managerial skills, a combination that is unfortunately too rare in science. It has been an honor working for and with him.

In addition, David's lab is filled with wonderful individuals who I look up to. Doing your Ph.D. while being surrounded by mostly postdocs who are seasoned scientists can be challenging but also incredibly inspiring, motivating, and valuable. I appreciate everyone who has been part of the lab throughout my time there. I admire them all for their unique characters and quirks. Particularly, Juliane and Augusto have been a continuous support and I am happy to call them not only coworkers but also close friends.

Furthermore, the various female role models and mentors that I have found in the lab and the Institute deserve a mention. I have never doubted I couldn't do something because of my gender, I and believe they all have had something to do with it.

I also want to thank Walter Witke, who as a co-advisor in Germany has helped me to graduate with a Dr.rer.nat. Similarly, I thank my other committee members in Bonn, Heinz Beck who I remember fondly from my IMPRS interviews back in 2018, and Michael Pankratz who also agreed to support me in my efforts towards a doctorate.

Furthermore, I would like to thank Robert Stackman and Rodney Murphey who also serve on my committee. However, their roles go further beyond this, as they have been continuous support in Florida and symbolize my ties with FAU and all I have learnt there. Thank you for supporting me throughout my doctoral work.

There a many more people to thank. Because ultimately, so many people have shaped me into who I am and what I have accomplished. Without my Acroyoga friends such as Gina, life would have been a lot less fun and I would be a lot less mentally and physically healthy. Without Carina, the second half of my time in Florida would have been a lot lonelier and with less culinary adventures. Without Kate and Matt, I may not have committed to a Ph.D. in Florida. Without Michael Hörner, I wouldn't

even have known about the Max Planck Institute in Florida. Without my friends in Göttingen, I may not have stuck with Neuroscience. Without my friends in Heidelberg, I would not have had the courage to switch from Physics to Neuroscience. The list goes on and I'm sure you all know who you are. Thank you Elsa, Vio, Eva, and Tirza for being my close friends throughout different stages of life so far and hopefully in the future, too.

And despite Frankie not being able to read this, as he is a cat, I also ascribe a lot of my mental health and well-being to him. He became my Ph.D. support animal. I always look forward to being greeting by him when I get home and hope he will have many more big stretches, snores, and zoomies.

A special thank goes to Nico, who has been there not only for most of my academic career but has also seen the full depth of personal growth. Thank you for your valuable advice, encouragement, care, and love in everyday life and moments of big decisions.

Last, but definitely not least, I want to thank my family. Their love, support, affirmation, and care is what has carried me through all of life and these words won't even do this justice. I am beyond grateful to have you, that you are always on my side, and will help my under any circumstances, even when I'm on another continent.

Contents

1. Introduction

Various senses have evolved to perceive the world around us and to guide behavior. For example, vision, hearing, touch, and olfaction are different modalities through which we perceive the world that we interact with. The brain has areas dedicated to each sensory modality, as well as areas to integrate different sensory streams. Multimodal integration of consistent stimuli is highly useful for perception and ultimately survival, as it has been shown to increase perceptual acuity and shorten reaction times [9, 10, 11, 12, 13, 14] . Similarly, combining information from separate sources of the same modality has behavioral benefits. For instance, binocular vision - seeing with two eyes - increases visual acuity, improves visual detection especially in low-light settings, and enhances depth perception [15, 16, 17, 18, 19].

The advantages of binocular vision come with the challenge of having to combine signals from distinct sources into one coherent percept. For binocular vision, the sensory modality and reference frame are the same, but horizontal eye displacement leads to two different projections on each eye's retina [20]. The brain then needs to merge the two retinal signals. Along the visual pathway of carnivores and primates, individual neurons in primary visual cortex (V1) are the first to show signatures of coherent binocular integration: They respond very similarly to stimuli presented to either eye, a property referred to as binocular alignment ([1, 2, 4, 21, 22, 23, 24, 25, 26].

The proper integration of sensory cues is not innate but is an experience-dependent process [12, 14, 27, 28]. This is also true for binocular alignment [4, 5, 8]. At early stages of development, neurons in the visual cortex exhibit less alignment and more dissimilar response properties between the eyes [4, 5, 7, 8]. A given neuron may respond strongest to horizontal edges when presented to the left eye but strongest to vertical edges when presented to the right eye. Only with visual experience, the responses to the same stimulus viewed with different eyes become more similar, i.e., aligned [4, 5, 8].

Previous work has elucidated how binocular alignment of single neurons changes after eye opening [4, 6, 7]. Yet it has remained elusive how binocular responses are driven by individual synaptic inputs and how changes in the input population could underlie the binocular alignment process over development. The prevailing hypothesis about binocular alignment is that of monocular convergence [29, 30, 31]. According to this hypothesis, monocular inputs arriving at the same neuron are initially misaligned. Via Hebbian plasticity (what fires together wires together; [32]) inputs with similar tuning from each eye would be selected for, ultimately leading to binocularly aligned responses of the soma. This idea is largely rooted in the persistent separation of eye-specific signals in the early parts of the visual system and the strong notion of feedforward driven response generation of single neurons in V1.

However, this hypothesis neglects prominent intracortical wiring in V1 [33, 34, 35,

36, 37]. Several models have proposed a crucial role of intracortical and recurrent connections for other emerging properties in V1 [38, 39, 40, 41, 42, 43]. Therefore, intracortical wiring and recurrent mechanisms may also play an important role for binocular alignment. So instead of monocular inputs, an intracortical binocular input network and its maturation would be key to generating binocularly aligned responses.

Testing these two hypotheses, feedforward driven monocular convergence vs. intracortical binocular interactions, requires functionally characterizing individual synaptic inputs and their response properties for right and left eye stimulation. Only thanks to technical advancements in calcium sensor development and microscopy, it has become possible to disentangle the functional properties of individual monocular and binocular inputs and their potential impact on somatic output [44, 45, 46].

Here, we investigate the integration of separate input sources, namely from the left and right eye, that leads to binocularly aligned responses. Specifically, we will focus on the alignment of orientation tuning, a hallmark property of visual cortical neurons, and how it improves following eye opening. We use *in-vivo* two-photon functional imaging of dendritic spines to address the role of excitatory synaptic inputs in shaping binocular alignment of orientation tuning in layer 2/3 neurons of the ferret primary visual cortex at different stages of development. We answer the following questions:

1) What are the functional properties of excitatory synaptic inputs and how are they contributing to binocularly aligned responses of V1 neurons in visually experienced animals?

2) What is the functional synaptic architecture prior to visual experience? What changes in synaptic connectivity occur with visual experience and how could they drive increases in binocular alignment?

The structure of this work is as follows: the introduction gives an overview of the visual system with key aspects related to binocular alignment and presents the most relevant concepts of visual processing in the brain. Normal developmental changes as well as effects of altered visual experience are discussed. Beyond that, the work is divided into two parts reflecting the two main questions of this work. The first chapter addresses the synaptic basis of binocular alignment in visually experienced animals. This work has been published previously and a short summary will highlight the key results of the study and my contributions. The second chapter describes the synaptic architecture in visually naïve animals and compares it with the mature state to explore how any changes may contribute to the developmental alignment process. To conclude, the presented findings are summarized and open questions are discussed.

1.1. The ferret as a model organism for visual development

The visual system and its development have been studied extensively in non-human primates, carnivores, including cats and ferrets, and, more recently, in mice [47, 48]. Mice have gained popularity as genetic tools became available for them and allowed highly targeted manipulation and measurements of neural activity. In contrast, non-human primates appreciated for their strong similarities with humans are decreasing in popularity due to ethical concerns and high costs. The ferret (*Mustela putorious furo*) not only seems to strike a balance as it conserves many functional and organizational features while being lower cost than primates [49]. But it is also a particularly well-suited model organism of binocular vision for multiple reasons.

First, the forward-facing eyes of ferrets result in a sizeable binocular visual field of about 80 degrees [50]. Moreover, like many other predatory animals, they exhibit high visual acuity [51, 52]. This is in stark contrast with mice that are nocturnal animals and therefore may not rely on vision as much as diurnal species. The rodent visual system is designed for low-light conditions and consequently their retina contains mostly rods and very few cones [53]. Moreover, mice do not have a fovea, which is an area of high cone density for high acuity vision at the focal point [54, 55]. Accordingly, they are reported to not make convergent eye movements when stimuli of different disparities (spatial offset) are presented [56]. Rodent eyes are more laterally located, which leads to a smaller binocular visual field, yet their primary visual cortex (V1) has a sizeable binocular zone where binocular alignment can be evaluated [57, 58]. Lastly, their smaller overall body size translates to smaller retinas and fewer photoreceptors, which results in their vision being less accurate. While mice can perform visually guided behavioral tasks, they have lower spatial resolution compared to ferrets, cats, or primates [59].

There is another important difference between the mouse visual system and that of other species that may limit how much certain findings translate. Indeed, neurons in mouse V1 exhibit similar functional properties and encode the same features (edge orientation, spatial frequency, etc.) as neurons in other species [58, 60]. Yet, certain functional properties emerge earlier within the visual pathway of the mouse and many of the characteristic organizational principles shared across carnivores and primates are absent (see 1.4.2 and 1.4.3). Thus, despite the similar functional properties present in rodent V1 as that in carnivores and primates, there may be different mechanisms underlying it. This implies that not all findings in the mouse visual system may translate to other species and vice versa. In contrast, the ferret visual system exhibits strong similarities in functional organization not only with other carnivores and primates, but also to the human brain [24, 34, 49, 61, 62, 63, 64, 65]. Therefore, when functional organization may play a crucial role, the ferret can be a more instructive model organism for visual processing.

Ferrets are a great model specifically for visual development as they are born at an early gestational age [49, 62]. This allows studying developmental processes in ferrets when they are several days or weeks of age, whereas the same processes occur for many other species in the womb or shortly after birth. Specifically, ferrets open their eyes

around postnatal day 30 (p30), so four to five weeks of age, whereas cats open their eyes within two weeks after birth. This discrepancy is partly due to the relatively short gestation period of ferrets of around 40 days, whereas for cats it is around 65 days. Consequently, while strong parallels between cat and ferret development are maintained, they are shifted by about 3 weeks (see Fig 7 in [62]). Similar to cats, mice open their eyes within 2 weeks after birth, around p11. Technical advances have also enabled studying the developing visual system in mouse [7, 66] yet the question about transferability of insights remain.

To summarize, while each species offers unique advantages and disadvantages when studying visual development and binocular alignment, the ferret stands out as a well-rounded model organism. The conservation of many properties from ferret to humans can lead to valuable insights, and the ferret's drawn out postnatal development allows to probe the system at various stages. In the future, genetic tools could become more accessible also for other species, and the toolbox to probe visual development in ferret may soon expand drastically and further our understanding of the intricate mechanisms underlying it.

1.2. Visual development

The onset of visually evoked response marks the beginning of interactions between the environment and the brain. In ferrets, visually evoked responses are first observed around p20 [67]. At this point the eyelids are still closed therefore, visual experience at this stage lacks defined edges or fine spatial structure. Instead, stimuli are largely changes in luminance.

The type of experience that animals receive changes drastically with eye opening, which in ferrets occurs around p30. Suddenly, visual input is highly structured, with sharp edges and varying shapes. These new images that are innervating the retina with unprecedented structure and statistics, are highly correlated between the eyes and have to be integrated and encoded in the visual system. Therefore, eye opening marks the transition from innate mechanisms to experience-dependent mechanisms, or, in other words, when nature and nurture begin to interact. Accordingly, with the start of patterned visual experience, the whole brain undergoes a rapid learning experience. After eye opening, the brain becomes progressively less plastic and sensory experience will less strongly alter connectivity and activity [62]. At this stage, the brain is considered to be "mature" having reached a stable representation of and interaction with the external world.

By knowing what the state of the brain is prior to eye opening, when it is largely governed by internal mechanisms, one can better appreciate how and why the brain may arrive at its mature state that is presumably optimized and shaped by experience. Thus, when studying the visual system, it is highly instructive to examine the experienced state of visually experienced animals as well as the naïve state prior to eye opening. Consequently, the following overview on the visual system aims to highlight the key properties pertaining to binocular alignment and how they change around and due to eye opening. While the ferret visual system is the focus, studies from other species are included to either provide supportive evidence, allow educated

guesses where studies in ferrets are missing, or point out species differences.

1.3. Primary visual pathway

1.3.1. The retina

In the retina, rods and cone cells transduce incoming light into membrane potential changes [68]. These fluctuations are passed on within the retinal circuitry and ultimately integrated by retinal ganglion cells (RGCs), where action potentials are first generated along the visual pathway. The receptive field (RF) of RGCs, the part of the visual field where light stimuli affect the firing rate, is characteristically circular. RGCs are categorized as ON-center or OFF-center based on whether increases in luminance in the RF center increase or decrease the firing rate, respectively [69, 70].

The spiking activity of RGCs travels along projections exiting the eyes through the optic tract and terminates in the lateral geniculate nucleus (LGN) of the thalamus (see Fig.1.1) [70, 71]. Along the optic tract, at the optic chiasm, most fibers cross onto the other hemisphere [65, 72, 73]. The right eye mostly covers the right visual hemifield and all those signals cross to the left hemisphere. In contrast, the signals in the right eye conveying information about the left hemifield, do not cross and stay on the right hemisphere, where the signals about the same hemifield but from the left eye are arriving (see Fig.1.1). To clarify and simplify from which eye signals are coming with reference to the brain hemisphere, one refers to signals from the opposite side as contralateral and to signals from the same side as ipsilateral, or contra and ipsi in short. While this partial cross-wiring of projections to LGN offers the first opportunity for signals from the same part of the visual field but from different eyes to converge, eye-specific signals stay mostly separated at this stage of the visual pathway of carnivores and primates [74, 75].

1.3.2. The lateral geniculate nucleus

LGN neurons display a similar RF structure as RGCs, namely quite circular with ON or OFF centers [70, 75, 76]. LGN is structurally and functionally organized. First, retinotopy is maintained therefore neurons representing neighboring fields in visual space are anatomically close (ferret: [76, 77], cat: [78]). Second, LGN of carnivores and primates displays a distinct laminar layout and organization ([79], cat: [80, 81], monkey: [82], ferret: [74, 83]). In ferret LGN, RGC axons from the contralateral eye almost exclusively terminate in layer A and RGC axons from the ipsilateral eye almost exclusively in layer A1 (see Fig.1.1) [74, 83]. This anatomical separation translates to the response properties of neurons: Neurons in each layer are monocular, i.e., they only respond to visual stimulation through one eye and not the other (ferret: [75, 84], cat: [78],). While layer C appears to be more functionally intermingled and extracellular multi-unit activity shows responses for right and left eye stimulation, single units are still monocular [75, 84]. Recent studies suggest that some degree of binocular interaction occurs [85, 86, 87], yet LGN in carnivores and primates is considered to be largely monocular. Mouse LGN is an exception to this strong monocularity, as it

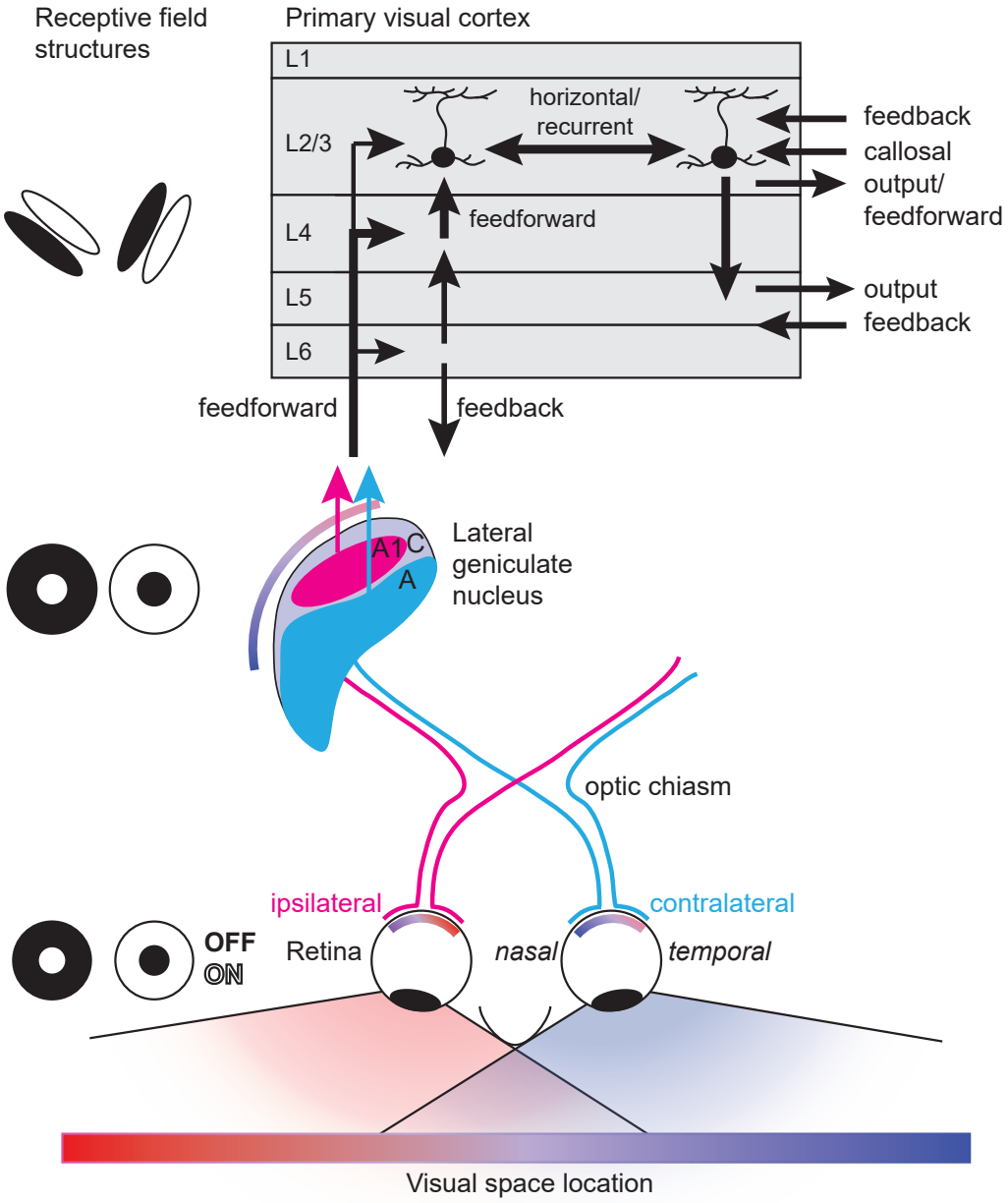

Figure 1.1.: Schematic illustration of the primary visual pathway and canonical laminar connectivity in primary visual cortex in the ferret
Left: two exemplary receptive field structures at the level of different stages of the visual pathway (from bottom to top: retina, lateral geniculate nucleus (LGN), primary visual cortex (V1)), illustrating the transformation from center-surround fields with ON or OFF centers to elongated fields in V1 where neurons become selective for edge orientation. Bottom: visual space is color-coded and its representation on the retinas and in LGN are illustrated. The temporal and nasal parts of each retina have different a wiring pattern so that each hemifield of visual space is mapped onto the contralateral (opposite) hemisphere of the brain. Top: V1 laminar structure and canonical connectivity patterns with focus on pyramidal neurons in layer 2/3 (layer 2/3 (L2/3)). Line thickness illustrates relative the strength of the connection.

displays substantial mixing of eye-specific inputs and neurons respond to stimulation of either eye [88].

Notably, the laminar segregation by eye is a developmental process. To study the emergence of the laminar, eye-specific layout of the LGN, the classical experimental approach is an injection of a transneuronally transported amino acid in one eye. Measuring the distribution and intensity of the radioactive decay of this tracer in autoradiographs of sections through the LGN at different ages allows visualizing projections originating from the injected eye. Using this technique in in developing carnivores and primates of various ages revealed that retino-geniculate projections are at first not separated by right and left eye, and the classical laminar structure is absent (monkey: [89, 90], cat: [91, 92], ferret: [74, 93]). In ferrets, the laminae slowly form around p4-p8 [74]. Aberrant axons retreat into their appropriate laminae starting p15. This anatomical restructuring during development is also reflected in functional changes, because LGN layers become more monocular (cat: [71], monkey: [94]). Ultimately, LGN reaches its mature laminar and eye-segregated structure after four weeks postnatal, shortly before eye opening in the ferret around p30 [74].

To investigate the role of neuronal activity in this segregation process, several studies used tetrodotoxin to block retinal or cortical activity in developing cats [95, 96, 97]. They found that the formation of LGN laminar requires neuronal activity. For instance, before being light-sensitive, each retina exhibits spontaneous, strong, and synchronous bursts of activity that travels as a wave within a given eye, but not across the eyes [98, 99]. These retinal waves become less frequent and decorrelated after p21 and disappear a few days before eye opening in the ferret which aligns well with the time course of RGC-LGN connection refinement [99, 100]. This uncorrelated activity between the eyes early in development may be taken advantage of to differentiate eye-specific inputs (ferret: [99, 101], cat: [102]). Further supportive work showed by either artificially increase activity levels in one eye of a ferret [102] or altering experience in one eye with monocular lid suture in cat [103], that the relative activity of signals from each eye has an impact on the relative size of the eye-specific LGN laminae.

1.4. Primary visual cortex

LGN neurons predominantly project to the V1 which in most species is located at the occipital lobe, around the posterior pole of the brain. There, significant signal transformations occur, and neurons exhibit selectivity for more complex features than ON or OFF centers. Notably, for the first time along the visual pathway, signals from the two eyes converge such that single neurons respond to stimuli through either eye, i.e., are binocularly responsive [2, 23, 24, 62, 104]. Besides responding to both eyes, neurons in V1 have elongated receptive fields and their activity is better driven by elongated bars than spots (see Fig.1.1) [23, 105]. Moreover, they exhibit orientation selectivity: the correct orientation of an edge or will increase their firing, whereas orthogonally oriented edges will increase their firing less or not at all. Similarly, the direction of a moving edge can affect the firing rate of a neuron (direction selectivity), [106, 107]. In short, V1 is considered the first stage in visual processing where binoc-

ularity and orientation selectivity emerge. Hereby it becomes apparent why binocular alignment is generally studied in V1 and most frequently with respect to orientation preference and tuning. The following sections will cover ocular dominance (1.4.2) and orientation selectivity (1.4.3) as well as the role of intracortical connectivity to provide some background on these aspects related to binocular alignment.

1.4.1. The cortical column

As at previous stages of visual processing, V1 displays strong functional organization. Functional properties such as orientation preference are organized across the cortical surface and extend in depth, across the six laminae of cortex [23, 106, 108, 109]. This organization has manifested as the idea of a functional column within which a feature is computed and represented [106, 108, 110, 111] (but see [111]). Tracing studies reveal vertical projection patterns within the cortex that support this vertical signal flow. [112, 113]. The six cortical layers can be distinguished based on their cytoarchitecture [114], but these layers also exhibit distinct connectivity patterns [115, 116]. Knowing this intralaminar network and the general signal flow is important to understand where and how feature representations may arise in V1 (see Fig.1.1).

In histological sections, V1 is easily identified due to a visually distinctive white stripe on the posterior pole which gave it the alternative name "striate cortex". This stripe is in fact a consequence of the high density of myelinated axons that originate in LGN and terminate most prominently in layer 4 (L4) of V1 [68, 93, 116, 117, 118]. Some LGN projections also arrive in layer 6, which in turn projects to L4, and a small fraction of LGN projection terminates in L2/3 [111, 115, 119, 120]. Regardless, L4 is the main recipient of the feed-forward LGN projections and thus the canonical thalamo-cortical input layer. L4 neurons project most prominently to L2/3, which contains mostly excitatory, pyramidal-type neurons, with numerous dendritic spines and a large dendritic tree that is particularly extensive for the apical part, i.e., towards the brain surface [116, 121]. Within L2/3, horizontal connections between L2/3 cells create high interconnectivity creating a recurrent network [33, 34, 35, 121, 122]. From L2/3 signals are sent to other visual cortical areas or are passed on to layer 5 [121], which is also an output layer for sending signals to other cortical areas. Layer 6 in turn is providing feedback to LGN [123]. For completeness one may add that layer 1 consists largely of axons and dendrites of varying origin and is therefore characterized by low neuronal density with the exception of a few presumably regulatory interneurons [115].

In short, for the purpose of this study, signals from thalamus reach L4 and are passed on to L2/3 which is strongly interconnected with itself. A more comprehensive overview of input sources to L2/3 neurons is given later as this layer has been the main focus for studies of binocular alignment, including this one.

1.4.2. Ocular dominance

V1 is considered the major place for signal convergence from both eyes and most neurons are binocular (monkey: [106], cat: [2, 23], ferret: [24, 62]). Accordingly, areas of V1 that represent parts of the visual field that are only accessible from one eye are monocular [24, 50, 124]. Despite the strong convergence of eye-specific signals,

binocular neurons still exhibit differences in response strength for one eye over the other [2]. This bias for one eye over the other is called ocular dominance and is spatially organized across the cortical surface such that neurons with similar degrees of eye preference are grouped together [93, 109, 125]. This organization appears as alternating bands of ocular dominance which also extend in depth, forming the so-called ocular dominance columns (ODC).

Anatomically, ODCs are rooted in organized thalamo-cortical projections to L4, the main thalamo-recipient layer [93, 116] and vertical projection patterns across the layers [112, 113]. Labeling with [3H]-proline proves useful not only for studying eye-specific projections toLGN but also to cortex, as it can travel across multiple synapses. This experimental approach employed in various species has shown thatLGN projections from each eye exhibit a stripy pattern in L4 (human and monkey: [126, 127], cat: [128], ferret: [93]). Tracing studies combined with electrophysiology corroborate the anatomical and physiological correspondence and confirmed that areas with high labeling density for a given eye corresponded with strong ocular dominance (monkey: [127], cat: [25, 128]). A tracing study in L2/3 further highlights the tight link of anatomy and function as it shows that these ODCs also coincide with long-range horizontal connections that link columns of the same eye preference together [129]. Notably, structurally as well as physiologically, ocular dominance bands are absent in mouse V1 [57, 58, 130]). This could relate to the fact that in mouse LGN, more neurons are binocular [88]. This suggests that signals from the two eyes may be combined at an earlier stage of the visual system in mice than in other species.

While carnivores and monkeys all display the characteristic eye-specific thalamocortical projection pattern, there seem to be differences regarding how directly these anatomical patterns translate to the functional properties in L4. In monkeys, physiology closely mirrors anatomy: neurons in thalamo-recipient layer L4c are still mostly monocular and binocularity emerges only in L2/3 [106, 131]. Eye-specific signals stay separated in L4 and only mix in superficial layers. A slightly different relationship is found in cats where many L4 neurons can be driven through either eye [128]. Nevertheless, L4 exhibits stronger ocular dominance than downstream L2/3 indicating that signals from both eyes are weakly combined in L4, and stronger mixing occurs in L2/3. This can be explained anatomically by the fact that L4 pyramidal neurons are receiving signals not only from highly monocular LGN projections, but also connect horizontally across domains and vertically across laminae [132]. In fact, it is estimated that only 5-6% of inputs to L4 are of thalamic origin and most inputs are cortico-cortical connections instead [116, 133]. Thalamocortical inputs tend to be larger and have more synaptic release sites than other inputs [134, 135] which could contribute to their disproportionate postsynaptic potentials [136]. Yet, nevertheless, the remaining significant contribution of intracortical inputs could blur the eye-specific signal separation and lead to binocularly responsive neurons in L4.

How monocular or binocular L4 is in the ferret remains unknown since no physiological measurements have been done so far. An anatomical study reports that in ferret about 13% of synaptic inputs to L4 neurons originate in LGN, thus are most likely monocular [137]. While this is about twice as much as in cats, their relative strength is largely unknown (but see [119]) and again intracortical inputs are a likely and relevant source of inputs to L4. Calcium imaging shows that in L2/3 most neu-

rons are binocular [4]. So while we lack a clear picture of L4 binocularity, considering the strong binocularity in L2/3 and the numerous similarities of ferrets with cats, L4 is assumed to be not purely but at least more monocular than L2/3. Due to this assumption and current limitations in imaging techniques, L2/3 has been the focus of studying binocular alignment.

OD during development Thalamocortical projections undergo a developmental process and refine in their laminar and horizontal innervation patterns. The axons of LGN neurons grow into L4 of ferret V1 around birth and start innervating it around p10/12 [138]. Thalamo-cortical inputs, albeit weak during early development, already exhibit laminar biases and preferentially target layer 4 and spare upper L2/3 [93, 120]. This projection bias further strengthens and increases its laminar specificity with age to form the innervation pattern observed in the mature animal. In those, L4 exhibits dense labeling, layer 6 presents as a weaker band, and L1 and L2/3 exhibit very little labeling.

In parallel with the laminar innervation pattern, the horizontal organization forming ocular dominance bands emerges. In essence, thalamocortical projection patterns mirror the initial overlap and later segregation of eye-specific inputs described earlier in the LGN (see Fig.1.3.2). Rakic [90] was the first to show how in embryonic monkeys that eye-specific inputs to L4 initially overlap before they separate. In ferret L4, ocular dominance bands in ferret were visible as early as p16, so well before eye opening [139]. The segregation into bands of eye-specific thalamo-cortical projection patterns is also reflected in cortical activity. Work in young kittens and monkeys shows that cortical cells in L4 are more binocular and become monocular for one eye on the same timescale as the separation of eye-specific projections [94, 120]. In contrast, in 3-week-old kittens, an increase in binocularly driven neurons is reported [140]. However, the authors do not comment on from which layer or at which depth these units are recorded. In ferret, extracellular recordings of neurons in V1 (presumably across all layers) were found to be less contra-dominated and more binocular in ferrets of p80 or older in comparison to ferrets younger then p65, suggesting an increased balance of drive from each eye over time [62]. Yet, two-photon calcium imaging of L2/3 cells shows that at eye opening, cells are highly binocular and become more monocular after about a week of visual experience [4].

The role of neuronal activity in ODC formation is not fully resolved. Crowley and Katz (2002) [139] report that when ODCs emerge in ferrets around p17, manipulation of retinal activity did not disturb the described patterns. In contrast, other studies in comparably more mature cats have found that retinal activity is required [141]. It appears that the role of neuronal activity may vary over development. It has been suggested that there may be distinct mechanisms driving ocular dominance, namely early innate and later activity-dependent ones [139].

In contrast to neuronal activity in general, many studies have probed the experience-dependent aspect of ocular dominance in V1. During the so-called critical period for ocular dominance, monocular deprivation creates a drastic shift of ocular dominance in cortical responses towards the non-deprived eye especially in the superficial layers (ferret: [62], cat: [103, 142], monkey: [143]). On the other hand, in older animals,

monocular deprivation has little to no effect suggesting reduced plasticity levels after development. In ferrets, this critical period lasts from p35 to p70 [62]. While the window for the critical period can be delayed by dark rearing [144, 145, 146], binocular lid suture had renders many cells unresponsive [147]. This suggests that no experience and diffuse, unpatterned experience through close eye lids can have different effects at certain dvelopmental stages. Lastly, not any kind of binocular experience is sufficient for normal development. Binocular experience with induced strabismus renders cells largely monocular suggesting an essential role of continuous, correlated activity from both eyes [148, 149, 150]. In humans, strabismus can occur at any age but is most frequent in children 6 years or younger [151]. This condition is reversible only at the early stage and a common treatment is ocular occlusion of one eye or vision correction [152].

To summarize, ocular dominance columns and the anatomical correlate of thalamocortical projections are formed prior to the onset of visual experience. However, they are not fully refined and still malleable. Therefore, the degree of how much and where exactly in V1 eye-specific inputs are combined appears to be established by the time of eye opening is susceptible to change under abnormal visual experience. In normal development, while some convergence may occur in L4, L2/3 is clearly combining inputs from both eyes. Ultimately, further studies and, importantly, physiological data are needed to clarify the exact timing of the anatomical and functional development of ocular dominance, especially in L4, in the developing ferret.

1.4.3. Orientation selectivity

As mentioned above, V1 is not only the initial hub for binocular interactions, but another feature emerges. Neurons selectively respond to edges of a certain orientation, and not or less to others. They display orientation selectivity. How orientation selectivity emerges from unselective LGN inputs to V1 has been the center of many studies. Shortly after Hubel and Wiesel first described orientation selective units in cat V1 in 1959 [23], they proposed a model about how this feature could be created on a single neuron level [2]. An orderly arrangement along one axis of the circular receptive fields of LGN could in summation lead to the elongated receptive fields and thereby generate orientation selective responses observed in V1, particularly in L4. This model relies on precise wiring of feed-forward inputs only. Many studies since then have investigated the emergence of orientation selectivity along the visual pathway and experimental evidence is largely in favor of this feed-forward model for V1 [153, 154, 155, 156, 157].

Orientation maps and their development Remarkably, the preference for edge orientation is organized in domains of similar preferences that again span all cortical layers, but orientation preference also varies smoothly across the cortical surface, forming a continuous orientation map that covers all angles [108, 109, 125]. Work in the tree shrew, a mammal with strong similarities in cortical organization with primates, shows that orientation maps can be ascribed to organized projections of on and off neurons [158] favoring a feedforward origin of this functional organization. On the other hand, theoretical and experimental work stress the role of intracortical connectivity in building and maintaining such large-scale organization [38, 39, 41, 42, 159,

160]. This is also supported by anatomical studies in carnivores and primates, where labeling a localized group of neurons reveals a modular pattern of the extensive horizontal connections in L2/3 as the axons show periodic biases for local, more frequent arborization [35, 160, 161]. This projection pattern matches the periodicity orientation maps, or in other words, axons preferentially connect to other cortical domains with similar orientation preference [122, 129, 162]. Therefore, horizontal connections are considered to be crucial for the layout of orientation maps.

The link of patchy projections and modular orientation representations is further supported by developmental studies of neuronal morphology and function. Tracings of axonal arbors of L2/3 pyramidal neurons in ferret have been used to study axonal projections. Over development, axons expand tangentially to the cortical surface, uniformly in direction, and already extend over 1mm before eye opening [33]. Around p32-p34, axons exhibit patchy organization with some areas showing higher density of axons and branching. By p45, axons show adult-like clusters and span several millimeters. Horizontal connections in L2/3 have also been assessed with retrograde labeling [35], photo stimulation and electrical stimulation essays [36, 37] in order to probe connectivity patterns during development. These studies further corroborate that horizontal connections are initially shorter-range and more uniform before they expand and exhibit a modular pattern.

Complementing these studies examining horizontal connectivity, are results from calcium imaging done at different developmental stages. Prior to visual experience, ferret V1 displays modular patterns of activity in response to stimulation by drifting gratings [4, 43, 163]. While these patterns are unreliable, biases in the responses reveal a primordial orientation map. Over a couple days with visual experience, responses to gratings become more reliable, orientation selectivity increases drastically, and the orientation map matures on a similar timescale as horizontal connections.

Moreover, there seems to be a link of innate connectivity and orientation maps. In the ferret, cortical spontaneous activity, presumably reflecting innate connectivity, has been observed as early as postnatal day 22 and already presents a modular structure [164, 165]. It even persists after optic nerve transection abolishing geniculate input [165] supporting its intracortical origin. Early spontaneous activity holds some predictive power of the orientation map at eye opening [43]. The similarity is not perfect, but the patterns of spontaneous and evoked activity become increasingly similar with the onset of visual experience. In essence, spontaneous, modular, cortical activity, shaped by intracortical and recurrent connections, may provide an initial structure for evoked responses before V1 refines to create a reliable orientation map after the onset of visual experience. For this maturation process visual experience is crucial. While dark rearing only delays the maturation of the orientation map, visual experience through closed eye lids past the point of natural eye opening deteriorates the initial orientation map and the horizontal connection pattern [160]. This mirrors the role of experience for ocular dominance insofar as it highlights that the statistics of visual experience (no patterns, vs. diffuse patterns) at specific stages of development matter. Yet, orientation selectivity is not a phenomenon that relies on inputs from both eyes and monocular deprivation as well as alternating monocular lid-suture still allowed for the maturation of orientation selectivity and orientation maps [166].

Comparison with mouse V1 It is worth briefly discussing how these findings in ferrets, cats, and primates translate to the mouse, another model organism for vision. Mouse V1 exhibits similar functional properties as V1 of ferrets, cats, and monkeys. Neurons exhibit orientation, spatial frequency, and direction selectivity similar to other higher order mammals [58]. But despite the similar functional properties present in rodent V1, there may be different mechanisms underlying it. For instance, while neurons in V1 also present retinotopic organization, additional large-scale organization like ocular dominance columns or an orientation map is absent [57, 58, 167]. Neurons with similar orientation preference do not cluster across the surface, but instead are intermingled, which has coined the term 'salt-and-pepper' organization. Accordingly, L2/3 horizontal connectivity does not exhibit a modular and patchy structure, yet a bias for like-to-like connectivity was found [168, 169] supporting a role of horizontal connectivity, even when is it not modular. Another key difference across species is that, in mouse retina, there are substantially more types of RGCs than in primates [170]. A significant portion of RGCs already exhibit orientation and direction selectivity, a property considered to only emerge in V1 of carnivores and primates [171, 172]. While more recently, and after designated efforts, direction-selective ganglion cells were also found in the primate retina [173], they seem to only constitute a small fraction. Some studies have reported orientation bias in the retina and LGN of the cat [157, 174, 175], in LGN of developing ferrets [176], and the retina of the primate [177]. However, orientation and direction selective cells were more numerous in LGN of the mouse than in these other species [178, 179, 180, 181]. Therefore, orientation selectivity in mouse V1 could be more feedforward-driven than in other species. Ultimately, it remains to be answered how across species the different numbers and degrees of orientation and direction selective neurons upstream to V1 contribute to functional properties in V1.

To conclude, orientation tuning is a hallmark feature of V1, across species. In carnivores and primates, there is evidence that this feature could be driven by orderly convergence of LGN inputs to cortex [2, 153, 154, 158]. Yet, intracortical such as horizontal connectivity within L2/3 also appears to be a crucial component of V1, in particular for features exhibiting modular activity patterns, such as orientation preference [35, 129, 162]. These two lines of research are representative of a longstanding discussion about the role of feed-forward and intracortical input in driving neuronal responses. This discussion takes place for various stages and features of visual processing and also extends to binocular alignment, as described in the following.

1.5. Binocular alignment

Having two eyes allows sampling many points of the visual scene twice. Generally, edges of objects produce nearly identical signals on each retina. However, they appear at different locations due to the horizontal offset of the eyes and their opposing inward rotation when focusing on an object [20]. Ultimately, cortical neurons should be able to match these spatially offset, but otherwise identical signals. While the spatial offset of receptive fields is a feature that is used for depth perception and neurons encoding different offsets (disparity) exist [182, 183, 184, 185, 186], the receptive field structure for each eye should match the other closely [3]. In other words, the functional

response properties, like orientation preference and tuning, should also align between the eyes and is considered to be required for binocular vision [187]. Furthermore, neurons responding equally to images from either the right or left eye is important for situations of monocular occlusion [188]. When an object is suddenly covering one eye, the representation of the visual scene still accessible with the other eye should ideally remain constant. Otherwise, downstream computational issues may arise. In sum, binocularly responding neurons are expected to present highly similar responses for right and left eye stimulation.

The earliest support for this hypothesis can be found in the early work by Hubel and Wiesel in 1962 [2]. They studied orientation selectivity in cat V1 and also assessed the receptive field structure of single units for right and left eye stimulation. Their findings suggest that the receptive field location and structure for each eye are very similar. The main difference they describe are not functional properties but the biases in response strength of single cells for one eye over another (ocular dominance, see 1.4.2), which became a highly studied phenomenon afterwards. Since then, many others have described the high degree of response similarity of binocularly responsive neurons across many species (macaque: [1], cat: [2, 21, 25, 189, 190], ferret: [4], mouse: [5, 6, 26]). Most studies specifically measure the matching of orientation preference since it is such a characteristic feature of V1. Some studies go beyond this functional property and compare monocular responses with respect to tuning selectivity, spatial frequency tuning, and other features [21]. Common to all these studies is the finding that responses for each eye show strong similarities. Despite these strong similarities it is important to highlight, that there is diversity in the degree of alignment and not all neurons exhibit perfect alignment.

1.5.1. Binocular alignment during development

Developmental studies regarding binocular vision have been focusing largely on ocular dominance, orientation selectivity, or disparity but less on orientation matching. A noteworthy exception is work by Blakemore and Sluyters (1972, 1974) [3, 191] who studied visual cortical neurons in kittens reared under normal or artificial conditions. Kittens that underwent binocular deprivation by suturing both eyelids shut or reverse suturing of one eye at a time of the course of weeks, exhibited a higher degree of orientation preference mismatch between the eyes than normally reared kittens. They conclude that normal, binocular vision is critical for orientation alignment between the eyes. Similar effects of normal and binocularly deprived visual experience was found by Crair *et al.*(1998) [192] when studying contra and ipsi eye orientation maps and their similarity. Other work studied the effects of induced strabismus in kittens. In strabismic kittens that undergo monocular deprivation, recovery of orientation selectivity and visual acuity is slower than in non-strabismic animals [193]. During normal rearing, induced strabismus maintains retinal and general signaling levels, yet the activity between the two eyes is less correlated which results in most V1 neurons becoming almost exclusively monocular as a result [147, 148]. This suggests that not only binocular but correlated vision through both eyes is essential for normal binocular responses.

A more thorough appreciation and description of the development of binocular align-

ment was given by Wang *et al.*(2010) [5] in the mouse. Around p20, therefore before the onset of the critical period for ocular dominance in mice, many binocularly responsive neurons exhibit significantly different orientation preferences for each eye. Responses become better aligned between the eyes over the next 2 weeks, which is also the closure of the critical period for ocular dominance in mice [194]. This alignment process requires binocular visual experience as monocular deprivation and dark rearing during this period prohibits orientation preferences for each eye to become better matched [5]. More recently, Chang *et al.*(2022) [4] reported similar findings in V1 of the ferret (see Fig.1.2a-b). At eye opening, neurons exhibit diverse levels of binocular orientation match which are above chance, but below what is seen in animals with several days of visual experience. Delaying eye opening by binocular lid-sutures leads to less orientation matching compared to visually naïve animals. Even multiple days of visual experience following binocular deprivation are not sufficient to reduce mismatch to the level of normally reared animals with comparable amounts of visual experience. Both studies in mouse and ferret reveal that in animals with no or little visual experience, many binocularly responsive neurons exhibit significantly different orientation preferences for each eye. Moreover, they demonstrate that binocular responses are not innately well aligned undergo a developmental process that requires binocular vision and leads to better alignment. Importantly, this phenomenon occurs across species and appears to be a fundamental part of visual development.

Intrigued by the experience-dependent integration of distinct sources, further experiments aimed to dissect the binocular alignment process. Chronic imaging of the same neurons during the alignment process revealed two distinct strategies of how visual cortex can arrive at increased response similarity between the two eyes: In the mouse visual cortex, the monocular and binocular neuronal population appear to undergo a sizeable restructuring after eye opening as early as p14 [6, 7, 8]. Specifically, binocular neurons with low orientation selectivity are largely rendered monocular, whereas well-tuned monocular neurons gain responsiveness to the other eye and become binocularly aligned [6]. Notably, given the initial contra dominance in neurons, it is more frequent that the ipsi eye response is added to match [6, 7]. Lastly, this reassignment is restricted to L2/3 neurons and is not observed in L4. In contrast, data from L2/3 in the ferret presents an alternative strategy for increasing binocular alignment [4]. Here, the tracked neurons do not undergo changes in ocular dominance, but instead shift their orientation preference for both monocular responses. Specifically, both monocular preferences become more similar with the preference measured during binocular stimulation of the naïve animal. These shifts tend to be more pronounced for the ipsi eye representation since the initial contra eye responses tend to be more similar than the ipsi eye response to the binocular response. Overall, the changes in both monocular orientation preferences leads to better alignment between the eyes after only 4 days of visual experience. To summarize, several studies suggest that especially changes in the response to ipsilateral stimulation are contributing to alignment, although there may be different underlying mechanisms across species.

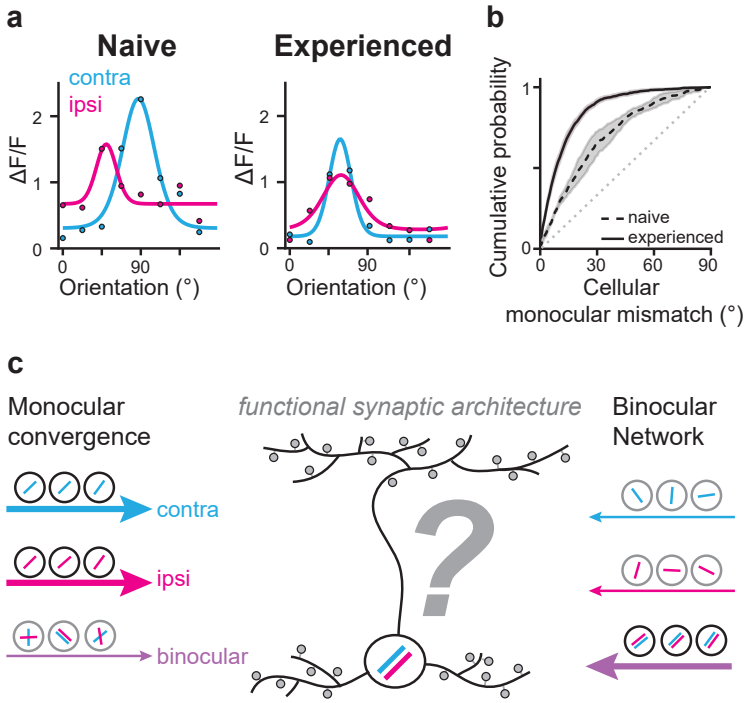

Figure 1.2.: The binocular alignment process and two hypotheses about its synaptic basis
(a) Cellular trial-averaged responses (median, circles) and fitted orientation tuning curves for and naïve and experienced animals. **(b)** Cumulative distributions of cellular monocular mismatch for naive and experienced animals (mean ± standard error). Mismatch is computed as difference in orientation preference for contra and ipsi eye responses. Diagonal (dotted grey line) indicates chance levels of mismatch. (a-b) are adapted with permission from [4]. **(c)** Illustration of the two main (not mutually exclusive) hypotheses about the synaptic basis of binocular alignment. Orientation preference for each eye of the soma and the inputs (circles) is illustrated as the angle of a bar. Monocular convergence predicts monocular contra and ipsi input streams to provide inputs matching each other in orientation preference, while binocular inputs would not be relevant and could be mismatched or absent. In contrast, binocularly aligned responses of the soma could be supported by binocular inputs that are aligned themselves. Monocular inputs could be mismatched to each other and the somatic preference or absent.

1.5.2. Hypotheses about the synaptic basis of binocular alignment

Several ideas about how binocular alignment and orientation preference matching develop have been put forward. In general, these ideas are tightly interwoven with orientation selectivity and ocular dominance. Early studies on the visual system were dominated by the idea of orderly feedforward drive (see above 1.4.2 and 1.4.3). The orderly of LGN inputs to create orientation selectivity in V1 is one example of that [2]. More recently, some studies argue that intracortical feedback and recurrent connectivity may also play a critical role in cortical computations, map formation, and may be sufficient to create or at least orientation selectivity from untuned inputs [38, 39, 41, 42, 159]. While studies approach the relevance of recurrent connections largely from a computational or modeling side, recently some experimental efforts in the somatosensory cortex were made to illustrate the role of recurrent networks [195].

A similar discussion about the relevance of feedforward and recurrent streams has extended to binocular vision and particularly binocular alignment (see Fig.1.2c). Upstream to V1, neurons are typically considered to be purely monocular (see 1.3). Consequently, in a feedforward framework binocular V1 neurons would have to not only ensure orderly LGN connectivity for gaining orientation selectivity but also do so for both monocular input streams in an aligned manner to generate their orientation-matched binocular responses (see Fig.1.2c, left) [30, 31, 196]. This concept is called "monocular convergence" and builds on strong or exclusively feedforward drive. During development, visual experience could drive the alignment via Hebbian plasticity mechanisms which postulates that coactivity of the pre- and postsynaptic neuron results in strengthening of their connection [32]. Binocular vision would result in frequent coactivation of monocular neurons that prefer the same stimulus orientation but are otherwise independent from each other. In a binocular neuron connected to these monocular neurons, coactivation of the presynaptic partners could trigger an action potential. This in turn could promote growth and stabilization of the co-tuned, monocular inputs, ultimately leading to a reliable, aligned response of the postsynaptic binocular neuron.

On the other hand, neurons in V1 have numerous intracortical connections. Especially neurons in L2/3 are part of a horizontally connected, recurrent network [33, 35, 37]. Accordingly, these neurons should receive numerous inputs from other binocularly responsive neurons. Moreover, studies have also reported a small percentage of binocular neurons in the LGN, which show varying degrees of binocular interactions (stimulation of the "silent" eye may affect the responses to the dominant eye) [85, 86, 87, 197, 198, 199]. Thus, V1 neurons may make use of both upstream binocular interactions and intracortical and recurrent connectivity with other binocular V1 neurons, to create orientation tuning that is matched between the eyes (see Fig.1.2c, right) . After eye opening, the onset of binocular vision leads to highly similar drive in both retinas. Highly correlated drive through both eyes has been shown to lead to stronger responses than stimulation of one eye alone [2, 200, 201, 202]. This implies that binocular vision could lead to preferential activation and increased plasticity of binocular neurons that have high response alignment over those that are less aligned or monocular. Instead of monocular inputs, the binocularly aligned input network

would be strengthened during development and stabilize aligned responses in V1 due to Hebbian or recurrent amplification mechanisms. Anatomically, the increase in L2/3 horizontal connectivity [33, 35, 36, 37] could serve as the structural basis. Notably, this idea of the binocular, intracortical, recurrent network playing the major role does not discard the monocular convergence idea. Monocular convergence may still occur at earlier stages of visual processing such as L4. However, it may be less relevant in driving the aligned responses particularly in superficial layers of V1.

The two hypotheses of monocular convergence and intracortical binocular connectivity make different predictions about the synaptic architecture of binocular aligned neurons (see Fig.1.2c) . Monocular convergence predicts that many inputs should be monocular and inputs from each eye should largely match the orientation preference of each other and that of the soma. This way, separate input streams can support aligned somatic output. On the other hand, the intracortical binocular hypothesis predicts that most inputs are binocular and should match orientation preference between the eyes and to the soma. This way, their aligned input would drive an aligned somatic output. Ultimately, the two hypotheses highlight different network structures, namely feedforward and intracortical/recurrent. Understanding which of these structures the brain employs for binocular alignment can yield important insights about information integration at the subcellular and network level.

An initial effort to address alignment at the subcellular level was undertaken by Gu *et al.*[203]. They used whole cell recordings and optogenetics to silence cortical activity in an effort to distinguish thalamo-cortical and cortico-cortical inputs and their respective contribution to binocularly aligned responses in mouse V1. In animals with mature levels of alignment, they find that cortical and thalamic inputs provide similar degrees of alignment between the eyes. In contrast, in younger animals with less alignment, the summed thalamic input exhibits better alignment and thus developmentally precedes that of cortical input. This suggests that at least early in development, there may be functionally distinct contributions of feedforward and recurrent connections to interocular alignment. However, whole cell recordings do not allow to disentangle the contributions of monocular and binocular inputs, as it can only measure the sum of all monocular and binocular inputs that are activated during stimulation of one eye.

How binocular alignment emerges in V1 has also been approached from the theoretical side and numerous models have aimed to describe or model this process. While these models capture various aspects of alignment and make several predictions, they can differ substantially in their architecture. Models may include no intracortical connectivity, i.e., are purely feedforward driven and thus reflect the monocular convergence hypothesis [29, 30, 31]. Others include or discuss intracortical connectivity, giving some room for the binocular intracortical hypothesis [204, 205]. Experimental data giving insights about whether and how monocular (feedforward) and binocular (intracortical/recurrent) inputs are involved in binocular alignment could help interpreting past and guiding future models.

To summarize, to which proportion monocular or binocular inputs occur and how they each contribute to binocularly aligned responses in V1 responses is unknown. To fill this gap, this work aims to give a detailed description of the synaptic architecture generating binocularly aligned responses in L2/3 of ferret V1.

1.5.3. Input sources for binocular alignment

When studying how excitatory synaptic inputs contribute to somatic output, it can be useful to know overall connectivity patterns to appreciate where inputs may come from. Some areas may have characteristic properties and as such may be more or less prone to contribute to the feature of interest in the postsynaptic cell. For binocular alignment, it can be important to differentiate between putative monocular and binocular input sources, or the degree of orientation selectivity. The following section will briefly discuss the main input sources for L2/3 neurons in ferret V1 and how their developmental changes could contribute to increases in binocular alignment.

The previous section (1.4.1) covered general cortical circuitry and developmental changes related to ocular dominance and orientation selectivity. In brief, L4 is the main thalamo-recipient layer and itself sends signals to L2/3. L2/3 has extensive horizontal connections and can be thought of as a strong intracortical, recurrent network. Thus, L2/3 neurons are considered to mostly receive inputs from other L2/3 neurons. L4 represents another major input source, and lastly, some thalamic projections also innervate L2/3. However, there are two additional sources for input to L2/3 that have not been discussed so far (see Fig.1.1).

Feedback connections Following the feed-forward stream of information and the hierarchical structure of the visual system, signals from V1, travel to V2, and further higher order visual areas. Higher order visual cortices are considered to belong to either the dorsal "what" or the ventral "where" pathway that are responsible for different aspects for visual processing [206]. Regardless of the pathway, the further up in the hierarchy, thus the further downstream, the larger receptive field size and the more complex the features that are represented become [207, 208]. Importantly, information does not only flow unidirectional and higher visual areas send feedback projections to V1 and could potentially be contributing to binocular alignment [209]. Retrograde labeling in cat V1 with choleratoxin b shows that feedback projections most frequently originate from excitatory neurons in L5/6 and less frequently in L2/3 [209, 210]. They terminate in layer 1, upper layer 2, and layers 5/6 in V1 [211, 212]. This laminar specificity of feedback projections sparing L4 is often contrasted with feedforward projections that preferentially target L4 [211, 213, 214, 215]. A study in ferrets shows that the closer in the hierarchy and the larger the cortical area, the more cells provide feedback to V1 [208, 209]. Moreover, feedback projections connect neurons representing the same part of the visual field across different areas [208, 216]. V2 which in the ferret is functionally very similar to V1 and also exhibits orientation selectivity, sends projections to V1 that appear to even match orientation domains [217]. Therefore, feedback projections display structural properties that make them a putative source of inputs contributing to binocular responses in L2/3 of V1.

However, the function of these feedback connections is not fully elucidated [218]. Because the projecting neurons have larger receptive fields than their targets and the retinotopically match their target location [208, 216, 219], feedback is considered to be important for providing visual context, or more technically speaking, support extra-classical receptive field modulation [217, 218, 220]. For binocular integration, they may provide an additional source of binocular inputs as higher visual areas are

increasingly binocular and disparity selective implying that binocular integration stays relevant downstream of V1 [185, 221].

Lastly, feedback connectivity to V1 observed around eye opening shares the basic properties that is found in the adult ferret. Only minor shifts in the relative contribution of different higher visual areas areas have been described [222]. These changes occur over the course of a couple weeks after eye opening which does not match the rapid increase of binocular alignment within days of experience onset [4]. However, higher visual areas may undergo functional changes around the same time as V1 [223], which could effectively alter the information they provide and potentially contribute to the binocular alignment process. Hopefully, future experiments on functional development of higher visual area and thorough mapping studies can elucidate the role of feedback projections to V1 throughout development.

Callosal connections Some cortical neurons send signals to the other hemisphere via callosal projections [214, 219, 224, 225]. These projections are mostly excitatory and in the visual cortex link retinotopic similar areas across the hemisphere. They originate in L2/3 and layer 6 of the other hemisphere and preferentially terminate in parts of the visual cortex representing the vertical midline of the visual field which is accessible for both eyes (ferret: [226, 227], cat: [219, 228, 229, 230]) indicating a potential role for binocular vision. In cats with surgically induced strabismus the termination zones of callosal input were larger than normal and thus less specific [231, 232] indicating how the alignment of the vertical meridian across eyes is required for the precise callosal mapping that happens in normal development.

While anatomy supports a role of callosal projections in binocular vision, especially in the visual field center, studies have disagreed on whether or not they substantially contribute to binocular responses in V1. For instance, deactivation of callosal connections by cooling the other hemisphere was found to only mildly affect orientation and direction tuning [233, 234]. A lesion study in cats further suggested only a limited contribution of callosal input to depth perception [235]. In the mouse, tetrodotoxin treatment of the other hemisphere, effectively blocking callosal input, consistently reduced the ipsilateral response [236]. Similarly, in another rodent study, suppressing callosal input reduced spiking in monocular and binocular neurons, yet activation of the callosal projecting neurons was not sufficient to drive V1 responses in the other hemisphere [237]. Nevertheless, unpublished work in the ferret reportedly indicates that callosal connections contribute specifically to cardinal orientation preferring neurons of the vertical meridian [238]. Yet in general, callosal projections in carnivores and primates are thought to facilitate rather than modulate functional properties in the other hemisphere.

At birth, neurons in the cat that are projecting callosally are more uniformly distributed across the cortical surface. The reorganization into zones occurs over the first month [239]. In ferrets, studies have been investigating the development only starting around 4 weeks of age [224]. After p28, callosal connections seem to undergo very few changes and even the laminar projection patterns are stable throughout development. In sum, callosal input may not be the main driver of changes after eye opening. But since both hemispheres are undergoing developmental refinement, the input provided

by these projections is likely to change functionally and could differentially influence or facilitate binocular responses over development.

Inhibition While the main focus is often on the excitatory drive that neurons receive, inhibitory input is also important to consider. Inhibition has been shown to play a critical role in shaping cortical activity and plasticity [240, 241, 242, 243]. While it was initially thought that inhibition would contribute to orientation selectivity by signaling for non-preferred orientation, inhibition is cotuned in orientation space to the excitatory input to a cell (cat: [244], mouse: [245], ferret: [246]. As such, inhibition has been regarded as an important mechanism of stabilizing recurrent cortical network activity [247, 248]. It does however contribute to direction selectivity by altering the excitation/inhibition balance for the null (non-preferred) direction [246].

Before visual experience, inhibitory neurons in the ferret exhibit spontaneous activity that is modular, similar to excitatory networks at this stage [249]. Yet, during evoked activity with drifting gratings, inhibitory neurons display non-modular, uniform and unselective activity [250]. While evoked activity patterns of inhibitory neurons become modular independent of visual experience, the development of orientation selectivity of inhibitory neurons is experience-dependent. In contrast to these findings in the ferret, inhibitory neurons in mouse V1 were found to become less orientation selective with visual experience [251].

The precise function of inhbitory neurons may not only vary across development and species, but also across inhibitory subtypes [241, 252, 253]. Moreover, *where* inhibitory neurons synapse onto excitatory neurons can have implication for the postsynaptic neurons integration of signals [254]. Unfortunately, studying not only the summed inhibitory input, but the function and spatial organization of individual inhibitory synapses onto excitatory neurons has proven difficult. Recent developments in detection of the primary inhibitory neurostransmitter γ-Aminobutyric acid (GABA) still lack the sensitivity and spatial resolution for measuring the synaptic architecture of inhibitory inputs [255].

Given these technical challenges and limited knowledge on inhibition, its role in binocular alignment is unknown and remains to be explored.

Developmental structural changes of neurons in L2/3 We still lack a good understanding on the relative proportion and influence that synaptic inputs from one source over another have in the mature state as well as during development. The relative contribution from feedforward, recurrent, feedback, callosal, and inhibitory inputs may change over development and thereby alter the synaptic composition and the somatic output of a L2/3 neuron. We can only make educated guesses in this regard from various studies that assess connectivity and functional properties. Feedback and callosal inputs appear to be mostly developed and refined by the time of eye opening again, only undergoing small changes. In contrast, the increase in horizontal connectivity suggests that recurrent connections may become increasingly influential [33, 35]. A qualitative study by Zervas and Walkley (1999) [256] on dendrite morphology in the ferret cortex (but not V1) describes a continued increase in basal branch complexity from p28 to p35 and states that L2/3 neurons reach their peak spine density by p35.

The increase in axon and dendrite length, as well as spine density, and structural changes of dendritic spines, have been observed in many species and brain areas (human: [257, 258], primate: [259, 260], cat: [261], ferret: [121, 256, 262], mouse: [263, 264, 265]). Importantly, these changes continue over weeks, months and years, starting before birth and extending past the onset of sensory experience. Repeatedly, neuronal activity has been shown to promote structural changes at various scales and structural plasticity is now considered to be the key mechanism for learning and memory [265, 266, 267, 268, 269, 270]. Thus, the synaptic weight as well as total numbers of inputs could change drastically and be involved in driving increased binocular alignment.

1.6. Functional two-photon imaging

How can we probe the role of synaptic inputs in driving somatic responses that are binocularly aligned? Electrophysiology has been a major driving force in neuroscience by enabling recording of neuronal activity at high temporal resolution [271]. Particularly, whole cell recordings have provided key insights into the relationship between sub-threshold inputs and supra-threshold outputs of a single neuron [272, 273]. However, whole-cell recordings reveal only the summed activity of all synaptic inputs at the level of the soma, and therefore cannot be used to study how individual synaptic inputs along the dendritic tree contribute to the neuron's activity. With the advent of *in-vivo* two-photon calcium imaging in dendritic spines, it has become possible to probe the functional properties of individual excitatory synaptic inputs arriving at a given cell.

1.6.1. Calcium Imaging

Functional optical imaging exploits optical changes in the brain induced by neuronal activity to deduce neuronal responses [274, 275, 276, 277] . While the temporal resolution is lower compared to electrophysiology, the advantage of functional imaging lies in the measurement of the time evolution of neuronal activity in relation to spatial organization of relevant structures. Fluorescence offers an excellent choice of optical mechanism to probe the brain due to its high sensitivity and specificity. In *in-vivo* fluorescence microscopy, fluorophores are introduced into the brain whose photon emission increases or decreases with neuronal activity. One type of fluorescence imaging that has evolved dramatically due to the advancements in molecular sensor development is calcium (Ca^{2+}) imaging. It is a powerful technique, because calcium ions are a key secondary messenger in many cell types, including neurons. Depolarization of the cell membrane triggers Ca^{2+} influx into the cell, thereby making the intracellular Ca^{2+} concentration a proxy for neuronal activity. Genetically encoded calcium indicators (GECIs) have become the most popular means for visualizing calcium. The most famous example is the engineered protein complex GCaMP [45]. It consists of three key domains: (i) the green fluorescent protein (GFP), (ii) the calcium-binding domain Calmodulin (CaM), and (iii) a peptide sequence that links them together. In a nutshell, when Ca^{2+} binds to GCaMP, it undergoes a conformational change that increases its photon emission (fluorescence) that can be detected via a microscope.

Thus, imaged increases in GCaMP fluorescence in labeled neurons represent increases in Ca^{2+} concentration and are interpreted as increases in neuronal activity. Continuous efforts in sensor development have improved the signal-to-noise ratio and temporal dynamics of GECIs which has ultimately contributed to its popularity.

Ca^{2+} imaging need not to be limited to the activity of a whole neuron but can also be used to record activity at the level of an individual synapse [275, 276]. At the classical chemical excitatory synapse, presynaptic release of glutamate into the synaptic cleft elicits a series of reactions at the postsynaptic site [68]. Initially, glutamate binds to postsynaptic α-amino-3-hydroxy-5-methyl-4-isoxazolepropionic acid (AMPA) receptors, triggering the influx of Na+ ions. The fast depolarization of the postsynaptic membrane induced by Na+ influx releases the Magnesium block on the N-methyl-D-aspartate (NMDA) receptors. NMDA receptors then induce further ion influx including Ca^{2+}, thereby causing increased intracellular Ca^{2+} concentration at the postsynaptic spine. With calcium sensors like GCaMP even such local changes in Ca^{2+} levels can be detected which forms the basis of functional spine imaging.

1.6.2. Two-photon microscopy

The small size of dendritic spines (a few micrometers in length and width) necessitates an imaging modality with high spatial resolution. Furthermore, the imaging technique must also provide high signal/background contrast few hundred microns deep into the brain, which is a highly scattering tissue. Therefore, for recording Ca^{2+} activity in dendritic spines, another technological advancement in the field of imaging has been crucial. The advent of two-photon microscopy enabled high-resolution fluorescence imaging deep into the cortex [44]. In two-photon imaging, excitation light with half the excitation energy of the fluorophore (e.g., the GFP in GCaMP) - and thus twice the wavelength – is used. Simultaneous absorption of two photons is required to excite the fluorophore – a process that relies heavily on the precise timing of two incoming photons. Laser pulses focused at one point in 3D maximize the probability of this process in a very restricted spatial zone. Any observed emitted photons are thus likely emitted from the precise focal plane of the laser beam. The emitted photons are then amplified in a photon-multiplier-tube (PMT) for the readout. Therefore, the rare process of two-photon excitation allows for higher spatial resolution especially in z (the depth) dimension compared to classical, one photon microscopy. Beyond increased spatial resolution, two-photon microscopy has the additional benefit of reduced light scattering due to the use of longer wavelength excitation beams, which allow imaging deeper into the tissue, up to 450 µm [278, 279, 280].

1.6.3. Challenges and insights of functional spine imaging

The combination of two-photon microscopy and functional calcium imaging is a powerful approach to visualize not only excitatory synaptic activity in single trials but also the spatial arrangement of inputs and their properties within the dendritic tree ("functional synaptic architecture") [46, 281, 282, 283]. However, there are some challenges associated with this approach. First, to acquire high-quality data for spines, it is important to get sufficiently sparse labeling of neurons with the fluorophore to

keep background activity low and improve the signal-to-background ratio, while at the same time achieving high fluorophore concentrations within the neuron being imaged. Genetic tools such as the Cre-Flex system allow delivery of large amounts of Flexed GCaMP whose expression is dependent on Cre [284, 285]. The Cre gene can be delivered in very small amounts and thus limit the number of neurons that express Cre, which in turn allows for the strong expression of GCaMP in a limited number of cells ([46], see Methods). Second, since calcium serves as a secondary messenger throughout the neuron, dendritic events involving calcium increase, such as back-propagating action potentials, may contaminate dendritic spine events [276, 277]. To avoid this, one can decrease the overall neuronal drive by reducing stimulus intensity, for example by reducing the contrast of the stimulus. Moreover, post-experimental analysis tools such as regressing out dendritic signals can help isolate the spine signals (see Methods). Third, it is important to note that calcium imaging in dendritic spines is not an exhaustive assessment of synaptic activity. Subthreshold activity that does not lead to significant intracellular calcium level increases and inhibitory synaptic activity, both are not captured by this technique but may still constitute important signaling in a neuron. Lastly, the fluoresence at the dendritic spines generally does not linearly scale with the input amplitude, making the strenght of the synaptic signal difficult to estimate [276, 286].

Despite these limitations and challenges, understanding the excitatory drive arriving at the dendritic spines has led and will continue to lead to important insights. For instance, previous work has shown that the combined synaptic input ("synaptic aggregate") to a cell predicts somatic orientation preference (mouse: [281, 287], ferret: [46]). Remarkably, a *post-hoc* study correlating *in-vivo* responses with *post-hoc* electron microscopy to link structure and function of dendritic spines, revealed that inputs with similar orientation preference as the soma did not exhibit larger synaptic weight, as would be expected from functional plasticity mechanisms such as long term potentiation (LTP) [288]. Instead, the *numbers* of active inputs for a given orientation are a good predictor of somatic preference. This study highlights how powerful sampling dendritic spine properties can be for predicting somatic output. Furthermore, the spatial arrangement of synaptic inputs at various spatial scales and its implications for subcellular computations have been described. In the mouse, spines with receptive fields further away from the somatic receptive field are biased to be on higher-order branches and thus anatomically further away from the soma [287], which might weaken their effect on depolarization of the membrane at the soma [289] unless compensatory mechanisms are at play [290]. In the ferret, while the summed input tuning predicted somatic orientation preference, the frequency of branches with low circular dispersion (low diversity of orientation preference of their synaptic inputs) predicts somatic orientation selectivity [46]. Beyond this branch homogeneity, no organizational principle with respect to soma distance or whether a spine is located on an apical or basal branch has been reported. But on a smaller scale ($<10\,\mu m$), inputs exhibit functional clustering: nearby spines exhibit increased tuning and trial-by-trial correlation [287, 291]. As spatial clustering appears to be reserved for spines with low synaptic weight [288], these inputs may employ local coactivity to induce non-linear dendritic integration effects to exert an increased, disproportionate impact on somatic activity [292, 293]. In sum, *in-vivo* functional imaging of dendritic spines can help understand how single

cells integrate their various excitatory synaptic inputs to generate somatic responses and what computations may be involved in this integration process.

2. The synaptic basis of binocular alignment in visually experienced animals

2.1. Summary of publication

The primary visual cortex (V1) of carnivores and primates is the first major place of convergence of eye-specific inputs. In V1 of visually experienced animals, most neurons are binocular (they can be driven by either eye) and exhibit high degrees of binocular alignment, i.e., their responses to oriented gratings are similar for right and left eye stimulation [1, 2, 4, 6, 7]. How these aligned responses are supported by synaptic inputs to individual neurons has remained unknown. A prevailing hypothesis for how binocular responses are shaped is monocular convergence. It proposes that monocular input streams from each eye converge on single neurons, and Hebbian plasticity mechanisms result in functional alignment of these two [29, 30, 31]. However, this idea neglects that cortical neurons are embedded in intracortical and recurrent, binocular networks, which could also contribute to binocular responses and their alignment [37, 39, 40, 41, 42, 93, 159, 294]. Previous studies have assessed binocular response properties from the network to the cellular level but have not been able to disentangle the relative contribution of individual monocular and binocular inputs [4, 5, 6, 203].

To address the role of excitatory synaptic inputs in driving binocularly aligned somatic responses, we used two-photon calcium imaging of dendritic spines in pyramidal layer 2/3 (L2/3) neurons of ferret V1. We measured postsynaptic and respective somatic responses to oriented gratings presented to the right and left eye separately.

We find that individual neurons receive a combination of monocular and binocular synaptic inputs. Within the binocular group, inputs exhibit a broad range of contra-ipsi tuning correlation ("congruency"). Those with high similarity in orientation tuning for both eyes ("congruent") are also highly orientation selective and closely match somatic orientation preference. Consequently, this input population provides highly specific, binocularly aligned input, making it a prime candidate to support binocularly aligned somatic responses. In contrast, monocular inputs alone cannot support binocular alignment. Specifically, monocular ipsi inputs are less matched to somatic output than monocular contra inputs, suggesting monocular convergence is not driving similar orientation preference for each eye in these neurons. However, functionally well-suited, binocular congruent spines constitute only around 1/3 of inputs, raising the question of how this subclass can drive somatic output.

To test whether binocular congruent inputs exhibit more synaptic strength, which could increase their contribution to somatic output, we used correlative light and

electron microscopy [295]. A subset of cells and spines that has been imaged and functionally characterized *in-vivo* was reconstructed *post-hoc* with electron microscopy, and proxies of synaptic strength were measured. Notably, we find no differences across input classes that would support biases in synaptic strength favoring binocular congruent spines. Instead, trial-by-trial simulations of synaptic events revealed that binocular congruent inputs exhibit strength in numbers of spines active: In trials where many spines are active, and a large fraction of them is binocular congruent, the total synaptic aggregate shows stronger binocular alignment between eyes and to the soma. We conclude that binocular congruent inputs may exert a disproportionate impact by their selective and reliable recruitment at the somatic preferred orientation, and this modulatory signal is further enhanced by the co-activation of monocular and noncongruent inputs. This led us to test whether cells with more binocular inputs congruent converging onto them are more aligned. Indeed, the relative proportion of binocular congruent inputs per cell predicts somatic congruency, further highlighting the importance of numbers, not strength. Markedly, the proportions of monocular inputs are uncorrelated with somatic congruency.

Altogether, our results show that at this stage of binocular processing, binocularly aligned responses are due to biases in the presynaptic binocular network rather than the monocular network.

The contributions to this publication from myself and the other authors are as follows. Co-first author Benjamin Scholl set up *in-vivo* spine imaging in the ferret and together we conceived the experiments described above. The two of us conducted the experiments together and performed the data analysis for all parts of the study except for the ultrastructure analysis. The ultrastructural study was conceived by Benjamin Scholl and conducted in collaboration with the Electron-Microscopy core team of Melissa Ryan, Connon Thomas, and Naomi Kamasawa. Together with Benjamin Scholl and David Fitzpatrick, I contributed to the first draft and multiple revisions that included feedback from the other authors. The work was conducted under the supervision of Naomi Kamasawa and David Fitzpatrick.

Reference:

[296] Benjamin Scholl*, Clara Tepohl*, Melissa A. Ryan, Connon I. Thomas, Naomi Kamasawa, David Fitzpatrick. "A binocular synaptic network supports interocular response alignment in visual cortical neurons". In: *Neuron* 110.9 (2022). 1573–1584.e4. Copyright Elsevier. DOI: 10.1016/j.neuron.2022.01.023.

* authors contributed equally

The full publication can be found in A.1.

3. The synaptic basis of binocular alignment in visually naïve animals

3.1. Introduction

Neurons in primary visual cortex (V1) are combining signals from the right and left eye for a coherent binocular percept [1, 2, 4, 5, 25]. Without substantial visual experience, neurons display diverse degrees of response alignment between both eyes but with visual experience, the responses become increasingly similar, i.e., aligned. The previous chapter has highlighted a critical role of binocular inputs, especially those that exhibit similar responses to each eye ("congruent") in driving aligned response in experienced animals by strongly influencing somatic contra and ipsi eye responses (see Chapter 2). How in visually naïve animals neuronal responses with more diverse degrees of alignment are generated from synaptic inputs has remained unclear but could help to uncover synaptic changes that occur with visual experience and an increase of binocular alignment.

Data in visual layer 2/3 (L2/3) neurons from experienced ferrets suggests a critical role of binocular synaptic inputs whereas the convergence of monocular inputs could not explain the high levels of somatic alignment (see Chapter 2)). Monocular convergence could be underlying binocular responses earlier in development, when somatic responses display lower levels of alignment. The increase of binocular alignment with visual experience would then be a result of the binocular network substituting the monocular networks. Alternatively, an immature binocular network may be present and drive somatic binocular alignment, but not achieve as good alignment as in the experienced state. The maturation of the binocular network would then lead to better somatic alignment. Anatomically, horizontal connections in L2/3 of ferret V1, considered a main contributor of binocular inputs, are present yet not as extensive at eye opening raising the question of how frequent and relevant the binocular network may be prior to visual experience [33, 35, 36, 37]. Functionally, visual cortex, and more specifically L2/3 neurons, are not only less binocularly aligned but also less orientation selective [4, 160, 163, 297] prior to visual experience which could further affect the functional properties of synaptic inputs and their impact on somatic tuning.

In short, it has remained unclear what the functional properties of dendritic spines are and how they support the somatic response prior to visual experience. Addressing this knowledge gap could not only elucidate the synaptic basis of the visually naïve state of cortex but could also expose changes in the functional synaptic architecture that develop with visual experience and improved binocular alignment.

Here we use *in-vivo* two photon calcium imaging of pyramidal neurons and their dendritic spines in L2/3 of V1 in ferrets without prior visual experience. We find that binocular neurons already receive monocular and binocular inputs, but binocular inputs are less congruent than those in experienced animals. Paralleling results in the experienced animal, the median congruency of binocular predicts somatic congruency, albeit lower levels of it. An increase of binocular, particularly congruent, inputs is likely to drive the improved binocular alignment of neurons after eye opening. Structural plasticity, such as the stark increase in spine density that we observed, could be a substrate for boosting this input population.

When measuring spine-soma mismatch of orientation preference as a proxy for how much somatic output is supported by individual inputs, increasing numbers of binocular congruent inputs appear to transform particularly the ipsi response.

In the naïve animals, all synaptic ipsi eye inputs appear to loosely match and thus contribute to the somatic ipsi preference, whereas after eye opening, binocular congruent spines are the main inputs to support the output ipsi eye preference. The relative reduction of binocular congruent inputs in the naïve could allow for their impact being outweighed by binocular noncongruent and monocular ipsi inputs resulting in less alignment. In contrast, for the somatic contra response, binocular congruent and monocular contra inputs are a provider of specific, supporting drive throughout development. This eye-specific distinction highlights a biased contribution of binocular congruent inputs to naïve somatic contra over ipsi eye responses but also distinct developmental changes for each eye. The data suggest that the somatic ipsi eye preference may change more than the contra one in order to achieve aligned responses and this ipsi change is largely ascribed to an increasingly dominating binocular congruent input network.

In sum, the binocular input network is driving somatic binocular responses even prior to visual experience. However, it is immature in its congruency which is associated with lower somatic congruency at this stage. In combination with data from experienced animals we conclude that the maturation and growth of the binocular input network remodels the somatic ipsi eye response to achieve better binocular alignment following eye opening.

3.2. Methods

Experimental Model and Subject Details

All procedures were performed according to NIH guidelines and approved by the Institutional Animal Care and Use Committee at Max Planck Florida Institute for Neuroscience. This study used exclusively female ferrets (*Mustelidae putorius furo*, Marshall Farms). Animals underwent survival injections at ages postnatal day p9-p21 and acute terminal experiments at ages p28-p36. Animals were housed in a 12 h light/8 h dark cycle in a vivarium. No *a priori* sample size estimation was performed, but sample sizes are similar to other studies which performed *in-vivo* two-photon imaging.

Method Details

The experiments followed closely the study of Scholl, Tepohl *et al.*(2022) [296] with only a few exceptions. The main difference is that animals were younger when undergoing the procedures and had not naturally opened their eyes until the day of the imaging.

Viral injections

Female ferrets (n = 19) at ages p9-p21 were anesthetized with isofluorane delivered in O_2. Atropine and a 1:1 mixture of lidocaine and bupivacaine or lidocaine and ropivacaine was given subcutaneously (SQ). The animal's heat rate, respiratory rate, and internal temperature was monitored and maintained within physiological limits. Under sterile surgical conditions, an incision was made over the visual cortex. One to three craniotomies over the posterior part of the lateral gyrus were made and a mixture of diluted AAV1.hSyn.Cre (1:40,000-1:100,000) and AAV1.Syn.FLEX.GCaMP6s (Addgene, 100842-AAV1) was injected through beveled glass micropipettes of 10-30 µm diameter at several depths up to 600 µm below the pia. In total, up to 30 µL were injected in one hemisphere. The craniotomy was filled with sterile agarose (type IIIa, Sigma-Aldrich) and the overlying fascia and skin sutured together. Animals received metacam 2 days post-operative and in some cases baytril for 5 days to manage infection and inflammation.

Cranial window

After 15-21 days of expression, the acute terminal experiment took place. Anesthesia was induced with Ketamine (12.5 mg/kg, intramuscular) and Isoflurane. Atropine and a 1:1 mixture of lidocaine and bupivacaine or lidocaine and ropivacaine was given SQ. The animal's heat rate, respiratory rate, endtidal CO_2, external and internal temperature was monitored and maintained within physiological limits. Intubation or tracheotomy allowed for artificial respiration and an intravenous catheter allowed for delivery of fluids. Isoflurane was delivered throughout the procedure to maintain a surgical plane of anesthesia. An incision was made and the scalp retracted. A custom titanium head plate was attached to the skull (Metabond, Parkell) above the visual cortex. A craniotomy was performed and the dura retracted. A stack of cover glasses (5 mm diameter, 0.7 mm thickness, Warner Instruments) attached to a larger coverglass (8 mm diameter, 0.7 mm thickness, Warner Instruments) held together with optical adhesive (71, Norland Products) was inserted into the well. The thickness of the stack was chosen so that mild but sufficient pressure was exerted on the brain to reduce biological motion during imaging. The eyes were opened manually for the first time. To dilate the pupils and retract the nictitating membranes, a 1:1 mixture of tropicamide ophthalmic solution (Akorn) and phenylephrine hydrochloride ophthalmic solution (Akorn) was applied to both eyes. Silicon oil was applied at the beginning and throughout the experiment to avoid drying out of the eyes. After the surgical procedure, isoflurane was reduced gradually and pancuronium (0.3 mg/kg/h) was delivered intravenously.

Visual Stimuli

Visual stimuli were generated using Psychopy (Peirce, 2007) and displayed on a monitor 25 cm away from the animal. For each soma and dendritic segment, square-wave drifting gratings were presented at 22.5° increments to each eye independently (1.5-2 second duration, 1-2 second inter-stimulus-intervals, 6-10 trials for each field of view). Automated eye-shutters for each eye controlled by an Arduino allowed to randomly interleave stimulation of the right an left eye.

Two-photon imaging

For two-photon imaging, a Bergamo II microscope (Thorlabs) controlled by Scanimage (Vidrio Technologies) [298] was used. An Insight DS+ (Spectraphysics) delivered dispersion-compensated excitation light at 940 nm. The power out of the objective was limited to less than 40 mW. Cells were selected for imaging based on their expression levels and responsiveness to visual stimuli. Images of 512-by-512 pixel resolution were collected at 30 Hz using bidirectional scanning. Somatic imaging was done with a resolution of 1.54-11.78 pixels/µm and spine imaging with a resolution of 6.14-13.31 pixels/µm.

Two-photon imaging analysis

Images were corrected for in-plan motion with a 2D cross-correlation based approach in MATLAB. If the registration was not successful or motion along the z-axis was detected, the imaging data was excluded. ROIs (region of interest) were drawn in Fiji [299]. Spine and soma ROIs were fit with custom software (Cell Magic Wand, github.com/fitzlab/CellMagicWand), dendritic ROIs spanned contiguous dendritic segments. Mean pixel values over time were extracted using MATLAB. For computing $\Delta F/F_o$, a time-averaged median filter was used to determine F_o.

For a subset of cells (n = 7/29), the somatic response was unreliable and an ROI of a dendrite was used instead. The $\Delta F/F_o$ traces were aligned to the stimuli triggers sent by Psychopy and recorded by Spike2. As done previously [46, 296], a scaled version of the dendritc signal was subtracted from the spine signal to remove contamination from back-propagating action potentials. Functional responses of dendritic spines were unrelated to the degree of residual correlation with dendritic activity.

Peak $\Delta F/F_o$ responses to bars and gratings were computed using the Fourier analysis to calculate mean and modulation amplitudes for each stimulus presentation, which were summed together. Spines qualified as responsive and were included in the analysis if: (1) the mean peak $\Delta F/F_o$ for any stimulus was > 20 % $\Delta F/F_o$, (2) the SNR for the same stimulus was > 1, (3) and spines were weakly correlated with the dendritic signal (Spearman's correlation, $r < 0.4$). All 3 criteria had to be met to qualify as responsive. This set of criteria was used for each eye condition separately to determine the ocular dominance class of each spine and soma. Specifically, if these criteria were passed for stimuli presented only to the contralateral eye (monocular contra), stimuli presented only to the ipsilateral eye (monocular ipsi), or for both (binocular). For binocular spines, congruency was computed as the Pearson's correlation (MATLAB) between mean responses driven by contralateral and ipsilateral stimulation.

Some spine traces contained negative events after subtraction of the regressed dendritic signal, so response properties were computed ignoring negative $\Delta F/F_o$ values. For evaluating orientation preference and orientation selectivity, we computed the vector sum across all stimulus direction, weighted by the mean response amplitude.

$$r = \sum_k R(\theta_k) exp(2i\theta_k) \tag{3.1}$$

Where θ_k are the $k = 16$ angles displayed, and $R(\theta_k)$ is the mean response for each angle condition. The orientation selectivity (OS) was computed from the normalized vector length of the vector sum.

$$OS = \|r\| = \left\| \sum_k \frac{R(\theta_k) exp(2i\theta_k)}{R(\theta_k)} \right\| \tag{3.2}$$

For responses of OS > 0.1, the preferred orientation was taken as the angle of the vector sum.

$$\theta_{pref} = arg(r) = tan^{-1} \frac{real(r)}{im(r)} \tag{3.3}$$

Quantification and Statistical Analysis

Statistical analyses are described in the main text. To avoid assumptions about the distributions of the data and because many of our measurement are bound, we used non-parametric statistical analyses (Wilcoxon's signed-rank test, Wilcoxon's rank sum test, circular Kruskal-Wallis test) or permutation tests. Quantitative approaches were not used to determine if the data met the assumptions of the parametric tests. Correlation coefficients r were computed with circular-linear correlation or Spearman's correlation. All correlation significance tests were one-sided unless specified otherwise. All statistical analysis was performed in MATLAB.

Airyscan imaging

After perfusion, the brain was cut tangentially to the surface into slices of 50-80 um thickness. Apical and basal branches of neurons in superficial layers were imaged on a ZEISS LSM 980 with Airyscan 2. The Zeiss Plan-Apochromat 63x/NA=1.4 Oil DIC M27 objective or the Zeiss Plan-Apochromat 20x/NA=0.8 M27 objective was used. Acquisition parameters were Nyquist optimized for most images and z-stacks were collected with a step size of $0.17-0.39\,\mu m$. Pixel size under the 63x objective was $0.043\,\mu m$ and under the 20x objective $0.08-0.104\,\mu m$. Dendrites were traced with SNT [300] and spines were selected manually. Spine density ρ_{spines} was computed per dendritic segment:

$$\rho_{spines} = \frac{\#spines}{dendriticlength} \tag{3.4}$$

3.3. Results

To address how synaptic inputs contribute to binocular responses in L2/3 of naïve ferret V1, we used *in-vivo* two-photon calcium imaging of dendritic spines and the respective soma. All ferrets included in this study had no prior visual experience and eyes were opened shortly before the start of the experiment. To compare results across development, we used data from experienced animals that has been published and summarized in the previous chapter (Chapter 2, A.1, [296]). For consistency, the data from experienced animals was put through the same analysis and inclusion criterion as data from naïve animals, leading to slight quantitative but not qualitative differences with the analyses in the previous chapter.

We first imaged somatic responses to visual stimuli and if the soma appeared visually responsive to both eyes, we proceeded to serially image dendritic spines. We interleaved presentation of drifting gratings to the right and left eye. We measured responsiveness and orientation tuning for each eye independently for somata and dendritic spines. While some neurons responded exclusively to one eye, we specifically targeted binocularly responsive neurons for this study. In total, we imaged 25 binocularly responsive cells and 1173 spines responsive for at least one eye (see Methods). Imaging was biased to more superficial branches so that 82% of responsive spines were located on apical branches.

We first characterized the response properties of the neurons imaged in naïve animals. As we are studying binocular alignment specifically in the context of orientation tuning, we first measured the orientation selectivity. By computing orientation selectivity (OS, using normalized circular vector length, see Methods) we find that naïve neurons display weaker orientation selectivity than neurons in experienced animals, consistent with the literature (Fig.3.1a-b; one-sided rank sum test naïve vs. experienced; contra: $p = 0.0006$; ipsi: $p = 0.0008$, [4]). In binocular neurons with sufficient orientation selectivity for both eyes (OS$>$ 0.1, 19/25 neurons) we computed the contra-ipsi mismatch of orientation preference. We find that contra-ipsi mismatch tends to be larger in naïve than in experienced animals (Fig.3.1c; one-sided rank sum test naïve-experienced: $p = 0.06$). In fact, the levels of naïve mismatch are comparable with what had been reported in a previous study with a larger sample size of neurons (mean $\pm$ s.e.: (here) 29.7° $\pm$ 5.7°;Chang *et al.*(2020) [4]: 27.9° $\pm$ 4.2°). The measure of orientation mismatch does not capture differences in the full orientation tuning curve such as selectivity between the eyes. To include such potential differences we also computed the contra-ipsi tuning correlation ("congruency", see Methods). High congruency is associated with strong tuning similarities between the eyes. Neurons exhibit a broad range of congruency (median = 0.30, interquartile range (IQR) = 0.80) but overall lower than that seen in neurons from experienced animals (Fig.3.1d; median = 0.55, IQR = 0.38, one-sided rank sum test $p = 0.05$). Congruency and contra-ipsi mismatch are highly correlated ($r_{C-I} = -0.8$, $p < 0.0001$ for both developmental groups), but in the following we use congruency as the more encompassing measure for binocular alignment. For consistency across the study, which for some analyses requires somatic preference, we include only binocularly selective neurons going forward (19/25 cells, 997 responsive spines). Importantly, none of the results were qualitatively affected by this criterion.

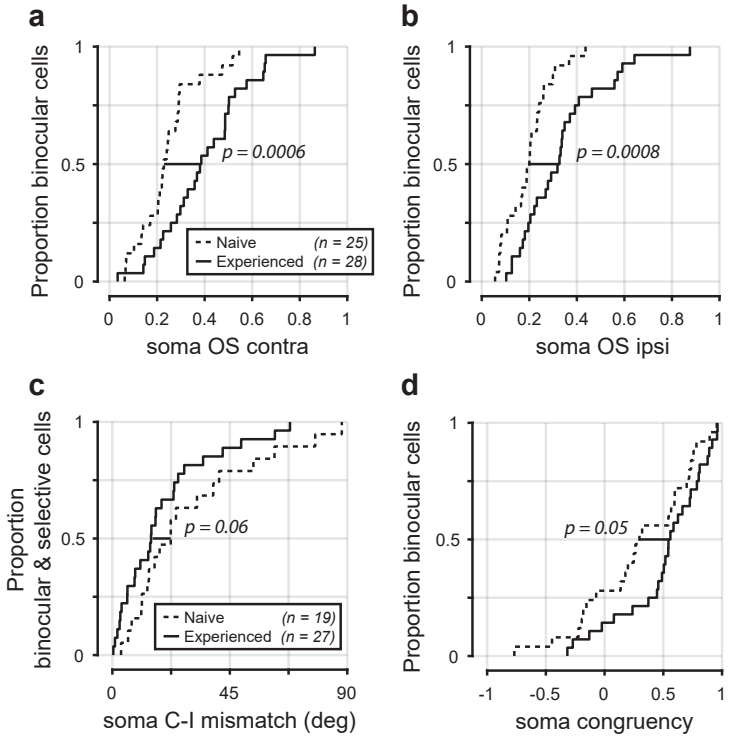

Figure 3.1.: Neurons of L2/3 neurons in naïve ferret V1 display immature orientation selectivity and binocular alignment
(a-b) Cumulative distribution plots of orientation selectivity (OS) of somatic responses to contralateral (a) and ipsilateral (b) stimulation of binocular neurons in visually naïve and experienced animals. **(c)** Cumulative distribution plots of orientation preference mismatch between contra and ipsi responses (C-I mismatch). Only for binocular neurons with an OS$>$ 0.1 for contra and ipsi orientation preference and C-I mismatch was computed. **(d)** Cumulative distribution plot of somatic response congruency (contra-ipsi tuning correlation, see Methods). All tests are one-sided Wilcoxon's rank sum tests

3.3.1. What is the role of monocular and binocular inputs in driving binocluar alignment in naïve animals?

Given the diverse yet immature levels of alignment at the cellular level, we wondered which synaptic input populations contribute to the initial binocular response. Given the predominant role of the binocular inputs and specifically of binocular congruent spines in the experienced animals, we wanted to test if a similar relationship would hold in the naïve, inexperienced visual cortex.

Inputs to neurons in naïve V1 exhibit ocular class diversity

First, we determined the proportion of monocular and binocular synaptic inputs available to layer 2/3 neurons at eye opening. For each spine, we assessed whether a significant response (see Methods) could be elicited by visual stimulation through the contralateral eye only (monocular contra), the ipsilateral eye only (monocular ipsi), or both eyes (binocular). We refer to this property as "ocular class" and examples for each class are shown in Fig.3.2b-c).

Prior to the onset of experience, spines are already diverse with respect to their ocular class, and this holds true at the level of input populations to single cells (see Fig.3.2d-e). Each binocularly responsive cell, except for one cell where only 20 spines were sampled, receives inputs from each ocular class, suggesting all three input subpopulations may contribute to somatic output. When considering the proportion of spines from each ocular class across cells, a dominant role of the binocular network becomes apparent. For both, contra, and ipsi eye stimulation, binocular inputs are more numerous than the respective monocular inputs (mean ± s.d.: binocular $56 \pm 17\%$, monocular contra: $28 \pm 15\%$, monocular ipsi: $16 \pm 11\%$).

In comparison with data from experienced animals, the balance of monocular and binocular inputs is marginally shifting after experience, with binocular inputs tending to become more frequent (mean ± s.d., rank sum test; binocular: (experienced) $65 \pm 12\%$, $p = 0.04$; monocular contra: (experienced) $23 \pm 11\%$, $p = 0.15$; monocular ipsi: (experienced) $13 \pm 10\%$, $p = 0.14$). Therefore, over development, binocular inputs may increase their impact on the somatic response.

To summarize, the data suggest that in visually naïve cortex, as in the experienced cortex, both monocular and binocular networks can contribute to binocular responses. Yet, consistently across development, the majority of the signals conveyed during monocular stimulation is conveyed by binocular afferents, which suggests that the binocular presynaptic network exerts a greater influence than monocular presynaptic network on somatic output.

Naïve binocular inputs exhibit diverse but low degrees of congruency

With the binocular network providing a substantial number of inputs, we next quantified how similar the input delivered by binocular spines is between eyes. We measured their degree of congruency and find that binocular spines cover a wide range of congruency values (Fig.3.3a; median = 0.20; inter-quartile range (IQR) = 0.65; $n = 558$). On average, congruency is above chance (mean ± s.d. congruency of randomized shift

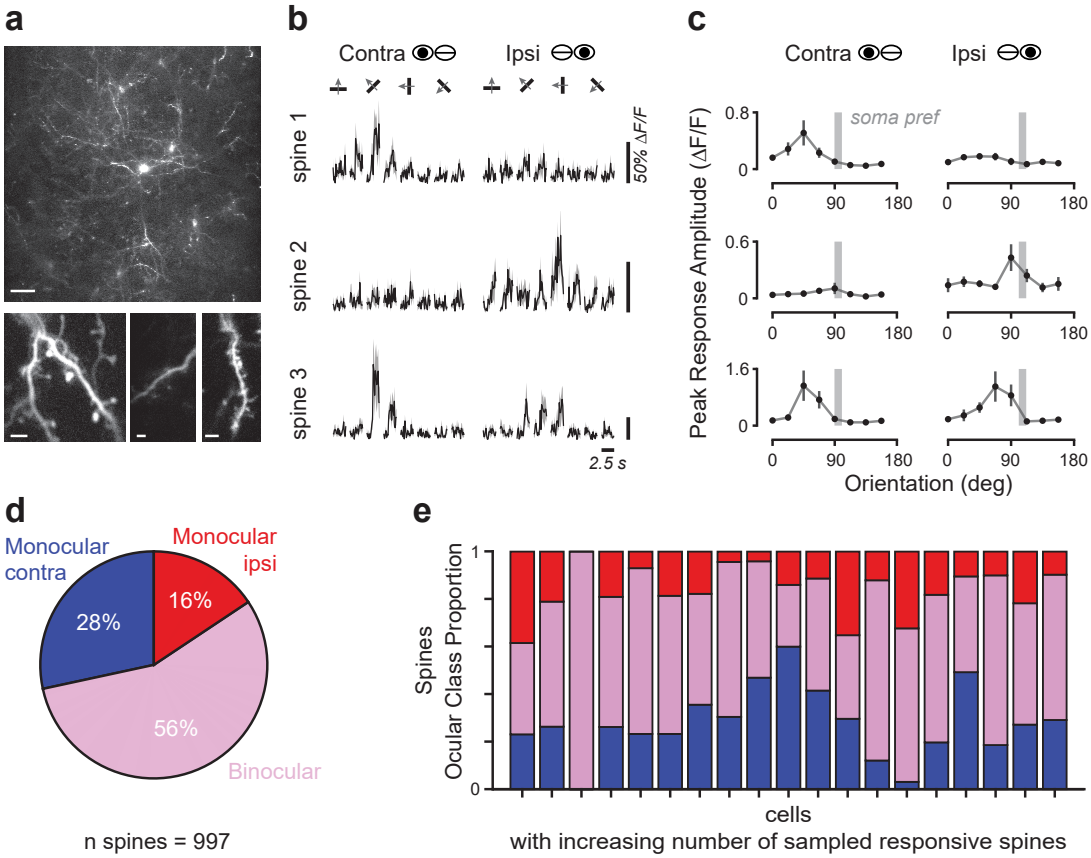

Figure 3.2.: Functional two-photon spine imaging in naïve ferret V1 reveals ocular class diversity

(a) Sparse labeling of neurons with GCaMP6s. Standard deviation projection of *in-vivo* images of a soma (top, z-projection) and subset of its dendritic branches with spines (bottom, time-projection of 1000 frames). Scale bars are 50 um (top, soma) and 5 um (bottom, branches) **(b)** Responses of three example spines belonging to the cell in (a) to drifting gratings presented to the contra and ipsi eye. Shown is the mean (black) and standard deviation (gray) across 2.5 seconds for each stimulus. The spines classify as monocular contra (spine 1), monocular ipsi (spine 2), and binocular (spine 3). The scale bar on the right is $50\%\Delta F/F_o$ for all three spines. **(c)** Peak amplitude mean (black dots) and standard deviation (lines) for the respective spines in orientation space. The preferred orientation of the soma for each eye condition ("soma pref") is indicated as a gray bar. **(d)** Proportions of all responsive spines sampled from binocular cells for each ocular class. **(e)** Proportions of spines from each ocular class for each binocularly responsive cell ($n = 25$). From left to right, an increasing number of responsive spines were sampled ($n_{min} = 13$, $n_{max} = 103$). Same color code as in (d).

of ipsi response:0.01 ± 0.39; rank sum test: $p < 0.0001$, effect size: 0.4), yet lower than that for experienced animals (Fig.3.3b; median = 0.39; IQR= 0.66; $n = 3011$, rank sum test: $p < 0.0001$). Especially spines with congruency values close to 1 are infrequent in the naïve state and the proportion of binocular spines of congruency > 0.8 triples from 5.2% to 15.3%. Consequently, using the cutoff of 0.5 previously used for experienced animals, only 25.3% (141/558) of binocular inputs classify as congruent ($r_{C-I} > 0.5$). On a cell-by-cell level, this equates to the proportion of binocular congruent inputs increasing 2-fold after eye opening (mean ± s.d.: naïve: $14 \pm 7\%$; experienced: $27 \pm 16\%$; rank sum test: $p = 0.0014$). It is important to note that we split the population to illustrate biases within the binocular population that correlate with congruency, and these will become apparent later on. The precise cutoff of 0.5 was chosen for consistency and comparability of the naïve and the experienced state. Wherever reasonable, we provide a quantification with the continuous measure of congruency. In short, we find that binocular inputs are substantially less congruent and mirror the less aligned state of V1 at eye opening.

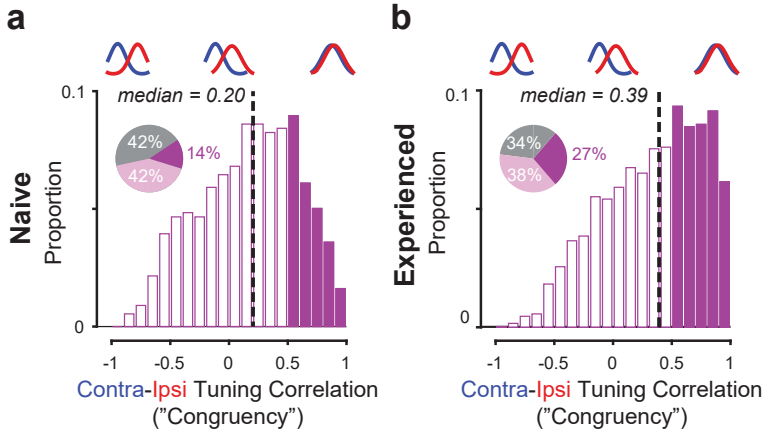

Figure 3.3.: Congruency of binocular inputs increases after eye opening
(a) Distribution of congruency (see Methods) for all binocular spines ($n = 558$) in visually naïve animals. Tuning curves above illustrate contra (blue) and ipsi (red) eye responses that would yield the different values of congruency. Spines with congruency values > 0.5 qualify as "congruent" (filled bars), spines with < 0.5 congruency are referred to as "noncongruent" (open bars). Inset shows the overall proportions of spines imaged that classify as monocular (gray), binocular noncongruent (light pink), and binocular congruent (dark purple). **(b)** Same as in (a) but for binocular spines ($n = 3011$) in visually experienced animals.

Congruency of the binocular input network predicts somatic congruency

While the binocular network is less congruent than in the experienced, it still provides the majority of inputs to a cell at this early developmental stage. Thus, we wondered whether the binocular input network plays the same role as later on where input congruency predicts somatic congruency.

We find that, indeed, the higher the median congruency of all binocular inputs to a cell, the more congruent the somatic response (Fig.3.4a; one-sided Spearman's correlation: $r = 0.62$, $p = 0.003$). In contrast, the proportion of monocular contra and ipsi inputs did not predict somatic congruency (Fig.3.4b; two-sided Spearman correlation: contra: $r = 0.03$, $p = 0.89$; ipsi: $r = 0.33$, $p = 0.18$). Both results recapitulate previous findings in experienced animals (Fig.3.4c-d).

These findings provide evidence that the same principle holds across both stages of development. Namely, the balance of binocular congruent and noncongruent inputs predicts somatic congruency. In contrast, the number of monocular inputs does not appear to play a crucial role. The key difference across development is the lower levels of congruency found at the level of spines and somas, suggesting a causal relationship.

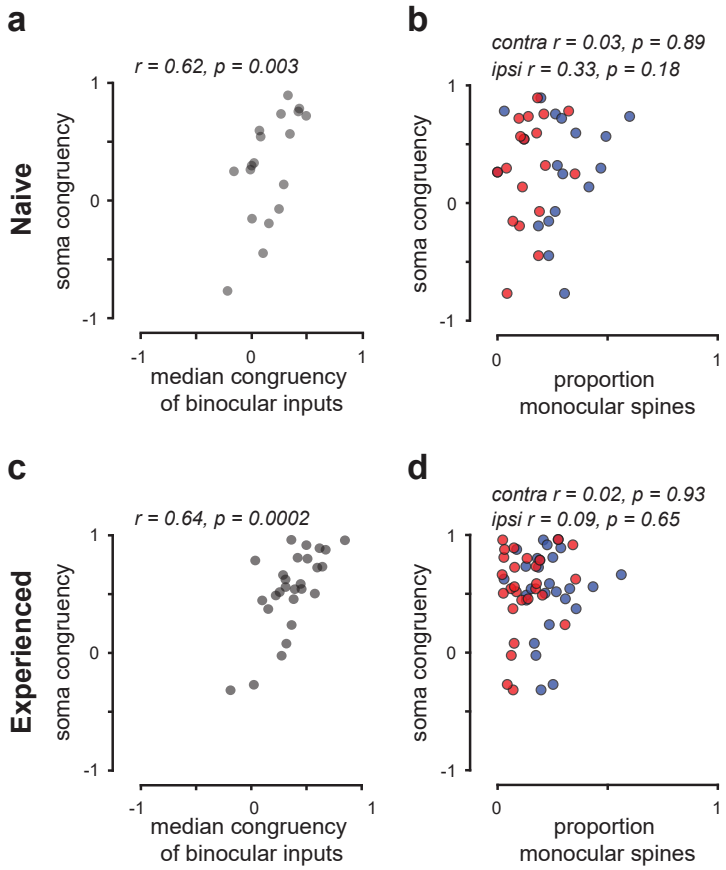

Figure 3.4.: Congruency of binocular inputs predicts somatic congruency
(a) Relationship of the median congruency of all binocular inputs on a cell and somatic congruency in visually naïve animals. One-sided Spearman's correlation. **(b)** Relationship between the proportion of monocular contra (blue) and monocular ipsi (red) spines converging onto a cell and somatic congruency. Each data point is from a single cell recorded in visually naïve animals. Two-sided Spearman's correlation. **(c-d)** Same as in (a-b) but for visually experienced animals.

Spine density increases after eye opening

How may a neuron increase its proportion of binocular congruent inputs? It could be the results of either converting binocular noncongruent inputs to congruent ones (presynaptic plasticity), or by increasing the number of synapses with presynaptic binocular congruent cells (structural plasticity). Previous reports in ferret have described increases in axonal spread following eye opening [33]. Studies in various other species and cortical areas complement these presynaptic changes with postsynaptic changes and report heightened dendrite and spine structural plasticity during experience driven learning [265, 266, 269, 270]. A functional bias in the addition of excitatory synapses could be a simple yet efficient way to increase the proportion of binocular congruent inputs.

During *in-vivo* imaging, dendritic branches in the naïve animal visually appeared to have less dendritic spines compared to the experienced state. To assess this more carefully and measure if and how much dendritic spine density increases after eye opening, we used post-hoc airy-scan imaging of L2/3 neurons and their respective dendrites.

Airy-scan imaging confirms that the overall density of dendritic spines increases substantially by around 42% after eye opening (Fig.3.5; naïve: median= 0.35, IQR = 0.15; experienced: median= 0.50, IQR = 0.38; rank sum test: $p = 0.0002$). Yet, there is diversity within and across cells of the same developmental stage.

Notably, if to the above-described proportions of binocular and monocular inputs of naïve animals only binocular inputs would be added to achieve such higher density, the resulting proportion of binocular inputs (69%) would be close to what is found in experienced animals (65%). Moreover, to match the proportion of binocular congruent inputs observed in experienced animals, only around 50% of these binocular inputs would have to be congruent. Dendrite length may also increase during this period and could act as a multiplicative factor for the number of spines that a neuron receives. In that case, a weaker bias for binocular (congruent) inputs would be sufficient to match the experienced proportions. Importantly, how these changes in spine density translate to active, functionally relevant synapses is not clear. Nevertheless, this structural change could serve as a substrate for an increase in binocular congruent inputs. This does not exclude the opportunity of presynaptic functional changes further boosting input congruency.

3.3.2. How are somatic changes supported by their synaptic inputs?

An increase in binocular congruent inputs is likely underlying the improved alignment at the somatic level. Such an increase in numbers of one input subpopulation could affect the relative contributions of all inputs to the somatic response.

There are other factors besides numbers that could alter the relative impact of input subpopulations such as orientation selectivity and orientation preference variance within a population (see Fig.A.2a), however, we find no evidence for these to be shifting the relative contribution of different input classes over development (A.2).

Thus, we wondered whether the lower numbers of binocular congruent inputs in the

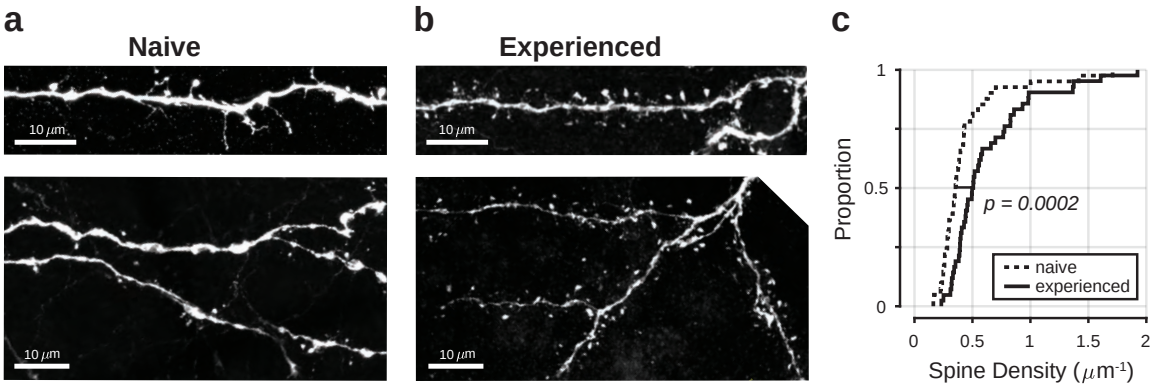

Figure 3.5.: Post-hoc airy-scan imaging reveals spine density increase after eye opening
(a-b) Example standard deviation images of dendritic branches from L2/3 neurons in visually naïve (a) and experienced (b) animals. Scale bars are 10 µm. **(c)** Cumulative distribution plots of measure spine density for branch segments in naïve ($n = 102$ segments, age p28-30) and experienced ($n = 95$ segments, age p38-47) animals. Wilcoxon's rank sum test.

naïve animals could result in responses being supported by spines from other ocular classes. Specifically, by probing the relative impact of binocular congruent inputs on somatic output over development, we can distinguish two hypothesis about a growing binocular congruent network may be building responses aligned between the eyes: In one scenario, the binocular congruent inputs provide a response equally (mis)matching somatic contra and ipsi eye response, in other words a middle ground. Increasing numbers of binocular congruent inputs that further support this middle ground preference, would boost their influence and translate to a symmetric convergence of somatic contra and ipsi preference towards the middle ground preference and improve binocular alignment. Alternatively, binocular congruent inputs could display asymmetric mismatch in the naïve state and more closely match one eye than the other. With increasing numbers of binocular congruent inputs, the somatic response more mismatched with their input would undergo larger changes to ultimately match the binocularly aligned preference conveyed by binocular congruent inputs. At the somatic level, orientation preference for each eye would exhibit different orientation preference stability over development.

Binocular congruent inputs are more specific to the somatic contra than ipsi output

To test these two hypotheses, we examined how inputs from different ocular classes functionally relate to the somatic output as a proxy for how much they each may contribute to somatic contra and ipsi eye orientation preference. In particular, we measured how closely the orientation preference of dendritic spines matches that of the respective soma ("soma mismatch") for the contra and ipsi eye separately (Fig.3.6a). Spines with a similar orientation preference as the soma (highly specific) are likely contributing to the output of the cell, whereas more mismatched (less specific) inputs

are presumably not eliciting spiking activity when they are active. Comparing soma mismatch for inputs from different ocular classes can give insights about how much monocular and binocular inputs may be contributing to the somatic contra and ipsi preference. As in our previous analysis, we only considered the orientation preference of spine responses with OS > 0.1.

	Median (IQR)	Binocular congruent	Binocular noncongruent	Monocular
	Contralateral responses			
Binocular congruent	16.0 (32.2)	-	p = 0.20	p = 0.24
Binocular noncongruent	19.4 (31.7)	-	-	p = 0.003
Monocular	12.8 (21.8)	-	-	-
	Ipsilateral responses			
Binocular congruent	27.1 (28.8)	-	p = 0.60	p = 0.93
Binocular noncongruent	23.6 (37.3)	-	-	p = 0.08
Monocular	26.6 (47.7)	-	-	-

Table 3.1.: Comparison of soma mismatch (in degree) across ocular classes or dendritic spines.
All statistical tests are Wilcoxon's rank sum test.

With respect to the somatic contra eye preference, monocular contra inputs match best (median = 12.8°), closely followed by binocular congruent and then noncongruent inputs (see Table 3.1, Fig.3.6b). Binocular noncongruent inputs are statistically less well matched to the soma than monocular contra inputs (rank sum test: $p = 0.003$). Yet, within the binocular input population soma mismatch is not correlated with their congruency (two-sided Spearman's correlation: $r = -0.08$, $p = 0.13$) suggesting equal levels of specificity and impact to somatic output of all binocular, orientation selective spines.

In contrast to the high specificity for contra eye responses, ipsi eye responses from monocular and binocular inputs were significantly less specific to the somatic ipsi output (contra-ipsi comparison, rank sum test: monocular: $p < 0.0001$, paired signed rank test: binocular congruent: $p = 0.003$, binocular noncongruent: $p = 0.05$). Among the three ocular classes, none exhibited higher specificity than the others (see Table 3.1) and for binocular inputs there is no correlation of congruency with mismatch (two-sided Spearman's correlation: $r = -0.05$, $p = 0.42$). This suggests that also the somatic ipsi eye response is a result of all its orientation selective inputs rather than a subset of inputs strongly affecting the output.

While soma mismatch is similar across inputs from different ocular classes, we observe a strong difference in mismatch between the eyes. The contra eye response appears supported by a highly specific input network, whereas ipsi inputs exhibit orientation preferences not as closely matched with the soma. This discrepancy in the naïve is particularly noteworthy for the binocular congruent inputs for two reasons. First, these inputs are per definition well aligned between eyes, but they do not generate the naïive levels of contra-ipsi alignment observed at the soma. Instead, their

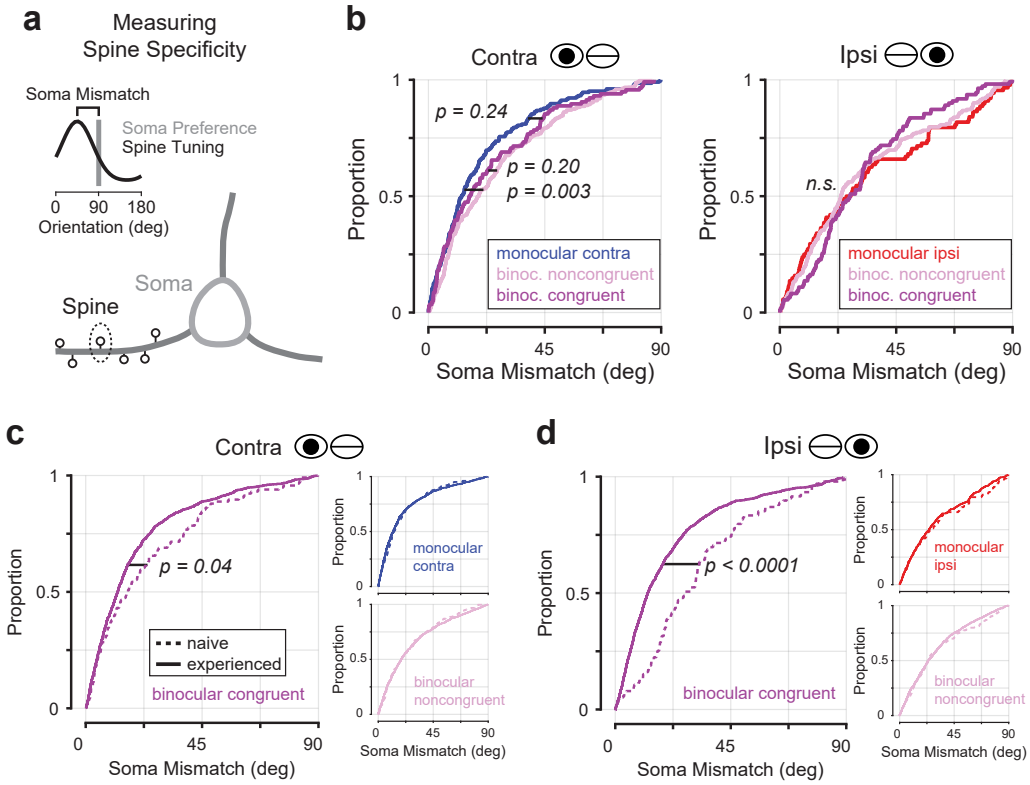

Figure 3.6.: Binocular congruent inputs reduce soma mismatch to the ipsi eye after eye opening

(a) Specificity is measured as mismatch in orientation preference of a given spine and the respective soma. **(b)** Cumulative distribution plots of spines' soma mismatch for contra (left) and ipsi (right) eye stimulation for monocular, binocular noncongruent, and binocular congruent spines in visually naïve animals. All statistical tests are Wilcoxon's rank sum test. **(c-d)** Cumulative distribution plots of soma mismatch for spines from different ocular classes in naïve and experienced animals for the contra (c) and ipsi (d) eye.

influence may be outweighed by other ipsi-responsive inputs resulting in somatic misalignment. Second, in experienced animals, this asymmetry is very small and binocular congruent inputs match contra and ipsi eye somatic preference closely (median mismatch: contra: 12.2°; ipsi: 12.6°, rank sum test: contra vs. ipsi: $p = 0.06$, effect size $= -0.05$) indicative of their role in driving an ipsi eye response of the soma that is aligned to the contra eye response. This developmental difference in ipsi specificity, exclusively for the binocular congruent, has an important implication: which synaptic subpopulations most strongly supports the ipsi eye response changes. Namely, the ipsi response becomes increasingly supported by matching binocular congruent inputs (Fig.3.6d; binocular congruent median mismatch for ipsi: naïve: 27.1°; experienced: 12.6°; rank sum test: $p < 0.0001$). On the other hand, the synaptic subpopulations underlying the contra response remain largely the same, yet binocular congruent inputs marginally improve their specificity (Fig.3.6c; binocular congruent mismatch for contra: naïve: 16.0°; experienced: 12.2°; rank sum test: $p = 0.04$). This distinction in development between the eyes could be a signature of the different degree of stability for somatic contra and ipsi eye responses.

The decrease in mismatch between soma and binocular congruent inputs for the ipsi eye could happen via two ways: 1) binocular congruent inputs shift their preference towards the somatic ipsi eye output or 2) somatic output shifts towards the preference conveyed by the binocular congruent input population. The data suggest that over development, binocular congruent inputs do not sacrifice their contra specificity to match ipsi eye output. At the same time, somatic contra-ipsi mismatch decreases (median mismatch: naïve: 22.4°; experienced: 14.8°). These two findings combined make the hypothesis of the soma shifting towards binocular congruent preference the more likely dominant developmental trajectory. In this scenario, the contra eye preference of a neuron and its input population could serve as an anchor or instructor to which the ipsi response is aligned. In other words, alignment could be viewed as the reshaping of the ipsi eye response instructed by a maturing and growing binocular congruent network.

3.4. Discussion

Most visual cortical neurons respond to stimulation through either eye, yet prior to visual experience, the orientation preference for each eye often differs significantly [4]. Only with visual experience, responses to each eye become increasingly similar and thereby improve binocular orientation preference alignment. While the binocular input network drives binocular alignment in neurons of experienced animals, the synaptic basis for naïve responses has remained unclear.

Here, we investigated the properties of the dendritic spines of individual L2/3 neurons in V1 of visually naïve ferrets to establish the state of binocular and monocular synaptic inputs to individual neurons prior to the onset of experience. By comparing the synaptic organization in visually naïve and experienced animals we hoped to gain new insights into the synaptic changes that lead to improved binocular alignment after eye opening.

We find that in naïve animals, individual neurons receive monocular (only respond-

ing to one eye) and binocular (responding to both eyes) inputs. Binocular inputs were marginally less frequent and overall exhibited lower congruency (contra-ipsi tuning correlation) than in the experienced. Nevertheless, the median congruency of binocular inputs to a cell predicted somatic congruency, suggesting a consistent role of the binocular presynaptic network in driving the degree of somatic alignment across development. The increase in spine density that we observe after eye opening could be a substrate for raising the numbers of binocular inputs, especially those that are highly congruent, and thereby enhancing somatic alignment.

Furthermore, the increase in binocular congruent inputs appears likely to drive enhanced somatic binocular alignment by altering the composition of synaptic inputs that determine the somatic responses to the ipsilateral eye. In the naïve animal, congruent inputs only match the somatic contra eye preference closely, but not the ipsi eye preference. This suggests that, early on, congruent inputs mixed with all the other synaptic inputs to the cell do not have enough weight to drive an ipsi eye somatic response that is aligned to the contra eye. This is in contrast to later in development when there is a greater percentage of binocular congruent spines and these inputs closely match the somatic preference for both eyes, thereby supporting binocularly aligned responses of the soma. Further support for the selective reorganization of the synaptic drive contributing to the ipsilateral somatic response comes from the fact that other input classes (monocular, binocular non-congruent) appear relatively stable in the degree to which they match the contra and ipsilateral eye somatic responses across development. We conclude that inputs from the binocular congruent network play a crucial role throughout development and propose that the binocular alignment process is predominantly the result of the ipsi eye somatic response being transformed by an increase in synaptic inputs from the binocular congruent network.

Differences in contra and ipsi responses and their development

We find distinct differences in the synaptic input populations underlying contra and ipsi eye responses which could have several implications for somatic properties. Somatic contra eye responses are supported by highly specific inputs, whereas inputs with ipsi eye responses exhibit less specificity. Consequently, considering trial-to-trial variability of neurons and synaptic inputs, the aggregate orientation preference may differ across trials and so may the somatic response [46]. This would result in less reliable and less orientation selective responses of the neuron for the ipsi eye specifically. Testing how trial-by-trial activity of contra and ipsi eye responses influences somatic tuning reliability would require sampling a large population of synaptic inputs and the somatic response. Technical advances allowing fast sampling in 3D of the dendritic tree would be needed to address this. Yet, it is curious to note that across the literature, several reports indicate that responses in V1 to the ipsi eye appear less developed than the contra responses early in development [4, 7, 25]. Anatomically, projections from the contra eye to ferret V1 are more pronounced than ipsi projections [93] and accordingly, ocular dominance is biased for the contra eye [62]. With respect to orientation selectivity a difference between the eyes is apparent as well. Orientation

discriminability is lower for ipsi responses than for contra responses in naïve ferret V1 [4].

Distinct changes of contra and ipsi responses of neurons have also been reported during development. In mouse V1, binocularly matched responses often achieved by monocular, selective neurons gaining a matched response to the other eye [6]. Markedly, the added response is more frequently the ipsi eye. Similarly, in the cat, the ipsi eye responses appear delayed in their development and increase orientation selectivity several days later than contra eye responses. Studies on binocular alignment rarely probe responses to binocular stimulation, yet work in the ferret finds a unique role of the binocular response. Binocular stimulation reveals a third response, which is distinct from the two monocular responses and not a linear sum of both of them [4]. Chronic wide-field imaging allowed tracking of network scale representations of orientation and reveals that monocular representations converge towards the binocular representation, as it was found to be the most stable. Moreover, the binocular representation, while not being a linear sum of the monocular representations, tended to share more similarity with the contra than ipsi representation. Accordingly, the ipsi representation tends to undergo a bigger change over development suggesting neurons may exhibit less orientation preference stability for the ipsi than the contra eye.

In line with these findings, our data indicate that the somatic response to ipsi stimulation is also likely to undergo a larger change than somatic response to contra stimulation over development. Comparisons of the synaptic makeup for somatic contra and ipsi eye responses over development, show that for the contra eye responses only a modest change occurs while the ipsi eye response is restructured and increasingly supported by binocular congruent inputs that align the ipsi to the contra eye response.

An efficient strategy for binocular alignment

Our data suggest that increasing numbers of binocular congruent inputs underlie improved somatic alignment primarily through remodeling of the ipsi eye somatic response. This appears to be not only a simple but also an efficient way to improve alignment. Neurons do not need to reconstruct their entire synaptic input populations. Rather, the increase of binocular congruent inputs could be sufficient to pull the ipsi eye response towards alignment. Monocular and binocular noncongruent inputs would have to undergo little change, thereby minimizing energetic cost of structural plasticity throughout the neuron. Besides this being an efficient strategy for improving alignment, it is possible that monocular ipsi and binocular noncongruent inputs serve a function not captured by our stimulus space or question and maintaining them could be valuable for some other reason. Assigning one subpopulation of inputs the main role for a feature, like binocular congruent inputs for alignment, is another way to efficiently use dendritic territory for a variety of computations performed by V1 neurons.

Potential origins of naïve levels of congruency

While the binocular input network is substantially less congruent in the naïve than in experienced state, congruency is still above chance. Similarly, contra-ipsi orientation

preference match observed across a population of L2/3 neurons at eye opening was better than random suggesting some developmental aspect prior to visual experience that biases the network for weak alignment. Spontaneous retinal waves have been reported to exhibit some synchronicity across retinas [301] and could provide an initial bias for cortical networks to be correlated in responses between eyes. Moreover, experience through closed eyelids is diffuse, yet can be sufficient to elicit orientation selective responses [67] and therefore could initiate an experience dependent alignment process that is eventually refined by highly structured, patterned experience after eye opening.

Possible functions of non-congruency

Initial low levels of congruency and orientation match may seem like a reflection of immaturity, or unfinished development. Yet, diversity in binocular congruency may be a feature that could support flexibility in accommodating natural sources of variability in the biology of eye alignment. Animal-to-animal variability in eye position and torsion may lead to different cells serving as the congruent population. Providing a diverse pool of neurons by eye opening could ensure that sufficient neurons exhibit an "aligned" responses that can then instruct the remaining network to adjust to a specific contra-ipsi configuration. The flexibility of a cortical network could be a critical factor for creating an ultimately coherent percept for each animal with its unique physical layout.

Notably, whether a neuron is congruent or noncongruent could change over development. The animal's head is still growing significantly, and so could eye positioning. Thus, our measurement may be a mere snapshot of what "aligned" means at this stage or for the current eye positions.

How aligned not only the experienced but the *mature* state is, is not clear. Previous work studying binocular alignment of cell populations has only assessed alignment in ferrets up to one week after eye opening since by then many features have assumed their putative mature form unless disturbed by abnormal experience [4, 62, 160]. The study on the synaptic layout in experienced animals included cells from ferrets up to 60 days old and these were not significantly more matched than neurons from younger animals suggesting alignment does not improve indefinitely. While it is it not known what degree of alignment is present in fully grown ferrets, other work in adult, i.e., mature monkeys and cats shows a significant fraction of cells with different orientation preferences for each eye, indicating V1 never becomes perfectly congruent [1, 3]. This could be deliberate as there is indeed a potential role for noncongruent responses. Viewing conditions where head tilt leads to eye torsion, a slant in depth, or motion in depth, all these result in images on each retina with different edge orientation and noncongruent inputs and cells could be relevant in signaling in these situations [3, 188, 302].

Potential sources of synaptic inputs

The diversity in the properties and roles of excitatory inputs to L2/3 neurons in V1 raises a question about the source of these inputs (see 1.5.3). Knowing the origin of the

synaptic partners could help to distinguish differential contribution of different circuit components for binocular integration. Based on anatomical studies, neurons residing in layer 4 (L4) and L2/3 are likely the most numerous and strongest presynaptic partners [116, 119, 134, 135]. Besides, some direct feedforward, thalamic projections to L2/3 exist [93, 303]. Feedback projections from higher order visual cortices and callosal projections from the other hemisphere are potential candidates for excitatory synaptic inputs [209, 222]. The precise proportions of connections provided by each source are not known and difficult to estimate. The functional properties such as ocular dominance of the different areas can also only allow limited insight as to if and which signals they may provide. Thalamic projections are plausible providers of monocular input, feedback projections are most likely binocular [184, 185]. L4 and callosal inputs could offer a mix of monocular and binocular inputs, but L4 neurons at the naïve stage appear not as orientation selective as L2/3 neurons on the other hemisphere [297]. Proximal L2/3 neurons are a likely contributor of binocular, selective inputs and could therefore form a recurrent network that is heavily involved in determining the somatic alignment of their postsynaptic targets. In line with this hypothesis is the expansion of L2/3 horizontal connections that could lead to the observed increase in binocular inputs after eye opening [33, 35]. Binocular alignment could then be a result of an increasingly strong connected recurrent network. Ultimately, to further support this idea, additional experiments are required. Rabies-tracing or other retrograde labeling could provide an estimate on the proportion of inputs provided by presynaptic partners and elucidate a more accurate understanding of L2/3 connectivity [304]. Retrograde labeling with a calcium sensor would allow to probe their functional properties, too [305]. Besides, recent advancements using a combination of *in-vivo* functional imaging and *post-hoc* source identification [306] could help to dissect the source as well as the functional properties of synaptic inputs. Lastly, to test the contribution and necessity of presynaptic partners, *in-vivo* imaging of somata and dendritic spines before and after selective manipulation of putative input sources could prove useful.

Chronic imaging for differentiating synaptic plasticity mechanisms

We find the congruency of the binocular input network is the key factor for somatic alignment in visually naïve and experienced animals. How the binocular congruent input network increases its influence on somatic output over development to enhance binocular alignment could be the consequence of three distinct, not mutually exclusive mechanisms.

First, dendritic spines could change their synaptic strength over time. This is often referred to as functional plasticity as the efficacy of the conveyed signal is altered. Data in experienced animals suggests that synaptic strength is not employed by the binocular congruent network, since ultrastructural correlates of this property is comparable across monocular, binocular congruent, and binocular noncongruent spines (A.1, [296]). It is therefore unlikely that this is a mechanism used by V1 to enhance binocular congruent drive. Instead, we find strength in numbers of binocular congruent inputs to be key. This leaves two further potential mechanisms to be explored.

Neurons may refine their synaptic connectivity via selective addition and deletion of binocular congruent and binocular noncongruent spines, respectively (structural plasticity). Such functional biases in spinogenesis and pruning would lead to a net gain of binocular congruent inputs. While our data indicate a strong gain of new dendritic spines by L2/3 cells after eye opening, whether this increase displays a bias for binocular congruent spines and thereby increases their proportion on the total synaptic population, is unclear.

Alternatively, no structural synaptic change with respect to strength or numbers need to occur. Instead, maintained, stable spines, may change the information they convey because of the presynaptic partner altering its response properties (presynaptic changes). Chronic imaging of L2/3 neurons following eye opening confirms that increased binocular alignment in the ferret is due to single cells staying responsive to both eyes and changing their monocular responses to become increasingly aligned [4]. This is in contrast to mouse V1, where binocular alignment was in part achieved by cells dropping out or joining the population of binocularly responsive neurons and functional biases within these transitioning cell groups leading to better alignment of binocular neurons overall [6]. Since L2/3 neurons are a major source of inputs to other L2/3 neurons, changes in presynaptic neurons are almost certainly contributing in ferret V1 to increasingly binocular congruent information received by postsynaptic neuron at dendritic spines.

To resolve the specific contribution of these two mechanisms to increased congruency in the synaptic input to L2/3 cells, we must follow structural changes and changes in functional properties of spines chronically following the onset of visual experience. Only by chronically tracking the response properties of spines that are maintained, and those that are lost and added, it would be possible to estimate the relative contribution of structural plasticity and presynaptic changes on the binocular alignment process.

A putative mechanism for the increase of binocular congruent inputs via structural plasticity

While we do not know whether the addition and pruning of dendritic spines (structural plasticity) is functionally biased, there is a potential mechanism supporting this hypothesis. Visual experience after eye opening is mostly binocular. Therefore, highly similar signals will be sent from each retina and passed along to cortex. Binocular neurons with orientation preferences matching closely what is conveyed through each eye (congruent) would be preferentially activated by binocular experience. Previous work in cats shows supportive evidence for this. When the two monocular receptive fields overlap perfectly during binocular stimulation, the resulting response will be larger than the two separate monocular responses, also called “binocular facilitation” [2, 200, 201, 202].

Increased activity levels of binocular congruent cells and reduced activity of noncongruent cells during binocular experience could lead to long term potentiation (LTP) and long term depression across the cortical network. Studies have shown that high frequency synaptic activation and LTP is associated with new spine formation in the vicinity of activated synapses and duplicating spines reaching the same axonal bouton

[269, 307, 308, 309]. Moreover, in a developmental period where new synapses are frequently formed frequently, activity is relevant for selectively stabilizing dendritic spines [310]. In sum, these effects could results in and increase in binocular congruent synaptic inputs and ultimately increase binocular alignment within the network.

4. Conclusion

The brain has to integrate signals from various sources to create a percept of the world before it can act within and upon it. Binocular vision is an accessible way to study coherent signal integration since both eyes convey signals about the same image from slightly different perspectives from which the brain generates a three-dimensional yet unified representation. In carnivores and primates, primary visual cortex (V1) is where right and left eye signals converge for the first time. Neurons in V1 then combine these signals to create a representation of edge orientation that remains constant whether the stimulus is perceived through either eye (binocularly aligned).

Across species, binocular alignment requires experience to mature, highlighting the necessity of sensory input to produce a coherent representation from signals provided by different organs. This developmental process has been studied at the level of network scale and single-cell responses. Yet, how individual V1 neurons shape their synaptic inputs to mix signals from the two eyes into a binocularly aligned representation has remained unknown. Only by studying the synaptic scale and disentangling the contribution of individual synaptic inputs, we can gain insights into the binocular alignment process over development. *In-vivo* two-photon functional imaging of dendritic spines and the respective soma of neurons in V1 has allowed us to examine the information conveyed by excitatory synaptic inputs that ultimately drive somatic output in visually naïve and experienced animals.

Synaptic inputs are diverse

Probing the functional properties of dendritic spines has revealed diversity in synaptic inputs at both stages of development. Diversity has been observed for several features by know and could be important for cortical computation [46, 291, 311]. Here, the diversity of ocular classes is highly relevant for binocular alignment: neurons in layer 2/3 (L2/3) of ferret receive not only monocular inputs (responsive only to one eye), but the majority of inputs are binocular (responsive to both eyes). Considering that upstream of V1, neurons are highly monocular, this hints at the abundance of intracortical, binocular connections in L2/3 and their potential strong influence on somatic responses. Despite monocular inputs being less frequent than binocular input, additional properties need to be evaluated to resolve the relative contribution of each group and weigh on the contrasting hypotheses of feedforward driven monocular convergence vs. recurrent binocular interaction.

Numbers of binocular congruent inputs are key for driving binocular alignment

We find from several lines of analyses that the binocular, not the monocular inputs are the key driver for binocular alignment in visually naïve and experienced animals. In particular, the overall congruency (contra-ipsi tuning correlation) of the binocular network predicted somatic congruency. In other words, the larger the proportion of binocular congruent inputs (those that convey responses that are highly aligned between the eyes) to a neuron, the more congruent the somatic response.

In the experienced animals, we were able to further evaluate the role of numbers of inputs exhibiting a certain feature. This concept has gained renewed attention due to recent work on orientation tuning [288]. Analysis of ultrastructure to estimate synaptic weight of dendritic spines imaged *in-vivo* revealed that strength in synaptic weight is not a mechanism that binocular congruent inputs employ to enhance their impact on somatic output. Instead, simulations of trial-by-trial activity of input populations showed that binocular congruent inputs exert a disproportionate impact by strength in numbers active for specific stimuli. Thereby, while on average constituting only around 30% of inputs to a neuron, their combined, highly specific, activity allowed them to drive binocularly aligned responses of the soma.

Not only in visually naïve and experienced animals is the critical role of numbers apparent. Comparing both stages shows a drastic increase of binocular input congruency, translating to a roughly two-fold increase in the proportion of binocular congruent inputs throughout the network after eye opening. This increase of binocular congruent inputs likely leads to the higher levels of congruency of somatic response following visual experience.

Lastly, the increased proportion of inputs that are binocular congruent appears to have distinct effects on how synaptic inputs constitute the somatic output.

Contra and ipsi eye responses have distinct synaptic compositions and development

At both developmental stages, the synaptic composition for somatic responses to contra and ipsi stimulation differs. For contra eye responses, monocular contra and binocular congruent inputs closely match somatic output preference, in the naïve as well as in the experienced animal. For ipsi eye responses, the synaptic contribution of different subpopulations is distinct for both developmental stages. In naïve animals, all synaptic inputs match the somatic output for the ipsi less than the output for the contra eye. In experienced animals, only binocular congruent inputs closely match the somatic preference for the ipsi eye.

From this we draw two conclusions. First, the synaptic composition specifically for the ipsi eye changes with visual experience. Prior to experience, for the ipsi eye response the impact of comparably rare binocular congruent inputs is outweighed by binocular noncongruent and monocular ipsi inputs. Later, the ipsi eye response becomes increasingly supported by binocular congruent inputs resulting in better binoc-

ular alignment of the ipsi. Second, in experienced animals, aligned responses rely on binocular congruent inputs shaping the ipsi response, not monocular ipsi inputs as would be predicted from the monocular convergence hypothesis.

In short, the response of the soma becoming increasingly aligned between eyes after eye opening appears to be predominantly a result of the binocular congruent network reconstructing the ipsi eye response to become aligned to the contra eye response.

Recurrent networks for visual processing

Overall, our results do not support the hypothesis of two converging monocular input streams supporting binocularly aligned response in L2/3 of ferret V1. Instead, the binocular inputs and their degree of alignment (congruency) plays a critical role in driving binocular alignment. While this does not rule out monocular convergence to occur elsewhere, layer 4 neurons for instance, it highlights how binocular aligned responses can be generated by neglecting monocular inputs, and instead rely on binocular inputs that enhance their impact by a variety of properties.

Anatomical and functional properties of the ferret visual system make horizontal, recurrent connections within L2/3 a likely source of binocular inputs. While initially neglected in many models, recurrent connectivity in V1 has gained increasing attention and recognition for its role in orientation selectivity and orientation maps [38, 41, 42, 43, 159]. Since visual scenes are largely constituted from continuous edges or structures, this tight interconnectedness can be useful for connecting functionally related neurons representing neighboring parts of the visual field. Unsurprisingly, in machine learning models, recurrent networks have gained popularity for applications that require temporal context integration such as video encoding and captioning [312, 313, 314]. Overall, recurrent network structures in machine learning as well as in the brain are increasingly recognized for their computational abilities and studying this further will almost certainly yield relevant insights in cortical and *in-silico* computations.

Bibliography

[1] Holly Bridge and Bruce G. Cumming. "Responses of Macaque V1 Neurons to Binocular Orientation Differences". In: *Journal of Neuroscience* 21.18 (2001), pp. 7293–7302. DOI: 10.1523/JNEUROSCI.21-18-07293.2001.

[2] D. H. Hubel and T. N. Wiesel. "Receptive fields, binocular interaction and functional architecture in the cat's visual cortex". In: *The Journal of Physiology* 160.1 (1962), pp. 106–154.2.

[3] Colin Blakemore, Adriana Fiorentini, and Lamberto Maffei. "A second neural mechanism of binocular depth discrimination". In: *The Journal of Physiology* 226.3 (1972), pp. 725–749. DOI: https://doi.org/10.1113/jphysiol.1972.sp010006.

[4] Jeremy T. Chang, David Whitney, and David Fitzpatrick. "Experience-Dependent Reorganization Drives Development of a Binocularly Unified Cortical Representation of Orientation". In: *Neuron* 107.2 (2020), 338–350.e5. DOI: 10.1016/j.neuron.2020.04.022.

[5] Bor-Shuen Wang, Rashmi Sarnaik, and Jianhua Cang. "Critical Period Plasticity Matches Binocular Orientation Preference in the Visual Cortex". In: *Neuron* 65.2 (2010), pp. 246–256. DOI: 10.1016/j.neuron.2010.01.002.

[6] Liming Tan et al. "Vision Changes the Cellular Composition of Binocular Circuitry during the Critical Period". In: *Neuron* 108.4 (2020), 735–747.e6. DOI: 10.1016/j.neuron.2020.09.022.

[7] Liming Tan, Dario L. Ringach, and Joshua T. Trachtenberg. "The Development of Receptive Field Tuning Properties in Mouse Binocular Primary Visual Cortex". In: *The Journal of Neuroscience* 42.17 (2022), pp. 3546–3556. DOI: 10.1523/JNEUROSCI.1702-21.2022.

[8] Liming Tan et al. "Vision is required for the formation of binocular neurons prior to the classical critical period". In: *Current biology : CB* 31.19 (2021), 4305–4313.e5. DOI: 10.1016/j.cub.2021.07.053.

[9] Guido T. Meijer et al. "Audiovisual Integration Enhances Stimulus Detection Performance in Mice". In: *Frontiers in Behavioral Neuroscience* 12 (2018).

[10] John Welhoff Todd. *Reaction to Multiple Stimuli*. Science Press, 1912. 78 pp.

[11] Barry E. Stein and M. Alex Meredith. "Multisensory Integration". In: *Annals of the New York Academy of Sciences* 608.1 (1990), pp. 51–70. DOI: 10.1111/j.1749-6632.1990.tb48891.x.

[12] E. I. Knudsen and M. S. Brainard. "Visual instruction of the neural map of auditory space in the developing optic tectum". In: *Science* 253.5015 (1991), pp. 85–87. DOI: 10.1126/science.2063209.

[13] Adele Diederich and Hans Colonius. "Crossmodal interaction in saccadic reaction time: separating multisensory from warning effects in the time window of integration model". In: *Experimental Brain Research* 186.1 (2008), pp. 1–22. DOI: 10.1007/s00221-007-1197-4.

[14] Barry E. Stein and Terrence R. Stanford. "Multisensory integration: current issues from the perspective of the single neuron". In: *Nature Reviews Neuroscience* 9.4 (2008), pp. 255–266. DOI: 10.1038/nrn2331.

[15] J. I. Nelson, H. Kato, and P. O. Bishop. "Discrimination of orientation and position disparities by binocularly activated neurons in cat striate cortex". In: *Journal of Neurophysiology* 40.2 (1977), pp. 260–283. DOI: 10.1152/jn.1977.40.2.260.

[16] R. Cagenello, A. Arditi, and D. L. Halpern. "Binocular enhancement of visual acuity". In: *Journal of the Optical Society of America. A, Optics, Image Science, and Vision* 10.8 (1993), pp. 1841–1848. DOI: 10.1364/josaa.10.001841.

[17] A S Hood and J D Morrison. "The dependence of binocular contrast sensitivities on binocular single vision in normal and amblyopic human subjects". In: *The Journal of Physiology* 540 (Pt 2 2002), pp. 607–622. DOI: 10.1113/jphysiol.2001.013420.

[18] J E Ross, D D Clarke, and A J Bron. "Effect of age on contrast sensitivity function: uniocular and binocular findings." In: *British Journal of Ophthalmology* 69.1 (1985), pp. 51–56. DOI: 10.1136/bjo.69.1.51.

[19] Jenny C.A. Read. "Binocular Vision and Stereopsis Across the Animal Kingdom". In: *Annual Review of Vision Science* 7.1 (2021), pp. 389–415. DOI: 10.1146/annurev-vision-093019-113212.

[20] Charles Wheatstone. "XVIII. Contributions to the physiology of vision. —Part the first. On some remarkable, and hitherto unobserved, phenomena of binocular vision". In: *Philosophical Transactions of the Royal Society of London* 128 (1997), pp. 371–394. DOI: 10.1098/rstl.1838.0019.

[21] B. C. Skottun and R. D. Freeman. "Stimulus specificity of binocular cells in the cat's visual cortex: ocular dominance and the matching of left and right eyes". In: *Experimental Brain Research* 56.2 (1984), pp. 206–216. DOI: 10.1007/BF00236275.

[22] Jonathan J. Nassi and Edward M. Callaway. "Parallel Processing Strategies of the Primate Visual System". In: *Nature reviews. Neuroscience* 10.5 (2009), pp. 360–372. DOI: 10.1038/nrn2619.

[23] D. H. Hubel and T. N. Wiesel. "Receptive fields of single neurons in the cat's striate cortex". In: *The Journal of Physiology* 148.3 (1959), pp. 574–591.

[24] Margaret I. Law, Kathleen R. Zahs, and Michael P. Stryker. "Organization of primary visual cortex (area 17) in the ferret". In: *The Journal of Comparative Neurology* 278.2 (1988), pp. 157–180. DOI: 10.1002/cne.902780202.

[25] M. C. Crair, D. C. Gillespie, and M. P. Stryker. "The role of visual experience in the development of columns in cat visual cortex". In: *Science (New York, N.Y.)* 279.5350 (1998), pp. 566–570.

[26] Rashmi Sarnaik, Bor-Shuen Wang, and Jianhua Cang. "Experience-Dependent and Independent Binocular Correspondence of Receptive Field Subregions in Mouse Visual Cortex". In: *Cerebral Cortex (New York, NY)* 24.6 (2014), pp. 1658–1670. DOI: 10.1093/cercor/bht027.

[27] Eric I. Knudsen. "Fused Binocular Vision is Required for Development of Proper Eye Alignment in Barn Owls". In: *Visual Neuroscience* 2.1 (1989), pp. 35–40. DOI: 10.1017/S0952523800004302.

[28] Mark T. Wallace et al. "Visual Experience Is Necessary for the Development of Multisensory Integration". In: *Journal of Neuroscience* 24.43 (2004), pp. 9580–9584. DOI: 10.1523/JNEUROSCI.2535-04.2004.

[29] Xize Xu, Jianhua Cang, and Hermann Riecke. "Development and binocular matching of orientation selectivity in visual cortex: a computational model". In: *Journal of Neurophysiology* 123.4 (2020), pp. 1305–1319. DOI: 10.1152/jn.00386.2019.

[30] Basabi Bhaumik and Nishal P. Shah. "Development and matching of binocular orientation preference in mouse V1". In: *Frontiers in Systems Neuroscience* 8 (2014). DOI: 10.3389/fnsys.2014.00128.

[31] Manula A. Somaratna and Alan W. Freeman. "A model for the development of binocular congruence in primary visual cortex". In: *Scientific Reports* 12.1 (2022), p. 12669. DOI: 10.1038/s41598-022-16739-6.

[32] D. O. Hebb. *The Organization of Behavior: A Neuropsychological Theory*. New York: John Wiley & Sons, Inc., 1949. 379 pp.

[33] Jeremy C. Durack and Lawrence C. Katz. "Development of Horizontal Projections in Layer 2/3 of Ferret Visual Cortex". In: *Cerebral Cortex* 6.2 (1996), pp. 178–183. DOI: 10.1093/cercor/6.2.178.

[34] K. S. Rockland. "Anatomical organization of primary visual cortex (area 17) in the ferret". In: *The Journal of Comparative Neurology* 241.2 (1985), pp. 225–236. DOI: 10.1002/cne.902410209.

[35] Edward S. Ruthazer and Michael P. Stryker. "The Role of Activity in the Development of Long-Range Horizontal Connections in Area 17 of the Ferret". In: *Journal of Neuroscience* 16.22 (1996), pp. 7253–7269. DOI: 10.1523/JNEUROSCI.16-22-07253.1996.

[36] Matthew B. Dalva and Lawrence C. Katz. "Rearrangements of Synaptic Connections in Visual Cortex Revealed by Laser Photostimulation". In: *Science* 265.5169 (1994), pp. 255–258. DOI: 10.1126/science.7912852.

[37] D. A. Nelson and L. C. Katz. "Emergence of functional circuits in ferret visual cortex visualized by optical imaging". In: *Neuron* 15.1 (1995), pp. 23–34. DOI: 10.1016/0896-6273(95)90061-6.

[38] P. Adorján et al. "A model for the intracortical origin of orientation preference and tuning in macaque striate cortex". In: *Visual Neuroscience* 16.2 (1999), pp. 303–318. DOI: 10.1017/S0952523899162114.

[39] R Ben-Yishai, R L Bar-Or, and H Sompolinsky. "Theory of orientation tuning in visual cortex." In: *Proceedings of the National Academy of Sciences of the United States of America* 92.9 (1995), pp. 3844–3848.

[40] A. P. Bartsch and J. L. van Hemmen. "Combined Hebbian development of geniculocortical and lateral connectivity in a model of primary visual cortex". In: *Biological Cybernetics* 84.1 (2001), pp. 41–55. DOI: 10.1007/s004220170003.

[41] Paul C Bressloff and Jack D Cowan. "A spherical model for orientation and spatial-frequency tuning in a cortical hypercolumn." In: *Philosophical Transactions of the Royal Society B: Biological Sciences* 358.1438 (2003), pp. 1643–1667. DOI: 10.1098/rstb.2002.1109.

[42] Ian K. Christie, Paul Miller, and Stephen D. Van Hooser. "Cortical amplification models of experience-dependent development of selective columns and response sparsification". In: *Journal of Neurophysiology* 118.2 (2017), pp. 874–893. DOI: 10.1152/jn.00177.2017.

[43] Sigrid Trägenap et al. *Experience drives the development of novel, reliable cortical sensory representations from endogenously structured networks*. 2022. DOI: 10.1101/2022.11.14.516507.

[44] Winifried Denk, James H. Strickler, and Watt W. Webb. "Two-Photon Laser Scanning Fluorescence Microscopy". In: *Science* 248.4951 (1990), pp. 73–76. DOI: 10.1126/science.2321027.

[45] Tsai-Wen Chen et al. "Ultrasensitive fluorescent proteins for imaging neuronal activity". In: *Nature* 499.7458 (2013), p. 295. DOI: 10.1038/nature12354.

[46] Daniel E. Wilson et al. "Orientation selectivity and the functional clustering of synaptic inputs in primary visual cortex". In: *Nature neuroscience* 19.8 (2016), pp. 1003–1009. DOI: 10.1038/nn.4323.

[47] Tania A. Seabrook et al. "Architecture, Function, and Assembly of the Mouse Visual System". In: *Annual Review of Neuroscience* 40.1 (2017), pp. 499–538. DOI: 10.1146/annurev-neuro-071714-033842.

[48] Nicholas J. Priebe and Aaron W. McGee. "Mouse vision as a gateway for understanding how experience shapes neural circuits". In: *Frontiers in Neural Circuits* 8 (2014). DOI: 10.3389/fncir.2014.00123.

[49] Carlotta Gilardi and Nereo Kalebic. "The Ferret as a Model System for Neocortex Development and Evolution". In: *Frontiers in Cell and Developmental Biology* 9 (2021), p. 1004. DOI: 10.3389/fcell.2021.661759.

[50] N Garipis and K.-P Hoffmann. "Visual field defects in albino ferrets (Mustela putorius furo)". In: *Vision Research* 43.7 (2003), pp. 793–800. DOI: 10.1016/S0042-6989(03)00015-4.

[51] U. Schmidt and Trude Pontenagel. "Untersuchungen zur Leistungsfähigkeit des Gesichtssinnes beim Frettchen, Mustela putorius f. furo L". In: 1979.

[52] G. Y. Wen, J. A. Sturman, and J. W. Shek. "A comparative study of the tapetum, retina and skull of the ferret, dog and cat". In: *Laboratory Animal Science* 35.3 (1985), pp. 200–210.

[53] Chang-Jin Jeon, Enrica Strettoi, and Richard H. Masland. "The Major Cell Populations of the Mouse Retina". In: *The Journal of Neuroscience* 18.21 (1998), pp. 8936–8946. DOI: 10.1523/JNEUROSCI.18-21-08936.1998.

[54] D. H. Rapaport and J. Stone. "The area centralis of the retina in the cat and other mammals: Focal point for function and development of the visual system". In: *Neuroscience* 11.2 (1984), pp. 289–301. DOI: 10.1016/0306-4522(84)90024-1.

[55] J. H. Chievitz. "Ueber das Vorkommen der Area centralis retinae in den vier höheren Wirbelthierklassen". In: Arch. Anat. Physiol. Lpz. Anat. Abs. Suppl. 1891.

[56] Jason M. Samonds, Veronica Choi, and Nicholas J. Priebe. "Mice Discriminate Stereoscopic Surfaces Without Fixating in Depth". In: *Journal of Neuroscience* 39.41 (2019), pp. 8024–8037. DOI: 10.1523/JNEUROSCI.0895-19.2019.

[57] U. C. Dräger. "Observations on monocular deprivation in mice". In: *Journal of Neurophysiology* 41.1 (1978), pp. 28–42. DOI: 10.1152/jn.1978.41.1.28.

[58] U. C. Dräger. "Receptive fields of single cells and topography in mouse visual cortex". In: *The Journal of Comparative Neurology* 160.3 (1975), pp. 269–290. DOI: 10.1002/cne.901600302.

[59] G. T. Prusky and R. M. Douglas. "Characterization of mouse cortical spatial vision". In: *Vision Research* 44.28 (2004), pp. 3411–3418. DOI: 10.1016/j.visres.2004.09.001.

[60] Cristopher M. Niell and Michael P. Stryker. "Highly Selective Receptive Fields in Mouse Visual Cortex". In: *The Journal of Neuroscience* 28.30 (2008), pp. 7520–7536. DOI: 10.1523/JNEUROSCI.0623-08.2008.

[61] Jihane Homman-Ludiye, Paul R. Manger, and James A. Bourne. "Immunohistochemical parcellation of the ferret (Mustela putorius) visual cortex reveals substantial homology with the cat (Felis catus)". In: *Journal of Comparative Neurology* 518.21 (2010), pp. 4439–4462. DOI: 10.1002/cne.22465.

[62] Naoum P. Issa et al. "The Critical Period for Ocular Dominance Plasticity in the Ferret's Visual Cortex". In: *Journal of Neuroscience* 19.16 (1999), pp. 6965–6978.

[63] Daniel L. Adams, Lawrence C. Sincich, and Jonathan C. Horton. "Complete Pattern of Ocular Dominance Columns in Human Primary Visual Cortex". In: *The Journal of Neuroscience* 27.39 (2007), pp. 10391–10403. DOI: 10.1523/JNEUROSCI.2923-07.2007.

[64] Gary G. Blasdel and Guy Salama. "Voltage-sensitive dyes reveal a modular organization in monkey striate cortex". In: *Nature* 321.6070 (1986), pp. 579–585. DOI: 10.1038/321579a0.

[65] Dagmar J. Vitek, Jeffrey D. Schall, and Audie G. Leventhal. "Morphology, central projections, and dendritic field orientation of retinal ganglion cells in the ferret". In: *The Journal of Comparative Neurology* 241.1 (1985), pp. 1–11. DOI: 10.1002/cne.902410102.

[66] Nathalie L. Rochefort et al. "Sparsification of neuronal activity in the visual cortex at eye-opening". In: *Proceedings of the National Academy of Sciences* 106.35 (2009), pp. 15049–15054. DOI: 10.1073/pnas.0907660106.

[67] Colin J. Akerman, Darragh Smyth, and Ian D. Thompson. "Visual Experience before Eye-Opening and the Development of the Retinogeniculate Pathway". In: *Neuron* 36.5 (2002), pp. 869–879. DOI: 10.1016/S0896-6273(02)01010-3.

[68] Donald H Edwards. "Neuroscience. Third Edition. Edited by Dale Purves, George J Augustine, David Fitzpatrick, William C Hall, Anthony-Samuel LaMantia, James O McNamara , and S Mark Williams." In: *The Quarterly Review of Biology* 81.1 (2006), pp. 86–87. DOI: 10.1086/504005.

[69] S. W. Kuffler. "Discharge patterns and functional organization of mammalian retina". In: *Journal of Neurophysiology* 16.1 (1953), pp. 37–68. DOI: 10.1152/jn.1953.16.1.37.

[70] W. Martin Usrey, John B. Reppas, and R. Clay Reid. "Specificity and Strength of Retinogeniculate Connections". In: *Journal of Neurophysiology* 82.6 (1999), pp. 3527–3540. DOI: 10.1152/jn.1999.82.6.3527.

[71] C. J. Shatz and P. A. Kirkwood. "Prenatal development of functional connections in the cat's retinogeniculate pathway". In: *Journal of Neuroscience* 4.5 (1984), pp. 1378–1397. DOI: 10.1523/JNEUROSCI.04-05-01378.1984.

[72] J. E. Morgan, Z. Henderson, and I. D. Thompson. "Retinal decussation patterns in pigmented and albino ferrets". In: *Neuroscience* 20.2 (1987), pp. 519–535. DOI: 10.1016/0306-4522(87)90108-4.

[73] I. D. Thompson and J. E. Morgan. "The development of retinal ganglion cell decussation patterns in postnatal pigmented and albino ferrets". In: *The European Journal of Neuroscience* 5.4 (1993), pp. 341–356. DOI: 10.1111/j.1460-9568.1993.tb00502.x.

[74] D. C. Linden, R. W. Guillery, and J. Cucchiaro. "The dorsal lateral geniculate nucleus of the normal ferret and its postnatal development". In: *The Journal of Comparative Neurology* 203.2 (1981), pp. 189–211. DOI: 10.1002/cne.902030204.

[75] MP Stryker and KR Zahs. "On and off sublaminae in the lateral geniculate nucleus of the ferret". In: *The Journal of Neuroscience* 3.10 (1983), pp. 1943–1951. DOI: 10.1523/JNEUROSCI.03-10-01943.1983.

[76] D. J. Price and J. E. Morgan. "Spatial properties of neurones in the lateral geniculate nucleus of the pigmented ferret". In: *Experimental Brain Research* 68.1 (1987), pp. 28–36.

[77] K. R. Zahs and M. P. Stryker. "The projection of the visual field onto the lateral geniculate nucleus of the ferret". In: *The Journal of Comparative Neurology* 241.2 (1985), pp. 210–224. DOI: 10.1002/cne.902410208.

[78] D. H. Hubel and T. N. Wiesel. "Integrative action in the cat's lateral geniculate body". In: *The Journal of Physiology* 155.2 (1961), pp. 385–398.1.

[79] J.H. Kaas, R.W. Guillery, and J.M. Allman. "Some Principles of Organization in the Dorsal Lateral Geniculate Nucleus". In: *Brain Behavior and Evolution* 6.1 (1972). DOI: 10.1159/000123713.

[80] B. D. Thuma. "Studies on the diencephalon of the cat. I. The cyto-architecture of the corpus geniculatum laterale". In: *Journal of Comparative Neurology* 46.1 (1928), pp. 173–199. DOI: 10.1002/cne.900460106.

[81] W. R. Hayhow. "The cytoarchitecture of the lateral geniculate body in the cat in relation to the distribution of crossed and uncrossed optic fibers". In: *Journal of Comparative Neurology* 110.1 (1958), pp. 1–63. DOI: 10.1002/cne.901100102.

[82] W. E. le Gros Clark. "The laminar organization and cell content of the lateral geniculate body in the monkey". In: *Journal of Anatomy* 75 (Pt 4 1941), pp. 419–433.

[83] K. J. Sanderson, R. W. Guillery, and R. M. Shackelford. "Congenitally abnormal visual pathways in mink (Mustela vison) with reduced retinal pigment". In: *Journal of Comparative Neurology* 154.3 (1974), pp. 225–248. DOI: 10.1002/cne.901540302.

[84] K. R. Zahs and M. P. Stryker. "Segregation of ON and OFF afferents to ferret visual cortex". In: *Journal of Neurophysiology* 59.5 (1988), pp. 1410–1429. DOI: 10.1152/jn.1988.59.5.1410.

[85] Kacie Dougherty et al. "Binocular Suppression in the Macaque Lateral Geniculate Nucleus Reveals Early Competitive Interactions between the Eyes". In: *eNeuro* 8.2 (2021), ENEURO.0364–20.2020. DOI: 10.1523/ENEURO.0364-20.2020.

[86] A. Maier et al. "Binocular Integration in the Primate Primary Visual Cortex". In: *Annual Review of Vision Science* 8.1 (2022), pp. 345–360. DOI: 10.1146/annurev-vision-100720-112922.

[87] Natalie Zeater et al. "Binocular Visual Responses in the Primate Lateral Geniculate Nucleus". In: *Current biology: CB* 25.24 (2015), pp. 3190–3195. DOI: 10.1016/j.cub.2015.10.033.

[88] Michael Howarth, Lauren Walmsley, and Timothy M. Brown. "Binocular integration in the mouse lateral geniculate nuclei". In: *Current biology: CB* 24.11 (2014), pp. 1241–1247. DOI: 10.1016/j.cub.2014.04.014.

[89] I Kostovic and P Rakic. "Development of prestriate visual projections in the monkey and human fetal cerebrum revealed by transient cholinesterase staining". In: *The Journal of Neuroscience* 4.1 (1984), pp. 25–42. DOI: 10.1523/JNEUROSCI.04-01-00025.1984.

[90] P. Rakic, Horace Basil Barlow, and Raymond Michael Gaze. "Prenatal development of the visual system in rhesus monkey". In: *Philosophical Transactions of the Royal Society of London. B, Biological Sciences* 278.961 (1977), pp. 245–260. DOI: 10.1098/rstb.1977.0040.

[91] David Sretavan and Carla J. Shatz. "Prenatal development of individual retinogeniculate axons during the period of segregation". In: *Nature* 308.5962 (1984), pp. 845–848. DOI: 10.1038/308845a0.

[92] DW Sretavan and CJ Shatz. "Prenatal development of cat retinogeniculate axon arbors in the absence of binocular interactions". In: *The Journal of Neuroscience* 6.4 (1986), pp. 990–1003. DOI: 10.1523/JNEUROSCI.06-04-00990.1986.

[93] Edward S. Ruthazer, G. E. Baker, and M. P. Stryker. "Development and Organization of Ocular Dominance Bands in Primary Visual Cortex of the Sable Ferret". In: *The Journal of comparative neurology* 407.2 (1999), pp. 151–165.

[94] D. H. Hubel et al. "Plasticity of ocular dominance columns in monkey striate cortex". In: *Phil. Trans. R. Soc. Lond. B* 278.961 (1977), pp. 377–409. DOI: 10.1098/rstb.1977.0050.

[95] Carla J. Shatz and Michael P. Stryker. "Prenatal Tetrodotoxin Infusion Blocks Segregation of Retinogeniculate Afferents". In: *Science* 242.4875 (1988), pp. 87–89. DOI: 10.1126/science.3175636.

[96] M. W. Dubin, L. A. Stark, and S. M. Archer. "A role for action-potential activity in the development of neuronal connections in the kitten retinogeniculate pathway". In: *The Journal of Neuroscience: The Official Journal of the Society for Neuroscience* 6.4 (1986), pp. 1021–1036. DOI: 10.1523/JNEUROSCI.06-04-01021.1986.

[97] David W. Sretavan, Carla J. Shatz, and Michael P. Stryker. "Modification of retinal ganglion cell axon morphology by prenatal infusion of tetrodotoxin". In: *Nature* 336.6198 (1988), pp. 468–471. DOI: 10.1038/336468a0.

[98] Rachel O. L. Wong. "Retinal Waves and Visual System Development". In: *Annual Review of Neuroscience* 22.1 (1999), pp. 29–47. DOI: 10.1146/annurev.neuro.22.1.29.

[99] M. Meister et al. "Synchronous bursts of action potentials in ganglion cells of the developing mammalian retina". In: *Science (New York, N.Y.)* 252.5008 (1991), pp. 939–943. DOI: 10.1126/science.2035024.

[100] R. O. L. Wong, M. Meister, and C. J. Shatz. "Transient period of correlated bursting activity during development of the mammalian retina". In: *Neuron* 11.5 (1993), pp. 923–938. DOI: 10.1016/0896-6273(93)90122-8.

[101] R. O. Wong and D. M. Oakley. "Changing patterns of spontaneous bursting activity of on and off retinal ganglion cells during development". In: *Neuron* 16.6 (1996), pp. 1087–1095. DOI: 10.1016/s0896-6273(00)80135-x.

[102] D. Stellwagen and C. J. Shatz. "An instructive role for retinal waves in the development of retinogeniculate connectivity". In: *Neuron* 33.3 (2002), pp. 357–367. DOI: 10.1016/s0896-6273(02)00577-9.

[103] Torsten N. Wiesel and David H. Hubel. "Single-cell responses in striate cortex of kittens deprived of vision in one eye". In: *Journal of Neurophysiology* 26.6 (1963), pp. 1003–1017. DOI: 10.1152/jn.1963.26.6.1003.

[104] E. Auerbach et al. "Electric potentials of retina and cortex of cats evoked by monocular and binocular photic stimulation". In: *Vision Research* 1.1 (1961), 166–IN8. DOI: 10.1016/0042-6989(61)90027-X.

[105] W. MARTIN USREY, MICHAEL P. SCENIAK, and BARBARA CHAPMAN. "Receptive Fields and Response Properties of Neurons in Layer 4 of Ferret Visual Cortex". In: *Journal of neurophysiology* 89.2 (2003), pp. 1003–1015. DOI: 10.1152/jn.00749.2002.

[106] D. H. Hubel and T. N. Wiesel. "Receptive fields and functional architecture of monkey striate cortex". In: *The Journal of Physiology* 195.1 (1968), pp. 215–243.

[107] Michael Weliky, William H. Bosking, and David Fitzpatrick. "A systematic map of direction preference in primary visual cortex". In: *Nature* 379.6567 (1996), pp. 725–728. DOI: 10.1038/379725a0.

[108] Wentao Hu et al. "Functional ultrasound imaging reveals 3D structure of orientation domains in ferret primary visual cortex". In: *NeuroImage* 268 (2023), p. 119889. DOI: 10.1016/j.neuroimage.2023.119889.

[109] David H. Hubel, Torsten N. Wiesel, and Michael P. Stryker. "Anatomical demonstration of orientation columns in macaque monkey". In: *Journal of Comparative Neurology* 177.3 (1978), pp. 361–379. DOI: 10.1002/cne.901770302.

[110] V. B. Mountcastle. "Modality and topographic properties of single neurons of cat's somatic sensory cortex". In: *Journal of Neurophysiology* 20.4 (1957), pp. 408–434. DOI: 10.1152/jn.1957.20.4.408.

[111] Jonathan C Horton and Daniel L Adams. "The cortical column: a structure without a function". In: *Philosophical Transactions of the Royal Society B: Biological Sciences* 360.1456 (2005), pp. 837–862. DOI: 10.1098/rstb.2005.1623.

[112] Nellie M. Bugbee and Patricia S. Goldman-Rakic. "Columnar organization of corticocortical projections in squirrel and rhesus monkeys: Similarity of column width in species differing in cortical volume". In: *Journal of Comparative Neurology* 220.3 (1983), pp. 355–364. DOI: 10.1002/cne.902200309.

[113] Daniel P. Buxhoeveden and Manuel F. Casanova. "The minicolumn hypothesis in neuroscience". In: *Brain* 125.5 (2002), pp. 935–951. DOI: 10.1093/brain/awf110.

[114] Korbinian Brodman. *Vergleichende Lokalisationslehre der Großhirnrinde : in ihren Prinzipien dargestellt auf Grund des Zellenbaues*. 1909. 324 pp.

[115] Kathleen S. Rockland. "What do we know about laminar connectivity?" In: *NeuroImage* 197 (2019), pp. 772–784. DOI: 10.1016/j.neuroimage.2017.07.032.

[116] Tom Binzegger, Rodney J. Douglas, and Kevan A. C. Martin. "A Quantitative Map of the Circuit of Cat Primary Visual Cortex". In: *Journal of Neuroscience* 24.39 (2004), pp. 8441–8453. DOI: 10.1523/JNEUROSCI.1400-04.2004.

[117] Jamie D. Boyd and Joanne A. Matsubara. "Laminar and columnar patterns of geniculocortical projections in the cat: Relationship to cytochrome oxidase". In: *Journal of Comparative Neurology* 365.4 (1996), pp. 659–682. DOI: 10.1002/(SICI)1096-9861(19960219)365:4<659::AID-CNE11>3.0.CO;2-C.

[118] D. H. Hubel and T. N. Wiesel. "Ferrier lecture - Functional architecture of macaque monkey visual cortex". In: *Proceedings of the Royal Society of London. Series B. Biological Sciences* 198.1130 (1976), pp. 1–59. DOI: 10.1098/rspb.1977.0085.

[119] Marc Nahmani and Alev Erisir. "VGluT2 immunochemistry identifies thalamocortical terminals in layer 4 of adult and developing visual cortex". In: *The Journal of Comparative Neurology* 484.4 (2005), pp. 458–473. DOI: 10.1002/cne.20505.

[120] S. LeVay, M. P. Stryker, and C. J. Shatz. "Ocular dominance columns and their development in layer IV of the cat's visual cortex: a quantitative study". In: *The Journal of Comparative Neurology* 179.1 (1978), pp. 223–244. DOI: 10.1002/cne.901790113.

[121] Victor Borrell and Edward M. Callaway. "Reorganization of Exuberant Axonal Arbors Contributes to the Development of Laminar Specificity in Ferret Visual Cortex". In: *Journal of Neuroscience* 22.15 (2002), pp. 6682–6695. DOI: 10.1523/JNEUROSCI.22-15-06682.2002.

[122] Dy Ts'o, Cd Gilbert, and Tn Wiesel. "Relationships between horizontal interactions and functional architecture in cat striate cortex as revealed by cross-correlation analysis". In: *The Journal of Neuroscience* 6.4 (1986), pp. 1160–1170. DOI: 10.1523/JNEUROSCI.06-04-01160.1986.

[123] Jennifer S. Lund and R. G. Boothe. "Interlaminar connections and pyramidal neuron organisation in the visual cortex, area 17, of the Macaque monkey". In: *Journal of Comparative Neurology* 159.3 (1975), pp. 305–334. DOI: 10.1002/cne.901590303.

[124] Leonard E. White et al. "Maps of Central Visual Space in Ferret V1 and V2 Lack Matching Inputs from the Two Eyes". In: *Journal of Neuroscience* 19.16 (1999), pp. 7089–7099. DOI: 10.1523/JNEUROSCI.19-16-07089.1999.

[125] C Redies, M Diksic, and H Riml. "Functional organization in the ferret visual cortex: a double-label 2- deoxyglucose study". In: *The Journal of Neuroscience* 10.8 (1990), pp. 2791–2803. DOI: 10.1523/JNEUROSCI.10-08-02791.1990.

[126] Jonathan C. Horton. "Ocular integration in the human visual cortex". In: *Canadian Journal of Ophthalmology* 41.5 (2006), pp. 584–593. DOI: 10.1016/S0008-4182(06)80027-X.

[127] S. LeVay, D. H. Hubel, and T. N. Wiesel. "The pattern of ocular dominance columns in macaque visual cortex revealed by a reduced silver stain". In: *The Journal of Comparative Neurology* 159.4 (1975), pp. 559–576. DOI: 10.1002/cne.901590408.

[128] C J Shatz and M P Stryker. "Ocular dominance in layer IV of the cat's visual cortex and the effects of monocular deprivation." In: *The Journal of Physiology* 281 (1978), pp. 267–283.

[129] R Malach et al. "Relationship between intrinsic connections and functional architecture revealed by optical imaging and in vivo targeted biocytin injections in primate striate cortex." In: *Proceedings of the National Academy of Sciences of the United States of America* 90.22 (1993), pp. 10469–10473.

[130] Ursula C. Dräger. "Autoradiography of tritiated proline and fucose transported transneuronally from the eye to the visual cortex in pigmented and albino mice". In: *Brain Research* 82.2 (1974), pp. 284–292. DOI: 10.1016/0006-8993(74)90607-6.

[131] M. G. Rosa et al. "Laminar, columnar and topographic aspects of ocular dominance in the primary visual cortex of Cebus monkeys". In: *Experimental Brain Research* 88.2 (1992), pp. 249–264. DOI: 10.1007/BF02259100.

[132] A Kossel, S Lowel, and J Bolz. "Relationships between dendritic fields and functional architecture in striate cortex of normal and visually deprived cats". In: *The Journal of Neuroscience* 15.5 (1995), pp. 3913–3926. DOI: 10.1523/JNEUROSCI.15-05-03913.1995.

[133] A. Peters and B. R. Payne. "Numerical relationships between geniculocortical afferents and pyramidal cell modules in cat primary visual cortex". In: *Cerebral Cortex (New York, N.Y.: 1991)* 3.1 (1993), pp. 69–78. DOI: 10.1093/cercor/3.1.69.

[134] Bashir Ahmed et al. "Polyneuronal Innervation of Spiny Stellate Neurons in Cat Visual Cortex". In: (1994).

[135] V. N. Kharazia and R. J. Weinberg. "Glutamate in thalamic fibers terminating in layer IV of primary sensory cortex". In: *The Journal of Neuroscience: The Official Journal of the Society for Neuroscience* 14.10 (1994), pp. 6021–6032. DOI: 10.1523/JNEUROSCI.14-10-06021.1994.

[136] S. Chung and D. Ferster. "Strength and orientation tuning of the thalamic input to simple cells revealed by electrically evoked cortical suppression". In: *Neuron* 20.6 (1998), pp. 1177–1189. DOI: 10.1016/s0896-6273(00)80498-5.

[137] Violeta Contreras Ramirez. "Refinement of feedforward projections, neuronal density, and characterization of synapsesin layer 4 of ferret primary visual cortex". PhD thesis. 2015.

[138] K. Herrmann, A. Antonini, and C. J. Shatz. "Ultrastructural evidence for synaptic interactions between thalamocortical axons and subplate neurons". In: *The European Journal of Neuroscience* 6.11 (1994), pp. 1729–1742. DOI: 10.1111/j.1460-9568.1994.tb00565.x.

[139] J. C. Crowley and Lawrence C. Katz. "Early Development of Ocular Dominance Columns". In: *Science* 290.5495 (2000), pp. 1321–1324. DOI: 10.1126/science.290.5495.1321.

[140] Y Frégnac and M Imbert. "Early development of visual cortical cells in normal and dark-reared kittens: relationship between orientation selectivity and ocular dominance." In: *The Journal of Physiology* 278.1 (1978), pp. 27–44. DOI: 10.1113/jphysiol.1978.sp012290.

[141] MP Stryker and WA Harris. "Binocular impulse blockade prevents the formation of ocular dominance columns in cat visual cortex". In: *The Journal of Neuroscience* 6.8 (1986), pp. 2117–2133. DOI: 10.1523/JNEUROSCI.06-08-02117.1986.

[142] D. H. Hubel and T. N. Wiesel. "The period of susceptibility to the physiological effects of unilateral eye closure in kittens". In: *The Journal of Physiology* 206.2 (1970), pp. 419–436.

[143] Simon Le Vay, Torsten N. Wiesel, and David H. Hubel. "The development of ocular dominance columns in normal and visually deprived monkeys". In: *Journal of Comparative Neurology* 191.1 (1980), pp. 1–51. DOI: 10.1002/cne.901910102.

[144] George D. Mower et al. "Comparison of the effects of dark rearing and binocular suture on development and plasticity of cat visual cortex". In: *Brain Research* 220.2 (1981), pp. 255–267. DOI: 10.1016/0006-8993(81)91216-6.

[145] M. Cynader and D. E. Mitchell. "Prolonged sensitivity to monocular deprivation in dark-reared cats". In: *Journal of Neurophysiology* 43.4 (1980), pp. 1026–1040. DOI: 10.1152/jn.1980.43.4.1026.

[146] G. D. Mower. "The effect of dark rearing on the time course of the critical period in cat visual cortex". In: *Brain Research. Developmental Brain Research* 58.2 (1991), pp. 151–158. DOI: 10.1016/0165-3806(91)90001-y.

[147] T. N. Wiesel and D. H. Hubel. "Comparison of the effects of unilateral and bilateral eye closure on cortical unit responses in kittens". In: *Journal of Neurophysiology* 28.6 (1965), pp. 1029–1040. DOI: 10.1152/jn.1965.28.6.1029.

[148] U. Yinon et al. "The ocular dominance of cortical neurons in cats developed with divergent and convergent squint". In: *Vision Research* 15.11 (1975), pp. 1251–1256. DOI: 10.1016/0042-6989(75)90170-4.

[149] David H. Hubel and Torsten N. Wiesel. "Binocular interaction in striate cortex of kittens reared with artificial squint". In: *Journal of Neurophysiology* 28.6 (1965), pp. 1041–1059. DOI: 10.1152/jn.1965.28.6.1041.

[150] Frank Sengpiel and Peter C. Kind. "The Role of Activity in Development of the Visual System". In: *Current Biology* 12.23 (2002), R818–R826. DOI: 10.1016/S0960-9822(02)01318-0.

[151] Venkata M. Kanukollu and Gitanjli Sood. "Strabismus". In: *StatPearls*. Treasure Island (FL): StatPearls Publishing, 2023.

[152] null Vaegan and D. Taylor. "Critical period for deprivation amblyopia in children". In: *Transactions of the Ophthalmological Societies of the United Kingdom* 99.3 (1979), pp. 432–439.

[153] R. C. Reid and J. M. Alonso. "Specificity of monosynaptic connections from thalamus to visual cortex". In: *Nature* 378.6554 (1995), pp. 281–284. DOI: 10.1038/378281a0.

[154] B Chapman, Kr Zahs, and Mp Stryker. "Relation of cortical cell orientation selectivity to alignment of receptive fields of the geniculocortical afferents that arborize within a single orientation column in ferret visual cortex". In: *The Journal of Neuroscience* 11.5 (1991), pp. 1347–1358. DOI: 10.1523/JNEUROSCI.11-05-01347.1991.

[155] Madineh Sedigh-Sarvestani et al. "Intracellular, In Vivo, Dynamics of Thalamocortical Synapses in Visual Cortex". In: *The Journal of Neuroscience: The Official Journal of the Society for Neuroscience* 37.21 (2017), pp. 5250–5262. DOI: 10.1523/JNEUROSCI.3370-16.2017.

[156] Benjamin Scholl et al. "Emergence of Orientation Selectivity in the Mammalian Visual Pathway". In: *Journal of Neuroscience* 33.26 (2013), pp. 10616–10624. DOI: 10.1523/JNEUROSCI.0404-13.2013.

[157] T. R. Vidyasagar and J. V. Urbas. "Orientation sensitivity of cat LGN neurones with and without inputs from visual cortical areas 17 and 18". In: *Experimental Brain Research* 46.2 (1982), pp. 157–169. DOI: 10.1007/BF00237172.

[158] Kuo-Sheng Lee, Xiaoying Huang, and David Fitzpatrick. "Topology of ON and OFF inputs in visual cortex enables an invariant columnar architecture". In: *Nature* 533.7601 (2016), pp. 90–94. DOI: 10.1038/nature17941.

[159] D. C. Somers, S. B. Nelson, and M. Sur. "An emergent model of orientation selectivity in cat visual cortical simple cells". In: *Journal of Neuroscience* 15.8 (1995), pp. 5448–5465. DOI: 10.1523/JNEUROSCI.15-08-05448.1995.

[160] Leonard E. White, David M. Coppola, and David Fitzpatrick. "The contribution of sensory experience to the maturation of orientation selectivity in ferret visual cortex". In: *Nature* 411.6841 (2001), p. 1049. DOI: 10.1038/35082568.

[161] W. H. Bosking et al. "Orientation selectivity and the arrangement of horizontal connections in tree shrew striate cortex". In: *The Journal of Neuroscience: The Official Journal of the Society for Neuroscience* 17.6 (1997), pp. 2112–2127.

[162] CD Gilbert and TN Wiesel. "Columnar specificity of intrinsic horizontal and corticocortical connections in cat visual cortex". In: *The Journal of Neuroscience* 9.7 (1989), pp. 2432–2442. DOI: 10.1523/JNEUROSCI.09-07-02432.1989.

[163] Barbara Chapman, Michael P. Stryker, and Tobias Bonhoeffer. "Development of Orientation Preference Maps in Ferret Primary Visual Cortex". In: *Journal of Neuroscience* 16.20 (1996), pp. 6443–6453.

[164] Gordon B. Smith et al. "Distributed network interactions and their emergence in developing neocortex". In: *Nature neuroscience* 21.11 (2018), pp. 1600–1608. DOI: 10.1038/s41593-018-0247-5.

[165] Chiayu Chiu and Michael Weliky. "Spontaneous Activity in Developing Ferret Visual Cortex In Vivo". In: *The Journal of Neuroscience* 21.22 (2001), pp. 8906–8914. DOI: 10.1523/JNEUROSCI.21-22-08906.2001.

[166] Imke Gödecke and Tobias Bonhoeffer. "Development of identical orientation maps for two eyes without common visual experience". In: *Nature* 379.6562 (1996), pp. 251–254. DOI: 10.1038/379251a0.

[167] Kenichi Ohki et al. "Functional imaging with cellular resolution reveals precise micro - architecture in visual cortex". In: *Nature* 433.7026 (2005), pp. 597–603. DOI: 10.1038/nature03274.

[168] Ho Ko et al. "Functional specificity of local synaptic connections in neocortical networks". In: *Nature* 473.7345 (2011), nature09880. DOI: 10.1038/nature09880.

[169] Daniel J. Denman and Diego Contreras. "The Structure of Pairwise Correlation in Mouse Primary Visual Cortex Reveals Functional Organization in the Absence of an Orientation Map". In: *Cerebral Cortex (New York, NY)* 24.10 (2014), pp. 2707–2720. DOI: 10.1093/cercor/bht128.

[170] Tom Baden et al. "The functional diversity of retinal ganglion cells in the mouse". In: *Nature* 529.7586 (2016), pp. 345–350. DOI: 10.1038/nature16468.

[171] David I. Vaney, Benjamin Sivyer, and W. Rowland Taylor. "Direction selectivity in the retina: symmetry and asymmetry in structure and function". In: *Nature Reviews Neuroscience* 13.3 (2012), pp. 194–208. DOI: 10.1038/nrn3165.

[172] Amurta Nath and Gregory W. Schwartz. "Cardinal Orientation Selectivity Is Represented by Two Distinct Ganglion Cell Types in Mouse Retina". In: *The Journal of Neuroscience* 36.11 (2016), pp. 3208–3221. DOI: 10.1523/JNEUROSCI.4554-15.2016.

[173] Yeon Jin Kim et al. "Origins of direction selectivity in the primate retina". In: *Nature Communications* 13.1 (2022), p. 2862. DOI: 10.1038/s41467-022-30405-5.

[174] TD Shou and AG Leventhal. "Organized arrangement of orientation-sensitive relay cells in the cat's dorsal lateral geniculate nucleus". In: *The Journal of Neuroscience* 9.12 (1989), pp. 4287–4302. DOI: 10.1523/JNEUROSCI.09-12-04287.1989.

[175] W. R. Levick and L. N. Thibos. "Orientation bias of cat retinal ganglion cells". In: *Nature* 286.5771 (1980), pp. 389–390. DOI: 10.1038/286389a0.

[176] Kristine Krug, Colin J. Akerman, and Ian D. Thompson. "Responses of Neurons in Neonatal Cortex and Thalamus to Patterned Visual Stimulation Through the Naturally Closed Lids". In: *Journal of Neurophysiology* 85.4 (2001), pp. 1436–1443. DOI: 10.1152/jn.2001.85.4.1436.

[177] Christopher L. Passaglia et al. "Orientation Sensitivity of Ganglion Cells in Primate Retina". In: *Vision research* 42.6 (2002), pp. 683–694. DOI: 10.1016/s0042-6989(01)00312-1.

[178] Benjamin Scholl, Johannes Burge, and Nicholas J. Priebe. "Binocular integration and disparity selectivity in mouse primary visual cortex". In: *Journal of Neurophysiology* 109.12 (2013), pp. 3013–3024. DOI: 10.1152/jn.01021.2012.

[179] Xinyu Zhao et al. "Orientation-selective Responses in the Mouse Lateral Geniculate Nucleus". In: *Journal of Neuroscience* 33.31 (2013), pp. 12751–12763. DOI: 10.1523/JNEUROSCI.0095-13.2013.

[180] James H. Marshel et al. "Anterior-Posterior Direction Opponency in the Superficial Mouse Lateral Geniculate Nucleus". In: *Neuron* 76.4 (2012), pp. 713–720. DOI: 10.1016/j.neuron.2012.09.021.

[181] Denise M. Piscopo et al. "Diverse Visual Features Encoded in Mouse Lateral Geniculate Nucleus". In: *The Journal of Neuroscience* 33.11 (2013), pp. 4642–4656. DOI: 10.1523/JNEUROSCI.5187-12.2013.

[182] B. G. Cumming and G. C. DeAngelis. "The Physiology of Stereopsis". In: *Annual Review of Neuroscience* 24.1 (2001), pp. 203–238. DOI: 10.1146/annurev.neuro.24.1.203.

[183] Andrew J. Parker. "Binocular depth perception and the cerebral cortex". In: *Nature Reviews. Neuroscience* 8.5 (2007), pp. 379–391. DOI: 10.1038/nrn2131.

[184] F Gonzalez and R Perez. "Neural mechanisms underlying stereoscopic vision". In: *Progress in Neurobiology* 55.3 (1998), pp. 191–224. DOI: 10.1016/S0301-0082(98)00012-4.

[185] J. H. Maunsell and D. C. Van Essen. "Functional properties of neurons in middle temporal visual area of the macaque monkey. II. Binocular interactions and sensitivity to binocular disparity". In: *Journal of Neurophysiology* 49.5 (1983), pp. 1148–1167. DOI: 10.1152/jn.1983.49.5.1148.

[186] Izumi Ohzawa, Gregory Deangelis, and R.D. Freeman. "Stereoscopic depth discrimination in the visual cortex: neurons ideally suited as disparity detectors". In: *Science (New York, N.Y.)* 249 (1990), pp. 1037–41. DOI: 10.1126/science.2396096.

[187] D. Marr and T. Poggio. "A computational theory of human stereo vision". In: *Proceedings of the Royal Society of London. Series B, Biological Sciences* 204.1156 (1979), pp. 301–328. DOI: 10.1098/rspb.1979.0029.

[188] Barton L. Anderson and Ken Nakayama. "Toward a general theory of stereopsis: Binocular matching, occluding contours, and fusion." In: *Psychological Review* 101.3 (1994), pp. 414–445. DOI: 10.1037/0033-295X.101.3.414.

[189] Phillip A. Romo et al. "Binocular Neurons in Parastriate Cortex: Interocular 'Matching' of Receptive Field Properties, Eye Dominance and Strength of Silent Suppression". In: *PLoS ONE* 9.6 (2014). Ed. by Daniel Osorio, e99600. DOI: 10.1371/journal.pone.0099600.

[190] R. D. Freeman and I. Ohzawa. "Development of binocular vision in the kitten's striate cortex". In: *Journal of Neuroscience* 12.12 (1992), pp. 4721–4736. DOI: 10.1523/JNEUROSCI.12-12-04721.1992.

[191] Colin Blakemore and Richard C. Van Sluyters. "Reversal of the physiological effects of monocular deprivation in kittens: further evidence for a sensitive period". In: *The Journal of Physiology* 237.1 (1974), pp. 195–216.

[192] Michael C. Crair, Deda C. Gillespie, and Michael P. Stryker. "The Role of Visual Experience in the Development of Columns in Cat Visual Cortex". In: *Science (New York, N.Y.)* 279.5350 (1998), pp. 566–570.

[193] Peter C. Kind et al. "Correlated binocular activity guides recovery from monocular deprivation". In: *Nature* 416.6879 (2002), pp. 430–433. DOI: 10.1038/416430a.

[194] Joshua A. Gordon and Michael P. Stryker. "Experience-Dependent Plasticity of Binocular Responses in the Primary Visual Cortex of the Mouse". In: *The Journal of Neuroscience* 16.10 (1996), pp. 3274–3286. DOI: 10.1523/JNEUROSCI.16-10-03274.1996.

[195] Simon Peron et al. "Recurrent interactions in local cortical circuits". In: *Nature* 579.7798 (2020), pp. 256–259. DOI: 10.1038/s41586-020-2062-x.

[196] Xize Xu, Jianhua Cang, and Hermann Riecke. *Development and Binocular Matching of Orientation Selectivity in Visual Cortex: A Computational Model*. preprint. Neuroscience, 2019. DOI: 10.1101/682211.

[197] H Suzuki and E Kato. "Binocular interaction at cat's lateral geniculate body." In: *Journal of Neurophysiology* 29.5 (1966), pp. 909–920. DOI: 10.1152/jn.1966.29.5.909.

[198] H. Kato, M. Yamamoto, and H. Nakahama. "Intracellular recordings from the lateral geniculate neurons of cats". In: *The Japanese Journal of Physiology* 21.3 (1971), pp. 307–323. DOI: 10.2170/jjphysiol.21.307.

[199] K. J. Sanderson, P. O. Bishop, and I. Darian-Smith. "The properties of the binocular receptive fields of lateral geniculate neurons". In: *Experimental Brain Research* 13.2 (1971), pp. 178–207. DOI: 10.1007/BF00234085.

[200] H. B. Barlow, C. Blakemore, and J. D. Pettigrew. "The neural mechanism of binocular depth discrimination". In: *The Journal of Physiology* 193.2 (1967), pp. 327–342. DOI: 10.1113/jphysiol.1967.sp008360.

[201] P. O. Bishop, G. H. Henry, and C. J. Smith. "Binocular interaction fields of single units in the cat striate cortex". In: *The Journal of Physiology* 216.1 (1971), pp. 39–68. DOI: 10.1113/jphysiol.1971.sp009508.

[202] J.D. Pettigrew, T. Nikara, and P.O. Bishop. "Binocular interaction on single units in cat striate cortex: Simultaneous stimulation by single moving slit with receptive fields in correspondence". In: *Experimental Brain Research* 6.4 (1968). DOI: 10.1007/BF00233186.

[203] Yu Gu and Jianhua Cang. "Binocular matching of thalamocortical and intracortical circuits in the mouse visual cortex". In: *eLife* 5 (2016). DOI: 10.7554/eLife.22032.

[204] Ed Erwin and Kenneth D. Miller. "Correlation-Based Development of Ocularly Matched Orientation and Ocular Dominance Maps: Determination of Required Input Activities". In: *The Journal of Neuroscience* 18.23 (1998), pp. 9870–9895. DOI: 10.1523/JNEUROSCI.18-23-09870.1998.

[205] Elie L Bienenstock, Leon N Cooper, and Paul W Munro. "Theory for the Development of Neuron Selectivity: Orientation Specificity and Binocular Interaction in Visual Cortex." In: (1982), p. 82.

[206] Ms Livingstone and Dh Hubel. "Psychophysical evidence for separate channels for the perception of form, color, movement, and depth". In: *The Journal of Neuroscience* 7.11 (1987), pp. 3416–3468. DOI: 10.1523/JNEUROSCI.07-11-03416.1987.

[207] D. H. Hubel and T. N. Wiesel. "Receptive Fields and functional architecture in two nonstriate visual areas (18 and 19) of the cat". In: *Journal of Neurophysiology* 28 (1965), pp. 229–289. DOI: 10.1152/jn.1965.28.2.229.

[208] Gina Cantone et al. "Feedback connections to ferret striate cortex: direct evidence for visuotopic convergence of feedback inputs". In: *The Journal of Comparative Neurology* 487.3 (2005), pp. 312–331. DOI: 10.1002/cne.20570.

[209] Reem Khalil et al. "Visual Corticocortical Inputs to Ferret Area 18". In: *Frontiers in Neuroanatomy* 14 (2020), p. 73. DOI: 10.3389/fnana.2020.581478.

[210] A. Batardiere et al. "Area-specific laminar distribution of cortical feedback neurons projecting to cat area 17: Quantitative analysis in the adult and during ontogeny". In: *Journal of Comparative Neurology* 396.4 (1998), pp. 493–510. DOI: 10.1002/(SICI)1096-9861(19980713)396:4<493::AID-CNE6>3.0.CO;2-X.

[211] K. S. Rockland and D. N. Pandya. "Laminar origins and terminations of cortical connections of the occipital lobe in the rhesus monkey". In: *Brain Research* 179.1 (1979), pp. 3–20. DOI: 10.1016/0006-8993(79)90485-2.

[212] John C. Anderson and Kevan A. C. Martin. "The Synaptic Connections between Cortical Areas V1 and V2 in Macaque Monkey". In: *The Journal of Neuroscience* 29.36 (2009), pp. 11283–11293. DOI: 10.1523/JNEUROSCI.5757-08.2009.

[213] Laura L. Symonds and Alan C. Rosenquist. "Laminar origins of visual corticocortical connections in the cat". In: *Journal of Comparative Neurology* 229.1 (1984), pp. 39–47. DOI: 10.1002/cne.902290104.

[214] Johannes Tigges et al. "Areal and laminar distribution of neurons interconnecting the central visual cortical areas 17, 18, 19, and MT in squirrel monkey (Saimiri)". In: *Journal of Comparative Neurology* 202.4 (1981), pp. 539–560. DOI: 10.1002/cne.902020407.

[215] Jennifer S. Lund et al. "The origin of efferent pathways from the primary visual cortex, area 17, of the macaque monkey as shown by retrograde transport of horseradish peroxidase". In: *Journal of Comparative Neurology* 164.3 (1975), pp. 287–303. DOI: 10.1002/cne.901640303.

[216] Leigh-Anne Dell et al. "Cortical and thalamic connectivity of occipital visual cortical areas 17, 18, 19, and 21 of the domestic ferret (Mustela putorius furo)". In: *The Journal of Comparative Neurology* 527.8 (2019), pp. 1293–1314. DOI: 10.1002/cne.24631.

[217] Alessandra Angelucci et al. "Circuits and Mechanisms for Surround Modulation in Visual Cortex". In: *Annual Review of Neuroscience* 40.1 (2017), pp. 425–451. DOI: 10.1146/annurev-neuro-072116-031418.

[218] Tian-De Shou. "The functional roles of feedback projections in the visual system". In: *Neuroscience Bulletin* 26.5 (2010), pp. 401–410. DOI: 10.1007/s12264-010-0521-3.

[219] D. H. Hubel and T. N. Wiesel. "Cortical and callosal connections concerned with the vertical meridian of visual fields in the cat". In: *Journal of Neurophysiology* 30.6 (1967), pp. 1561–1573. DOI: 10.1152/jn.1967.30.6.1561.

[220] Jennifer S. Lund, Alessandra Angelucci, and Paul C. Bressloff. "Anatomical Substrates for Functional Columns in Macaque Monkey Primary Visual Cortex". In: *Cerebral Cortex* 13.1 (2003), pp. 15–24. DOI: 10.1093/cercor/13.1.15.

[221] Frank H. Baker, Peter Grigg, and Gunter K. von Noorden. "Effects of visual deprivation and strabismus on the response of neurons in the visual cortex of the monkey, including studies on the striate and prestriate cortex in the normal animal". In: *Brain Research* 66.2 (1974), pp. 185–208. DOI: 10.1016/0006-8993(74)90140-1.

[222] Reem Khalil and Jonathan B. Levitt. "Developmental remodeling of corticocortical feedback circuits in ferret visual cortex: Corticocortical Feedback Circuits". In: *Journal of Comparative Neurology* 522.14 (2014), pp. 3208–3228. DOI: 10.1002/cne.23591.

[223] Augusto A Lempel and Kristina J Nielsen. "Development of visual motion integration involves coordination of multiple cortical stages". In: *eLife* 10 (2021). Ed. by Chris I Baker, Tatiana Pasternak, and Robbe Goris, e59798. DOI: 10.7554/eLife.59798.

[224] Reem Khalil et al. "Developmental refinement of visual callosal inputs to ferret area 17". In: *Journal of Comparative Neurology* 530.5 (2022), pp. 804–816. DOI: 10.1002/cne.25246.

[225] Tommaso Bocci et al. "Visual callosal connections: role in visual processing in health and disease". In: *Reviews in the Neurosciences* 25.1 (2014). DOI: 10.1515/revneuro-2013-0025.

[226] G. M. Innocenti. "Architecture and Callosal Connections of Visual Areas 17, 18, 19 and 21 in the Ferret (Mustela putorius)". In: *Cerebral Cortex* 12.4 (2002), pp. 411–422. DOI: 10.1093/cercor/12.4.411.

[227] P. R. Manger. "The Representation of the Visual Field in Three Extrastriate Areas of the Ferret (Mustela putorius) and the Relationship of Retinotopy and Field Boundaries to Callosal Connectivity". In: *Cerebral Cortex* 12.4 (2002), pp. 423–437. DOI: 10.1093/cercor/12.4.423.

[228] B. P. Choudhury, D. Whitteridge, and M. E. Wilson. "The Function of the Callosal Connections of the Visual Cortex". In: *Quarterly Journal of Experimental Physiology and Cognate Medical Sciences* 50.2 (1965), pp. 214–219. DOI: 10.1113/expphysiol.1965.sp001783.

[229] G. Berlucchi and G. Rizzolatti. "Binocularly driven neurons in visual cortex of split-chiasm cats". In: *Science (New York, N.Y.)* 159.3812 (1968), pp. 308–310. DOI: 10.1126/science.159.3812.308.

[230] B. R. Payne. "Neuronal interactions in cat visual cortex mediated by the corpus callosum". In: *Behavioural Brain Research* 64.1 (1994), pp. 55–64. DOI: 10.1016/0166-4328(94)90118-X.

[231] Nancy E. Berman and Bertram R. Payne. "Alterations in connections of the corpus callosum following convergent and divergent strabismus". In: *Brain Research* 274.2 (1983), pp. 201–212. DOI: 10.1016/0006-8993(83)90697-2.

[232] R. D. Lund and D. E. Mitchell. "Asymmetry in the visual callosal connections of strabismic cats". In: *Brain Research* 167.1 (1979), pp. 176–179. DOI: 10.1016/0006-8993(79)90274-9.

[233] Thomas Wunderle, David Eriksson, and Kerstin E. Schmidt. "Multiplicative Mechanism of Lateral Interactions Revealed by Controlling Interhemispheric Input". In: *Cerebral Cortex* 23.4 (2013), pp. 900–912. DOI: 10.1093/cercor/bhs081.

[234] Valeri A. Makarov et al. "Stimulus-Dependent Interaction between the Visual Areas 17 and 18 of the 2 Hemispheres of the Ferret (Mustela putorius)". In: *Cerebral Cortex* 18.8 (2008), pp. 1951–1960. DOI: 10.1093/cercor/bhm222.

[235] B. Timney, A. J. Elberger, and M. L. Vandewater. "Binocular depth perception in the cat following early corpus callosum section". In: *Experimental Brain Research* 60.1 (1985), pp. 19–26. DOI: 10.1007/BF00237014.

[236] Xinyu Zhao, Mingna Liu, and Jianhua Cang. "Sublinear Binocular Integration Preserves Orientation Selectivity in Mouse Visual Cortex". In: *Nature communications* 4 (2013), p. 2088. DOI: 10.1038/ncomms3088.

[237] Vishnudev Ramachandra et al. "Impact of visual callosal pathway is dependent upon ipsilateral thalamus". In: *Nature Communications* 11.1 (2020), pp. 1–13. DOI: 10.1038/s41467-020-15672-4.

[238] Kerstin E. Schmidt. "The Visual Callosal Connection: A Connection Like Any Other?" In: *Neural Plasticity* 2013 (2013), e397176. DOI: 10.1155/2013/397176.

[239] G. M. Innocenti and R. Caminiti. "Postnatal shaping of callosal connections from sensory areas". In: *Experimental Brain Research* 38.4 (1980), pp. 381–394. DOI: 10.1007/BF00237518.

[240] Daniëlle van Versendaal and Christiaan N. Levelt. "Inhibitory interneurons in visual cortical plasticity". In: *Cellular and Molecular Life Sciences* 73.19 (2016), pp. 3677–3691. DOI: 10.1007/s00018-016-2264-4.

[241] Olivia K. Swanson and Arianna Maffei. "From Hiring to Firing: Activation of Inhibitory Neurons and Their Recruitment in Behavior". In: *Frontiers in Molecular Neuroscience* 12 (2019).

[242] Jeffry S. Isaacson and Massimo Scanziani. "How Inhibition Shapes Cortical Activity". In: *Neuron* 72.2 (2011), pp. 231–243. DOI: 10.1016/j.neuron.2011.09.027.

[243] T.P. Vogels and L.F. Abbott. "Gating Multiple Signals through Detailed Balance of Excitation and Inhibition in Spiking Networks". In: *Nature neuroscience* 12.4 (2009), pp. 483–491. DOI: 10.1038/nn.2276.

[244] J. S. Anderson, M. Carandini, and D. Ferster. "Orientation tuning of input conductance, excitation, and inhibition in cat primary visual cortex". In: *Journal of Neurophysiology* 84.2 (2000), pp. 909–926. DOI: 10.1152/jn.2000.84.2.909.

[245] Andrew Y. Y. Tan et al. "Orientation Selectivity of Synaptic Input to Neurons in Mouse and Cat Primary Visual Cortex". In: *The Journal of Neuroscience* 31.34 (2011), pp. 12339–12350. DOI: 10.1523/JNEUROSCI.2039-11.2011.

[246] Daniel E. Wilson, Benjamin Scholl, and David Fitzpatrick. "Differential tuning of excitation and inhibition shapes direction selectivity in ferret visual cortex". In: *Nature* 560.7716 (2018), pp. 97–101. DOI: 10.1038/s41586-018-0354-1.

[247] Yue Kris Wu and Friedemann Zenke. "Nonlinear transient amplification in recurrent neural networks with short-term plasticity". In: *eLife* 10 (2021). Ed. by Timothy O'Leary and Ronald L Calabrese, e71263. DOI: 10.7554/eLife.71263.

[248] Daniel B. Rubin, Stephen D. Van Hooser, and Kenneth D. Miller. "The Stabilized Supralinear Network: A Unifying Circuit Motif Underlying Multi-Input Integration in Sensory Cortex". In: *Neuron* 85.2 (2015), pp. 402–417. DOI: 10.1016/j.neuron.2014.12.026.

[249] Haleigh N. Mulholland et al. "Tightly coupled inhibitory and excitatory functional networks in the developing primary visual cortex". In: *eLife* 10 (2021), e72456. DOI: 10.7554/eLife.72456.

[250] Jeremy T. Chang and David Fitzpatrick. "Development of visual response selectivity in cortical GABAergic interneurons". In: *Nature Communications* 13.1 (2022), p. 3791. DOI: 10.1038/s41467-022-31284-6.

[251] Sandra J. Kuhlman, Elaine Tring, and Joshua T. Trachtenberg. "Fast-spiking interneurons have an initial orientation bias that is lost with vision". In: *Nature neuroscience* 14.9 (2011), pp. 1121–1123. DOI: 10.1038/nn.2890.

[252] Ryoma Hattori et al. "Functions and dysfunctions of neocortical inhibitory neuron subtypes". In: *Nature Neuroscience* 20.9 (2017), pp. 1199–1208. DOI: 10.1038/nn.4619.

[253] Yoshiyuki Kubota et al. "The Diversity of Cortical Inhibitory Synapses". In: *Frontiers in Neural Circuits* 10 (2016).

[254] Josiah R. Boivin and Elly Nedivi. "Functional implications of inhibitory synapse placement on signal processing in pyramidal neuron dendrites". In: *Current opinion in neurobiology* 51 (2018), pp. 16–22. DOI: 10.1016/j.conb.2018.01.013.

[255] Jonathan S. Marvin et al. "A genetically encoded fluorescent sensor for in vivo imaging of GABA". In: *Nature Methods* 16.8 (2019), pp. 763–770. DOI: 10.1038/s41592-019-0471-2.

[256] Mark Zervas and Steven U. Walkley. "Ferret pyramidal cell dendritogenesis: Changes in morphology and ganglioside expression during cortical development". In: *Journal of Comparative Neurology* 413.3 (1999), pp. 429–448. DOI: 10.1002/(SICI)1096-9861(19991025)413:3<429::AID-CNE6>3.0.CO;2-7.

[257] Huttenlocher Peter R. "Synaptic density in human frontal cortex — Developmental changes and effects of aging". In: *Brain Research* 163.2 (1979), pp. 195–205. DOI: 10.1016/0006-8993(79)90349-4.

[258] L. J. Garey and C. de Courten. "Structural development of the lateral geniculate nucleus and visual cortex in monkey and man". In: *Behavioural Brain Research* 10.1 (1983), pp. 3–13. DOI: 10.1016/0166-4328(83)90145-6.

[259] P. Rakic et al. "Concurrent overproduction of synapses in diverse regions of the primate cerebral cortex". In: *Science (New York, N.Y.)* 232.4747 (1986), pp. 232–235. DOI: 10.1126/science.3952506.

[260] Guy N. Elston and Ichiro Fujita. "Pyramidal cell development: postnatal spinogenesis, dendritic growth, axon growth, and electrophysiology". In: *Frontiers in Neuroanatomy* 8 (2014). DOI: 10.3389/fnana.2014.00078.

[261] B. G. Cragg. "The development of synapses in the visual system of the cat". In: *The Journal of Comparative Neurology* 160.2 (1975), pp. 147–166. DOI: 10.1002/cne.901600202.

[262] Edward M. Callaway and Víctor Borrell. "Developmental Sculpting of Dendritic Morphology of Layer 4 Neurons in Visual Cortex: Influence of Retinal Input". In: *The Journal of Neuroscience* 31.20 (2011), pp. 7456–7470. DOI: 10.1523/JNEUROSCI.5222-10.2011.

[263] David A. Orner et al. "Alterations of dendritic protrusions over the first postnatal year of a mouse: an analysis in layer VI of the barrel cortex". In: *Brain Structure & Function* 219.5 (2014), pp. 1709–1720. DOI: 10.1007/s00429-013-0596-5.

[264] Susanne Falkner et al. "Transplanted embryonic neurons integrate into adult neocortical circuits". In: *Nature* 539.7628 (2016), pp. 248–253. DOI: 10.1038/nature20113.

[265] Sarah E.V. Richards et al. "Experience-Dependent Development of Dendritic Arbors in Mouse Visual Cortex". In: *The Journal of Neuroscience* 40.34 (2020), pp. 6536–6556. DOI: 10.1523/JNEUROSCI.2910-19.2020.

[266] Hongbo Yu, Ania K. Majewska, and Mriganka Sur. "Rapid experience-dependent plasticity of synapse function and structure in ferret visual cortex in vivo". In: *Proceedings of the National Academy of Sciences* 108.52 (2011), pp. 21235–21240. DOI: 10.1073/pnas.1108270109.

[267] Pico Caroni, Flavio Donato, and Dominique Muller. "Structural plasticity upon learning: regulation and functions". In: *Nature Reviews Neuroscience* 13.7 (2012), pp. 478–490. DOI: 10.1038/nrn3258.

[268] Nora Jamann, Merryn Jordan, and Maren Engelhardt. "Activity-Dependent Axonal Plasticity in Sensory Systems". In: *Neuroscience*. Barrel Cortex Function 368 (2018), pp. 268–282. DOI: 10.1016/j.neuroscience.2017.07.035.

[269] Rafael Yuste and Tobias Bonhoeffer. "Morphological Changes in Dendritic Spines Associated with Long-Term Synaptic Plasticity". In: *Annual review of neuroscience* 24 (2001), pp. 1071–89. DOI: 10.1146/annurev.neuro.24.1.1071.

[270] Sonja B. Hofer et al. "Experience leaves a lasting structural trace in cortical circuits". In: *Nature* 457.7227 (2009), pp. 313–317. DOI: 10.1038/nature07487.

[271] Massimo Scanziani and Michael Häusser. "Electrophysiology in the age of light". In: *Nature* 461.7266 (2009), pp. 930–939. DOI: 10.1038/nature08540.

[272] Nicholas J. Priebe et al. "The contribution of spike threshold to the dichotomy of cortical simple and complex cells". In: *Nature Neuroscience* 7.10 (2004), pp. 1113–1122. DOI: 10.1038/nn1310.

[273] Nicholas J. Priebe and David Ferster. "Direction Selectivity of Excitation and Inhibition in Simple Cells of the Cat Primary Visual Cortex". In: *Neuron* 45.1 (2005), pp. 133–145. DOI: 10.1016/j.neuron.2004.12.024.

[274] Elizabeth M. C. Hillman. "Optical brain imaging in vivo: techniques and applications from animal to man". In: *Journal of biomedical optics* 12.5 (2007), p. 051402. DOI: 10.1117/1.2789693.

[275] Christine Grienberger and Arthur Konnerth. "Imaging Calcium in Neurons". In: *Neuron* 73.5 (2012), pp. 862–885. DOI: 10.1016/j.neuron.2012.02.011.

[276] Michael J. Higley and Bernardo L. Sabatini. "Calcium Signaling in Dendrites and Spines: Practical and Functional Considerations". In: *Neuron* 59.6 (2008), pp. 902–913. DOI: 10.1016/j.neuron.2008.08.020.

[277] Farhan Ali and Alex C. Kwan. "Interpreting *in vivo* calcium signals from neuronal cell bodies, axons, and dendrites: a review". In: *Neurophotonics* 7.1 (2019), p. 011402. DOI: 10.1117/1.NPh.7.1.011402.

[278] Martin Oheim et al. "Two-photon microscopy in brain tissue: parameters influencing the imaging depth". In: *Journal of Neuroscience Methods* 111.1 (2001), pp. 29–37. DOI: 10.1016/S0165-0270(01)00438-1.

[279] Kevin Takasaki, Reza Abbasi-Asl, and Jack Waters. "Superficial Bound of the Depth Limit of Two-Photon Imaging in Mouse Brain". In: *eNeuro* 7.1 (2020). DOI: 10.1523/ENEURO.0255-19.2019.

[280] Patrick Theer and Winfried Denk. "On the fundamental imaging-depth limit in two-photon microscopy". In: *Journal of the Optical Society of America. A, Optics, Image Science, and Vision* 23.12 (2006), pp. 3139–3149. DOI: 10.1364/josaa.23.003139.

[281] Xiaowei Chen et al. "Functional mapping of single spines in cortical neurons *in vivo*". In: *Nature* 475.7357 (2011), p. 501. DOI: 10.1038/nature10193.

[282] Hongbo Jia et al. "Dendritic organization of sensory input to cortical neurons *in vivo*". In: *Nature* 464.7293 (2010), p. 1307. DOI: 10.1038/nature08947.

[283] Zsuzsanna Varga et al. "Dendritic coding of multiple sensory inputs in single cortical neurons in vivo". In: *Proceedings of the National Academy of Sciences* 108.37 (2011), pp. 15420–15425. DOI: 10.1073/pnas.1112355108.

[284] Nat Sternberg and Daniel Hamilton. "Bacteriophage P1 site-specific recombination: I. Recombination between loxP sites". In: *Journal of Molecular Biology* 150.4 (1981), pp. 467–486. DOI: 10.1016/0022-2836(81)90375-2.

[285] Micheal A. McLellan, Nadia A. Rosenthal, and Alexander R. Pinto. "Cre-loxP-Mediated Recombination: General Principles and Experimental Considerations". In: *Current Protocols in Mouse Biology* 7.1 (2017), pp. 1–12. DOI: 10.1002/cpmo.22.

[286] Ian Nauhaus, Kristina J. Nielsen, and Edward M. Callaway. "Nonlinearity of two-photon Ca2+ imaging yields distorted measurements of tuning for V1 neuronal populations". In: *Journal of Neurophysiology* 107.3 (2012), pp. 923–936. DOI: 10.1152/jn.00725.2011.

[287] M. Florencia Iacaruso, Ioana T. Gasler, and Sonja B. Hofer. "Synaptic organization of visual space in primary visual cortex". In: *Nature* 547.7664 (2017), pp. 449–452. DOI: 10.1038/nature23019.

[288] Benjamin Scholl et al. "Cortical response selectivity derives from strength in numbers of synapses". In: *Nature* 590.7844 (2021), pp. 111–114. DOI: 10.1038/s41586-020-03044-3.

[289] W Rall. "Handbook of physiology, the nervous system, Vol 1, Cellular biology of neurons". In: (1977).

[290] J. C. Magee and E. P. Cook. "Somatic EPSP amplitude is independent of synapse location in hippocampal pyramidal neurons". In: *Nature Neuroscience* 3.9 (2000), pp. 895–903. DOI: 10.1038/78800.

[291] Benjamin Scholl, Daniel E. Wilson, and David Fitzpatrick. "Local Order within Global Disorder: Synaptic Architecture of Visual Space". In: *Neuron* 96.5 (2017), 1127–1138.e4. DOI: 10.1016/j.neuron.2017.10.017.

[292] Matthew E Larkum and Thomas Nevian. "Synaptic clustering by dendritic signalling mechanisms". In: *Current Opinion in Neurobiology*. Signalling mechanisms 18.3 (2008), pp. 321–331. DOI: 10.1016/j.conb.2008.08.013.

[293] Guy Major, Matthew E. Larkum, and Jackie Schiller. "Active properties of neocortical pyramidal neuron dendrites". In: *Annual Review of Neuroscience* 36 (2013), pp. 1–24. DOI: 10.1146/annurev-neuro-062111-150343.

[294] Akiyuki Anzai, Izumi Ohzawa, and Ralph D. Freeman. "Neural Mechanisms for Processing Binocular Information I. Simple Cells". In: *Journal of Neurophysiology* 82.2 (1999), pp. 891–908. DOI: 10.1152/jn.1999.82.2.891.

[295] Connon I Thomas et al. "Targeting Functionally Characterized Synaptic Architecture Using Inherent Fiducials and 3D Correlative Microscopy". In: *Microscopy and Microanalysis* 27.1 (2021), pp. 156–169. DOI: 10.1017/S1431927620024757.

[296] Benjamin Scholl et al. "A binocular synaptic network supports interocular response alignment in visual cortical neurons". In: *Neuron* 110.9 (2022), 1573–1584.e4. DOI: 10.1016/j.neuron.2022.01.023.

[297] B. Chapman and M. P. Stryker. "Development of orientation selectivity in ferret visual cortex and effects of deprivation". In: *Journal of Neuroscience* 13.12 (1993), pp. 5251–5262.

[298] Thomas A. Pologruto, Bernardo L. Sabatini, and Karel Svoboda. "ScanImage: Flexible software for operating laser scanning microscopes". In: *BioMedical Engineering OnLine* 2 (2003), p. 13. DOI: 10.1186/1475-925X-2-13.

[299] Johannes Schindelin et al. "Fiji: an open-source platform for biological-image analysis". In: *Nature Methods* 9.7 (2012), pp. 676–682. DOI: 10.1038/nmeth.2019.

[300] Cameron Arshadi et al. "SNT: a unifying toolbox for quantification of neuronal anatomy". In: *Nature Methods* 18.4 (2021), pp. 374–377. DOI: 10.1038/s41592-021-01105-7.

[301] James B. Ackman, Timothy J. Burbridge, and Michael C. Crair. "Retinal waves coordinate patterned activity throughout the developing visual system". In: *Nature* 490.7419 (2012), pp. 219–225. DOI: 10.1038/nature11529.

[302] Hal S. Greenwald and David C. Knill. "Orientation Disparity: A Cue for 3D Orientation?" In: *Neural Computation* 21.9 (2009), pp. 2581–2604. DOI: 10.1162/neco.2009.08-08-848.

[303] Simo Vanni et al. "Anatomy and Physiology of Macaque Visual Cortical Areas V1, V2, and V5/MT: Bases for Biologically Realistic Models". In: *Cerebral Cortex (New York, NY)* 30.6 (2020), pp. 3483–3517. DOI: 10.1093/cercor/bhz322.

[304] J. Michael Hasse et al. "Morphological heterogeneity among corticogeniculate neurons in ferrets: quantification and comparison with a previous report in macaque monkeys". In: *The Journal of comparative neurology* 527.3 (2019), pp. 546–557. DOI: 10.1002/cne.24451.

[305] Yajie Tang et al. "In Vivo Two-photon Calcium Imaging in Dendrites of Rabies Virus-labeled V1 Corticothalamic Neurons". In: *Neuroscience Bulletin* 36.5 (2019), pp. 545–553. DOI: 10.1007/s12264-019-00452-y.

[306] Juliane Jaepel et al. *Two novel approaches for source identification of functional synaptic input architecture*. 2022. URL: https://www.abstractsonline.com/pp8/#!/10619/presentation/84062 (visited on 06/24/2023).

[307] M. Maletic-Savatic, R. Malinow, and K. Svoboda. "Rapid Dendritic Morphogenesis in CA1 Hippocampal Dendrites Induced by Synaptic Activity". In: *Science* 283.5409 (1999), pp. 1923–1927. DOI: 10.1126/science.283.5409.1923.

[308] Florian Engert and Tobias Bonhoeffer. "Dendritic spine changes associated with hippocampal long-term synaptic plasticity". In: *Nature* 399.6731 (1999), pp. 66–70. DOI: 10.1038/19978.

[309] N. Toni et al. "LTP promotes formation of multiple spine synapses between a single axon terminal and a dendrite". In: *Nature* 402.6760 (1999), pp. 421–425. DOI: 10.1038/46574.

[310] Jean-Vincent Le Bé and Henry Markram. "Spontaneous and evoked synaptic rewiring in the neonatal neocortex". In: *Proceedings of the National Academy of Sciences of the United States of America* 103.35 (2006), pp. 13214–13219. DOI: 10.1073/pnas.0604691103.

[311] Benjamin Scholl and David Fitzpatrick. "Cortical synaptic architecture supports flexible sensory computations". In: *Current Opinion in Neurobiology*. Systems Neuroscience 64 (2020), pp. 41–45. DOI: 10.1016/j.conb.2020.01.013.

[312] Zachary C. Lipton, John Berkowitz, and Charles Elkan. *A Critical Review of Recurrent Neural Networks for Sequence Learning*. 2015. arXiv: 1506.00019[cs].

[313] Subhashini Venugopalan et al. *Sequence to Sequence – Video to Text*. 2015. DOI: 10.48550/arXiv.1505.00487. arXiv: 1505.00487[cs].

[314] Nitish Srivastava, Elman Mansimov, and Ruslan Salakhutdinov. *Unsupervised Learning of Video Representations using LSTMs*. 2016. DOI: 10.48550/arXiv.1502.04681. arXiv: 1502.04681[cs].

A. Appendix

A.1. Original publication

Neuron

Article

A binocular synaptic network supports interocular response alignment in visual cortical neurons

Graphical abstract

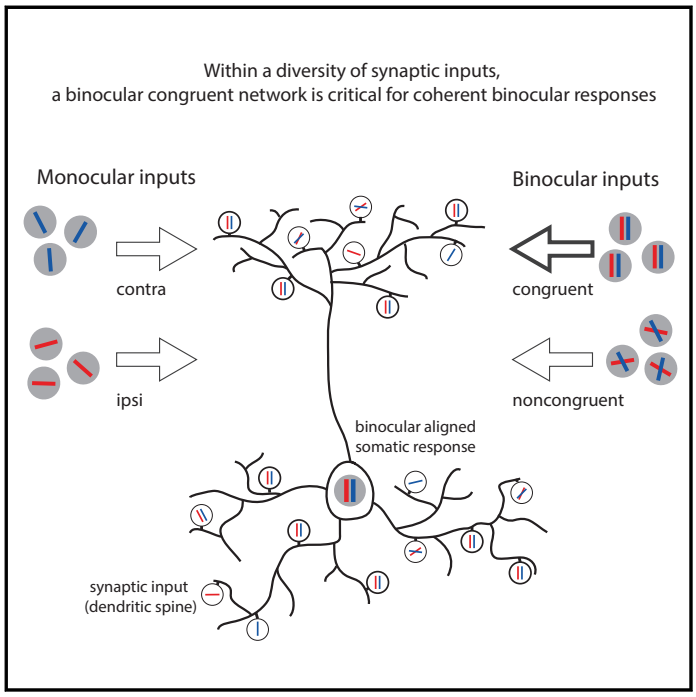

Authors

Benjamin Scholl, Clara Tepohl, Melissa A. Ryan, Connon I. Thomas, Naomi Kamasawa, David Fitzpatrick

Correspondence

benjamin.scholl@pennmedicine.upenn.edu

In brief

Scholl, Tepohl, et al. investigate how signals from the two eyes are combined within synaptic populations of individual neurons to shape a coherent representation. Rather than a convergence of monocular streams, they find that intracortical binocular networks are key to shaping alignment in cortical layer 2/3.

Highlights

- Layer 2/3 neurons in visual cortex receive monocular and binocular synaptic inputs
- Monocular inputs alone cannot account for somatic binocular alignment
- Binocular congruent inputs exhibit functional properties ideally suited for alignment
- Dominant influence of binocular congruent inputs derives from strength in numbers

Scholl et al., 2022, Neuron *110*, 1573–1584
May 4, 2022
https://doi.org/10.1016/j.neuron.2022.01.023

CellPress

Neuron

CellPress

Article

A binocular synaptic network supports interocular response alignment in visual cortical neurons

Benjamin Scholl,[3,4,5,*] Clara Tepohl,[1,4] Melissa A. Ryan,[2] Connon I. Thomas,[2] Naomi Kamasawa,[2] and David Fitzpatrick[1]
[1]Functional Architecture and Development of Cerebral Cortex, Max Planck Florida Institute for Neuroscience, 1 Max Planck Way, Jupiter, FL, USA
[2]Electron Microscopy Core Facility, Max Planck Florida Institute for Neuroscience, 1 Max Planck Way, Jupiter, FL, USA
[3]Department of Neuroscience, Perelman School of Medicine, University of Pennsylvania, Philadelphia, PA, USA
[4]These authors contributed equally
[5]Lead contact
*Correspondence: benjamin.scholl@pennmedicine.upenn.edu
https://doi.org/10.1016/j.neuron.2022.01.023

SUMMARY

In visual cortex, signals from the two eyes merge to form a coherent binocular representation. Here we investigate the synaptic interactions underlying the binocular representation of stimulus orientation in ferret visual cortex with *in vivo* calcium imaging of layer 2/3 neurons and their dendritic spines. Individual neurons with aligned somatic responses received a mixture of monocular and binocular synaptic inputs. Surprisingly, monocular pathways alone could not account for somatic alignment because ipsilateral monocular inputs poorly matched somatic preference. Binocular inputs exhibited different degrees of interocular alignment, and those with a high degree of alignment (congruent) had greater selectivity and somatic specificity. While congruent inputs were similar to others in measures of strength, simulations show that the number of active congruent inputs predicts aligned somatic output. Our study suggests that coherent binocular responses derive from connectivity biases that support functional amplification of aligned signals within a heterogeneous binocular intracortical network.

INTRODUCTION

Neural circuits in the central nervous system combine independent sources of sensory information to form coherent percepts and guide motor actions. In the visual system, a critical step in building coherent neural representations is combining signals from the two eyes. Binocular convergence is the basis of cyclopean perception, stereopsis, and increased acuity and sensitivity (Barendregt et al., 2015; Parker, 2007; Scholl et al., 2013a). In carnivores and primates, binocular convergence first occurs in the primary visual cortex (V1) where individual neurons respond selectively to sensory stimulation of one or both eyes (Hubel and Wiesel, 1962, 1965; Ohzawa and Freeman, 1986a; Priebe, 2008). Cortical neurons are also selective for edge orientation (Hubel and Wiesel, 1962; Priebe and Ferster, 2012), and in all mammals investigated, most binocular neurons exhibit matched orientation preferences for stimuli presented to each eye (Bridge and Cumming, 2001; Chang et al., 2020; Ferster, 1981; Hubel and Wiesel, 1962; Nelson et al., 1977; Skottun and Freeman, 1984; Wang et al., 2010). While interocular alignment is considered to be a prerequisite for binocular vision (Marr and Poggio, 1979), the synaptic basis of this phenomenon is poorly understood.

Ultimately, interocular alignment in the responses of individual neurons reflects the population of excitatory inputs synapsing onto their dendritic arbors. Receptive field properties resulting from the activity of synapses driven by the contralateral eye must be matched with those driven by the ipsilateral eye. In the simplest case, this can be conceptualized as the integration of separate, matched monocular streams converging on a postsynaptic neuron. Experimental studies and theoretical models of interocular response alignment typically focus on this perspective, proposing that contra- and ipsilateral eye-driven synapses with strong, correlated sensory-driven activity are strengthened and/or maintained during development (Bhaumik and Shah, 2014; Bienenstock et al., 1982; Erwin and Miller, 1998; Gu and Cang, 2016; Hofer et al., 2009; Mrsic-Flogel et al., 2007; Sarnaik et al., 2014; Smith and Trachtenberg, 2007; Tan et al., 2020; Wang et al., 2010; Xu et al., 2020).

Overlooked from this monocular framework, however, is the fact that much of the synaptic input a cortical neuron receives during stimulation of either eye arises from other cortical neurons that are binocular, especially in superficial layers of V1 (Anzai et al., 1999; Ohzawa and Freeman, 1986b; Scholl et al., 2013b; Skottun and Freeman, 1984). Thus, for most binocular cortical neurons, synaptic input derived from both monocular and

CellPress

Neuron
Article

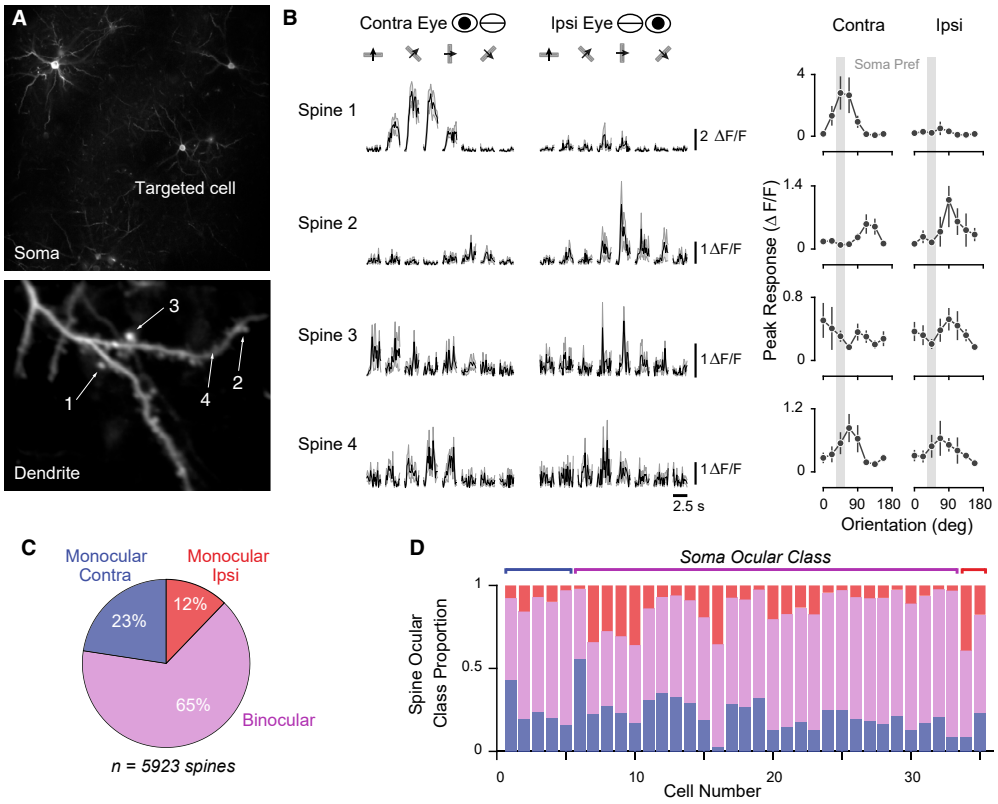

Figure 1. Mapping synaptic input ocularity in layer 2/3 cortical neurons with two-photon imaging of dendritic spines

(A) Sparse labeling of neurons in ferret V1 with GCaMP6s. Standard deviation projection of an example cell (top) and one of its dendrites (bottom) with visible spines.

(B) Responses of four example spines shown in (A) to drifting gratings presented to the contra and ipsi eye. Shown are mean (black) and standard deviation (gray) responses to each stimulus (n = 8 trials) presented to the contra (left) and ipsi (right) eyes. Also shown (right column) are the peak amplitude response mean (black dots) and standard deviation (lines). The preferred orientation of the soma is indicated as a vertical gray bar. For more binocular noncongruent examples see also Figure S1.

(C) Proportions of spines of each ocular class.

(D) Proportions of spines from each ocular class for individual neurons of each ocular class (see bar above), sorted by increasing proportion of binocular spines (purple). Same color scheme as in (C).

binocular neurons could play a role in interocular response alignment. While whole-cell recordings have measured monocular and binocular excitatory synaptic conductances (Gu and Cang, 2016; Longordo et al., 2013; Scholl et al., 2013b; Zhao et al., 2013), this technique cannot disentangle the response properties of individual synaptic inputs. Consequently, the specific contributions of monocular and binocular inputs to interocular response alignment remain unresolved.

To address this issue, we used *in vivo* two-photon microscopy to visualize layer 2/3 neurons in ferret V1 expressing GCaMP6s (Scholl et al., 2021; Wilson et al., 2016). We characterized the ocular class and orientation preference of individual dendritic spines, the postsynaptic sites of excitatory synapses on pyramidal neurons. We measured responses to stimulation of either eye and compared this to the somatic output. Individual neurons with binocularly aligned somatic responses received both monocular and binocular inputs. The response properties of monocular inputs alone could not explain binocular somatic alignment. Binocular inputs themselves exhibited a varying degree of interocular alignment, which we quantified using the cross-correlation between each eye's orientation tuning, termed "congruency." Binocular congruent inputs were functionally distinct, exhibiting a high degree of orientation selectivity and match to the somatic output orientation preference. A trial-based simulation of synaptic integration incorporating stimulus-driven activity demonstrated a predominate role for binocular congruent inputs in shaping the interocular response alignment of cortical neurons. Finally, we found that somatic alignment, across our entire population of cells, was predicted by binocular synaptic network properties, but not monocular ones. Our results emphasize a critical role for intracortical binocular network interactions in shaping the interocular response alignment of cortical neurons.

Neuron
Article

CellPress

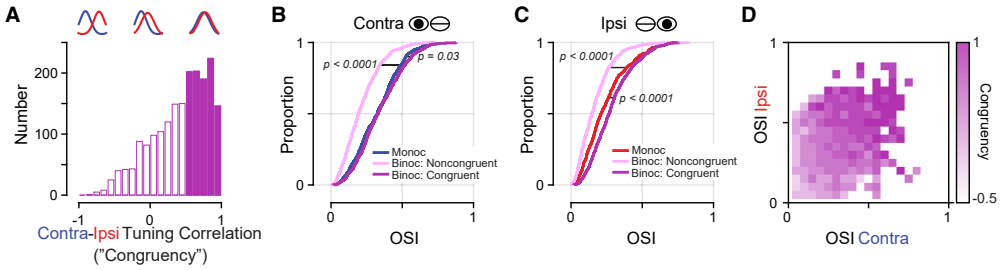

Figure 2. Binocular congruent inputs are most selective for orientation

(A) Distribution of binocular input "congruency": correlation coefficient between contra and ipsi orientation tuning. Binocular inputs with a correlation >0.5 are defined as congruent (filled bars).

(B and C) Cumulative distribution of OSI for monocular, binocular noncongruent, and binocular congruent synapses for contra (B) and ipsi (C) stimulation. Note, monocular contra inputs are more selective than monocular ipsi inputs (p = 0.0001, Wilcoxon rank-sum test).

(D) Heatmap of mean congruency of binocular inputs with respect to contra and ipsi OSI. See also Table 1.

RESULTS

Individual layer 2/3 cortical neurons receive synaptic inputs with diverse ocular properties

To investigate how monocular and binocular synaptic networks contribute to ocular alignment, we performed *in vivo* two-photon calcium imaging of layer 2/3 cells in ferret visual cortex sparsely labeled with GCaMP6s (Figure 1A; see STAR Methods). Ferrets had at least 1 week of visual experience. For each cell, we optimized visual stimuli while imaging the soma. We then serially imaged visible dendritic spines on apical and basal dendrites during visual stimulation. For each imaging location, we used drifting gratings of different orientations presented to each eye independently and analyzed their responses to characterize orientation tuning (Figures 1B and S1; see STAR Methods). In total we characterized 5,923 visually responsive (see STAR Methods) dendritic spines from 35 cells.

Ocular classes for each soma and dendritic spine were based on whether a significant response (see STAR Methods) was elicited by visual stimulation of only the contralateral eye (contra), only the ipsilateral eye (ipsi), or both eyes (binocular). A majority of dendritic spines were classified as binocular (Figure 1C) and a similar trend was found for individual cells (Figure 1D; mean = 64% ± 11% SD). All cells examined received synaptic inputs from each ocular class, displaying a functional diversity of synaptic populations that has been reported for other visual features, sensory areas, and species (Scholl and Fitzpatrick, 2020).

In this study, we aim to determine how synaptic populations with distinct ocular properties contribute to aligned responses at the soma. Thus, we focus exclusively on binocular cells, as defined by somatic responses (n = 28/35).

Binocular synapses vary in degree of congruency

Individual binocular synapses varied in the degree of similarity in orientation tuning between contra and ipsi eye stimulation. To characterize contra-ipsi similarity, we computed the Pearson correlation coefficient between responses evoked by stimulation for each eye. Henceforth, we define this metric as the degree of "congruency." Two binocular example spines are shown in Figure 1B for comparison (spine 3 and spine 4, congruency = 0.16 and 0.84, respectively). Binocular inputs exhibited a wide range of congruency but were biased toward positive values (median = 0.39, IQR = 0.68, n = 3117; Figure 2A). For subsequent comparisons, we split these synapses into two synaptic groups: binocular congruent ($r_{C\text{-}I} > 0.5$, n = 1,296 spines, 42% of all binocular inputs) and binocular noncongruent ($r_{C\text{-}I} < 0.5$, n = 1,802 spines, 58% of all binocular inputs). Splitting binocular synapses into two groups will be important for later analyses, as we will show that binocular congruent inputs have distinct functional properties and play a unique role in determining a cell's feature alignment. We note that the exact cutoff value does not affect our results and, for transparency, also report analyses without this categorization. We repeated our analysis with a bootstrapped measure of congruency but found no qualitative difference in our results (Figure S2).

Our goal is to examine how monocular and binocular synaptic networks contribute to interocular response alignment in binocular cells. However, our dataset includes binocular cells with poor alignment, similar to previous reports in visually experienced animals (Bridge and Cumming, 2001; Chang et al., 2020). Thus, we focus exclusively on binocular cells with congruent ($r_{C\text{-}I} > 0.5$) somatic orientation tuning between the two eyes (n = 16/28) and their synapses (n = 2,933, binocular spines n = 1,920, median congruency = 0.5) for the remainder of this study. Overall, congruency was directly related to interocular orientation preference difference, a measure used in previous studies of visual cortical neurons (circular-linear correlation = 0.74, p < 0.0001, n = 2,558 binocular spines with selective tuning for each eye [see STAR Methods]). Based on this relationship, our chosen cut-off ($r_{C\text{-}I} = 0.5$) equates to ~19 degrees of orientation preference mismatch.

Binocular congruent synapses exhibit high orientation selectivity and connection specificity

We first investigated the response characteristics of the synapses for each ocular class (monocular, binocular congruent, and binocular noncongruent), focusing on response selectivity and connection specificity. These two properties provide a measurement of how well a synapse conveys a given stimulus feature (selectivity) and how well synapses align to the orientation

Table 1. Comparing selectivity and specificity (soma mismatch) between spine ocular classes

	Binocular Congruent	Binocular Noncongruent	Monocular
Orientation Selectivity			
Contralateral responses			
Median (IQR)	*0.33 (0.24)*	*0.19 (0.18)*	*0.32 (0.23)*
Binocular Congruent	–	$p < 0.0001$	$p = 0.03$
Binocular Noncongruent	–	–	$p < 0.0001$
Ipsilateral responses			
Median (IQR)	*0.27 (0.20)*	*0.15 (0.16)*	*0.21 (0.20)*
Binocular Congruent	–	$p < 0.0001$	$p < 0.0001$
Binocular Noncongruent	–	–	$p < 0.0001$
Specificity			
Contralateral Responses			
Median (IQR)	*10.6 (16.3)*	*18.0 (37.5)*	*12.8 (21.0)*
Binocular Congruent	–	$p < 0.0001$	$p = 0.18$
Binocular Noncongruent	–	–	$p < 0.0001$
Ipsilateral Responses			
Median (IQR)	*11.5 (18.4)*	*20.8 (29.4)*	*22.5 (46.9)*
Binocular Congruent	–	$p < 0.0001$	$p < 0.0001$
Binocular Noncongruent	–	–	$p = 0.62$

All statistical tests are Wilcoxon's rank-sum test. Soma mismatch is in degree.

preference of the somatic output (specificity). Both properties are key factors in the interocular alignment of synaptic populations within a neuron. Additionally, we consider these properties for stimulation of the contra- and ipsilateral eye separately for the three ocular classes. This allows a straightforward comparison of the properties of monocular and binocular inputs driven by the contra- and ipsilateral eye.

Binocular congruent inputs exhibited the greatest degree of orientation selectivity (see STAR Methods) for responses elicited by contra and ipsi stimulation (Figures 2B and 2C; Table 1; median orientation selectivity index [OSI] = 0.26). This ocular class was more selective than binocular noncongruent inputs (Table 1), monocular ipsi inputs, and slightly more selective than monocular contra inputs. Notably, binocular noncongruent inputs were the least selective for orientation overall, and monocular contra inputs were more selective than monocular ipsi inputs ($p < 0.0001$, Wilcoxon rank-sum test). There was also a strong positive correlation between congruency and selectivity for contra and ipsi stimulation (contra: Spearman's $r = 0.47$, $p < 0.0001$; ipsi: Spearman's $r = 0.50$, $p < 0.0001$; Figure 2D).

To evaluate connection specificity, we measured the mismatch between the preferred orientation of each spine and that of their corresponding somatic output (Figure 3A); a mismatch closer to 0 equates to greater specificity. For this analysis we excluded spines unselective for orientation (OSI < 0.10). Binocular congruent inputs were most aligned to the somatic output (Figures 3B and 3C; Table 1). These inputs exhibited less mismatch than monocular ipsi inputs. A similar, but non-significant, trend was found for monocular contra inputs. Binocular noncongruent inputs, on the other hand, exhibited the most mismatch for contra stimulation, significantly less than corresponding monocular inputs. For ipsi stimulation, binocular noncongruent inputs were indistinguishable from monocular inputs. Consistent with the differences between binocular categories, mismatch was inversely correlated with congruency (contra: circular-linear $r = -0.30$, $p < 0.0001$; ipsi: circular-linear $r = -0.34$, $p < 0.0001$). Remarkably, monocular contra inputs displayed less mismatch than monocular ipsi inputs ($p = 0.001$, circular Kruskal-Wallis test; Figures 3B and 3C), highlighting a difference between monocular input streams. Importantly, the exact method for computing congruency and defining binocular congruent inputs had no impact on these findings (Figure S2).

The weak specificity and selectivity evident in monocular ipsi inputs clearly demonstrates that monocular input streams alone cannot be the basis of interocular alignment. Instead, we find that a subset of binocular synapses are most selective and functionally specific and are best positioned to support the binocularly aligned responses of layer 2/3 neurons.

Monocular and binocular synapses are similar in ultrastructural anatomy

While the distinct functional properties of binocular congruent inputs could support interocular response alignment, they comprise only ~1/3 of a cell's total inputs (binocular congruent: 33% ± 18%, binocular noncongruent: 32% ± 11%, monocular: 35% ± 13%; proportion mean ± SD). However, the impact of binocular congruent synapses could be enhanced by increased strength. As synaptic strength is reflected in the ultrastructural anatomy (Holler et al., 2021; Lee et al., 2016; Scholl et al., 2021), one possibility is that binocular congruent synapses also share distinct ultrastructural properties.

We recently developed a method to correlate light and electron microscopy at the synaptic level (Figure 4; see STAR Methods), allowing comparison of the same synapses (Thomas et al., 2021). For four binocular congruent cells that had been imaged *in vivo*, we anatomically reconstructed dendritic spines from basal dendrites. In a subset of responsive spines ($n = 103$), we classified ocularity based on the criteria used in this study (see STAR Methods). Spines sampled from the cells used for reconstruction exhibited similar ocular properties as cells which only underwent two-photon imaging. From the reconstruction dataset, we examined three basic anatomical features: spine head volume, postsynaptic density (PSD) area, and spine neck length (Figure 4D). Spine head volume and PSD area are positively correlated with synapse strength (Bourne and Harris, 2011; Toni et al., 1999), while spine neck length can attenuate synapse strength (Araya et al., 2006).

Overall, binocular congruent inputs were similar in ultrastructure compared to other ocular classes (Figure S3; Table S1). This was supported by a nonparametric one-way analysis of variance of spine head volume ($p = 0.58$), spine PSD area ($p = 0.098$), and spine neck length ($p = 0.093$). We also found no relationship between congruency and any other anatomical feature (spine head volume: Spearman's $r = 0.003$, $p = 0.49$; PSD area: Spearman's $r = 0.10$, $p = 0.21$; neck length: Spearman's $r = -0.009$, $p = 0.47$). We found similar results when considering

Neuron
Article

CellPress

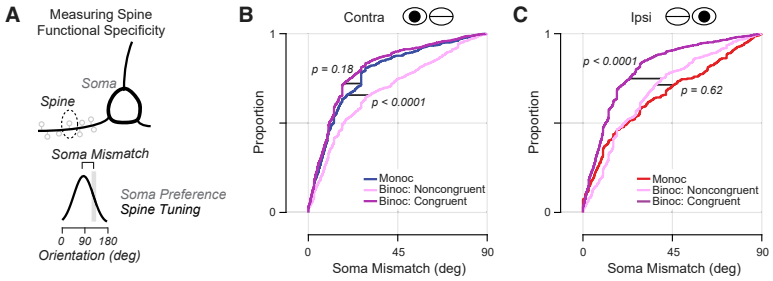

Figure 3. Binocular congruent inputs exhibit highest degree of connection specificity

(A) Connection specificity measured by comparing mismatch in orientation preference between individual spines and the soma.

(B and C) Cumulative distribution of soma mismatch for monocular, binocular noncongruent, and binocular congruent inputs for contra (B) and ipsi (C) stimulation. See also Table 1.

a metric of synaptic strength that combines multiple anatomical features and their interactions (e.g., synapse PSD area and neck length inversely regulate synapse strength). We used a NEURON model of each synapse, incorporating all anatomical features, and simulated the somatic depolarization due to a single action potential (see STAR Methods). This showed that binocular congruent inputs were similar in effective strength to other ocular classes ($p = 0.50$, nonparametric one-way ANOVA; Figure 4E; Table S1). Likewise, congruency was unrelated to simulated somatic input amplitude (Spearman's $r = 0.07$, $p = 0.71$). Altogether, our data demonstrate that binocular congruent synapses are similar in ultrastructural anatomy and simulated effective strength compared to monocular and binocular noncongruent synapses.

Simulating synaptic population activity and the emergence of interocular aligned responses

Binocular congruent synapses have distinct response properties, suggesting they are uniquely positioned to support interocular alignment. But their ultrastructural features (a measurement of strength) are largely similar to other ocular classes, suggesting that synaptic strength is not a mechanism to enhance drive. Strength alone, however, cannot predict how synapses might drive somatic activity during visual stimulation. Somatic activity derives from the "activity patterns" of functionally diverse populations of monocular and binocular synapses that are jointly recruited by a particular stimulus. Activity patterns are not only driven by synapse response properties but also their reliability in activation. This raises the question of whether reliability could be another factor contributing to interocular alignment. In fact, we found that binocular congruent inputs were more reliable in response to preferred stimuli compared to other ocular classes (Figure S4). This made us wonder how sensory-driven activity, stimulus selectivity, connection specificity, and reliability of activation altogether produce an aligned somatic response on a trial-by-trial basis.

To understand how activity patterns of monocular and binocular synapses act in concert to shape alignment, we devised a simple simulation of the aggregate synaptic drive onto each neuron (drawn from each neuron's measured synaptic population). Our simulation incorporates only synaptic calcium activity (converting $\Delta F/F$ into binary events) during presentations of visual stimuli (example branch shown in Figure 5A). For each simulation iteration, a random trial of one set of stimuli was chosen, and the activity across all dendrites and all groups of spines was summed to create an aggregate, simulating somatic aggregate input for each cell (Figures 5B–5D). This procedure was repeated 10,000 times for contra and ipsi visual stimulation. Simulation of the total aggregate for a representative binocular congruent cell is shown in Figure 5D ($n = 197$ spines). While we ignore factors such as dendritic compartmentalization and active nonlinearities, this simulation provides an estimate of stimulus-driven input to the soma from each ocular class.

Across all cells ($n = 14$, total spines $= 192 \pm 69$, mean $\pm$ SD), the number of active spines was greatest at the somatic preferred orientation (contra: $18.6\% \pm 2.2\%$, ipsi: $11.5\% \pm 2.1\%$, mean $\pm$ SE; Figure 6A) and the proportion of active synapses at somatic preferred orientation was similar for each group (binocular congruent: 6.5% and 5.4%; binocular noncongruent: 5.9% and 4.8%; monocular: 6.1% and 3.9%; mean proportion active for contra and ipsi eyes; Figure 6A). In contrast, for nonpreferred orientations, monocular and binocular noncongruent inputs were recruited more readily (binocular congruent: 1.4% and 1.3%, binocular noncongruent: 3.0% and 2.8%, monocular: 2.5% and 2.6%, mean proportion active for contra and ipsi eyes; Figure 6A).

We next examined aggregate specificity across all simulation iterations. Preferred orientation was defined as the stimulus evoking the largest proportion of active spines, similar to a maximum *a posteriori* estimate (Figure 6B). Not surprisingly, binocular congruent aggregates were more frequently aligned than monocular or noncongruent aggregates ($p = 0.006$ and $p = 0.018$, respectively, sign-rank one-sided test; Figure 6B). While frequency of alignment for all ocular classes was correlated with the total aggregate (monocular: Spearman $r = 0.75$, $p < 0.0001$; binocular congruent: Spearman $r = 0.93$, $p < 0.0001$; binocular noncongruent: Spearman $r = 0.82$, $p < 0.0002$, one-sided tests), binocular noncongruent and monocular aggregates were consistently *less* aligned than the total ($p = 0.002$ and $p = 0.01$, respectively, sign-rank one-sided test). In contrast, binocular congruent aggregates were indistinguishable from the total aggregate ($p = 0.33$, sign-rank one-sided test, mean difference $= -0.01 \pm 0.06$ SD). Adding a dendritic nonlinearity (i.e., nonlinear synaptic summation) to our simulation did not appreciably change these results (Figure S5).

Our simulation suggests that (1) a greater number of active synapses contribute to the somatic preferred orientation for both eyes, and (2) the binocular congruent synapse population exhibits a degree of alignment similar to the total population. These analyses, however, do not consider variation across

CellPress

Neuron
Article

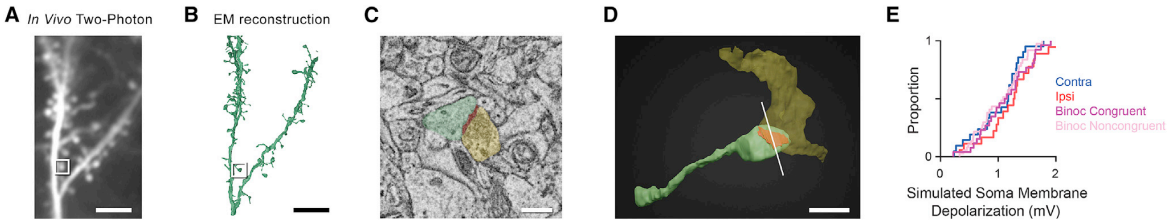

Figure 4. Correlation of light and electron microscopy at synaptic resolution

(A) Example *in vivo* two-photon standard deviation projection of dendrite and spines. Scale bar is 10 μm.

(B) Same dendrite and spines reconstructed from an electron microscopy volume. Scale bar is 10 μm.

(C) Electron micrograph of an example synapse in (A and B) showing the presynaptic bouton (yellow), postsynaptic density (red), and dendritic spine head (green). Scale bar is 500 nm.

(D) Full 3D reconstruction of the example synapse shown in (A–C). The white bar represents the cross section in (C). Scale bar is 1 μm.

(E) Cumulative distributions of simulated soma membrane potential depolarization for synapses of each ocular class. Postsynaptic anatomical measurements were combined in a NEURON model to simulate effective somatic input (see STAR Methods). See also Figure S3 and Table S1.

each simulation run, nor a possible relationship between the number of active synapses and degree of alignment. Further, as the total aggregate (Figure 6A, top) is most akin to subthreshold input that might elicit somatic action potentials, we wanted to understand how the number of active synapses from each ocular class contributes to the total aggregate and its alignment. Accordingly, we measured the total aggregate alignment (defined as the distance from the somatic preferred orientation) and the total number of active synapses at the preferred orientations (Figure 6C, black circles) for each simulation iteration. We then examined the contribution of different ocular classes of synapses at preferred orientations (Figure 6C, right). As shown for individual simulation runs in Figure 6C, an aligned total aggregate coincided with a large number of active synapses at the somatic preferred orientation, with binocular congruent synapses being the largest contributor. In contrast, a misaligned total aggregate showed less activation overall and more input from binocular noncongruent and monocular synapses.

Across our population of cells, we found that with a large number of active synapses where a large fraction is binocular congruent, the total aggregate is more aligned (Figure 6D, top). For binocular noncongruent synapses, we observed a different relationship: alignment correlated with fewer active binocular noncongruent synapses and greater activation of the total population (Figure 6D, middle). For monocular ipsi synapses, we observed a similar relationship as for binocular noncongruent synapses (Figure 6D, bottom right), and the fraction of monocular contra synapses recruited showed little relationship to alignment or the total synapses active (Figure 6D, bottom left). Multivariate linear regression models largely confirmed these observations (Table S2, see STAR Methods), but for contra visual stimulation, the total number of active synapses was a weak predictor. These relationships were also found for individual cells; the total number of active spines was positively related to alignment in a majority of cells (contra: binocular congruent = 10/14, binocular noncongruent = 9/14, monocular = 10/14; ipsi: binocular congruent = 14/14, binocular noncongruent = 14/14, monocular = 14/14 cells). With respect to each ocular class, a majority of cells showed that the fraction of binocular congruent spines was positively related to alignment (contra: 8/14; ipsi: 9/14), while binocular noncongruent and monocular fractions were inversely related to alignment (contra: 10/14 and 9/14, respectively; ipsi: 9/14 and 12/14, respectively). Interestingly, if an interaction term was included in the linear regression model, it was weighted more heavily (Table S2), providing further evidence that alignment is predicted by the total number of active synapses and total fraction of those that are binocular congruent.

Our simulation suggests that interocular alignment depends on the contribution of binocular congruent populations *and* the total number of active synapses. While binocular congruent inputs do not constitute the majority of inputs to a cell overall, they are selectively recruited at the somatic preferred orientation, resulting in a disproportionate impact. This impact is likely enhanced by co-active monocular and binocular noncongruent inputs to increase synaptic drive overall, potentially increasing the probability of generating spiking activity at the soma. This could also coincide with nonlinearities that trigger dendritic spikes, enhancing somatic drive and aggregate specificity. Altogether, it is clear that binocular congruent synapses strongly support feature-matched responses between the two eyes.

Somatic congruency is predicted by the relative proportion of binocular synaptic inputs

While we have focused solely on synaptic inputs to binocular congruent cells, it is possible that diversity in somatic congruency derives from the underlying synaptic inputs. We wondered whether characteristics of our synaptic populations could predict the degree of congruency of their respective soma; specifically, we wondered whether the number of available inputs from each ocular class could predict somatic congruency. Not surprisingly, binocular noncongruent cells (n = 12) had significantly less binocular congruent synaptic inputs than binocular congruent cells (18% ± 8% and 33% ± 18%, respectively, mean ± SD, p = 0.01, one-sided Wilcoxon rank-sum test). Therefore, we compared the proportion of spines from each ocular class to somatic congruency. We observed a tradeoff between binocular congruent and noncongruent synapses: the proportion of binocular congruent synapses was positively correlated with somatic congruency (r = 0.47, p = 0.006, one-sided Spearman correlation; Figure 7A) and the proportion of binocular

Neuron
Article

CellPress

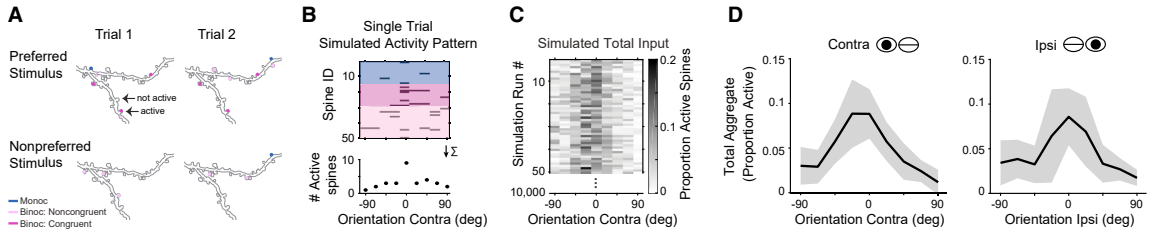

Figure 5. A simple model simulating synaptic input aggregates

(A) Example trial-to-trial activity of dendritic spines at the somatic preferred and non-preferred stimulus. Dendritic spines filled with color are those that are active.

(B) Activity pattern (discrete calcium events, shown in black, see STAR Methods) of a subset of spines (n = 50) for a single simulation iteration. Shown is activity driven by contra stimulation, with respect to the somatic preferred orientation. Spines are grouped and color coded by their ocular class. To estimate total aggregate input for a single trial, the activity of all spines is summed (bottom).

(C) Individual total aggregates for 50 (out of 10,000) simulation runs. Data are the proportion of possible spines active (here 197 spines).

(D) Total synaptic aggregate estimated for contra and ipsi stimulation. Shown are the mean and standard deviation.

noncongruent synapses was inversely correlated with somatic congruency ($r = -0.63$, $p < 0.0002$, one-sided Spearman correlation; Figure 7B). In contrast, the proportion of monocular spines was unrelated to somatic congruency (contra: $r = -0.07$, $p = 0.7$, ipsi: $r = 0.04$, $p = 0.8$, two-sided Spearman correlation; Figure 7C), highlighting the unique influence of binocular populations.

In sum, our results suggest that binocular congruency of somatic responses derives from a balance of intracortical subnetworks: aligned, selective, binocular congruent and less selective, misaligned, binocular noncongruent inputs.

DISCUSSION

Visual cortical neurons exhibit binocularly matched responses, yet it is unknown how this coherent representation emerges from converging sets of synapses that originate from monocular and binocular neurons. In this study we examined synaptic populations on individual layer 2/3 neurons in ferret visual cortex to determine how different networks contribute to the interocular alignment of orientation preference. All cells were innervated by inputs driven by stimulation of the ipsilateral or contralateral eye (monocular) and inputs driven by stimulation of either eye (binocular). Binocular inputs could be split into two groups (congruent and noncongruent), depending on the degree of correlation between contra and ipsi orientation tuning. Binocular congruent inputs were distinct as they were most selective for orientation and exhibited the highest degree of connection specificity. To better understand monocular and binocular synaptic integration, we devised a simple simulation combining sensory-driven synaptic activity. This simulation revealed a predominate role for binocular congruent inputs, contributing a selective and highly aligned aggregate input. This arose through the combination of their connection specificity, tuning selectivity, and strength in numbers. Finally, we observed that somatic response alignment of binocular cells was predicted by the relative percentage of binocular congruent and noncongruent inputs that synapse onto a neuron.

Our study shows how a distinct binocular synaptic network shapes interocular response alignment in layer 2/3 neurons, suggesting that alignment in these cells emerges through intracortical circuitry. While we do not know the precise origin of synapses imaged in this study, we base this conclusion on two observations: (1) inputs to layer 2/3 pyramidal neurons are primarily intracortical (Binzegger et al., 2004) and (2) cells in the lateral geniculate nucleus of carnivores and primates are almost exclusively monocular.

As cortical binocularity emerges over development in carnivores (Casagrande and Boyd, 1996; Chang et al., 2020; Hubel and Wiesel, 1965), intracortical networks might involve recurrent amplification, such as found for stimulus-tuned attractor networks (Ahmadian et al., 2013; Ben-Yishai et al., 1995). Visual stimuli preferred by the soma could be amplified by binocular congruent synapses, as they provide highly specific (and aligned) excitatory drive. Noncongruent inputs might provide nonspecific excitatory drive, depolarizing the soma closer to spike threshold and increasing the probability of eliciting spikes (Priebe, 2008). Altogether, it is clear that at this cortical processing stage, binocular, rather than monocular, synaptic networks are most important in shaping interocular alignment of neural response properties.

Comparison with monocular convergence models

Conventional models of binocular alignment focus on converging monocular input streams. In these models, contra and ipsi inputs onto single neurons become matched with one another through correlation-based plasticity mechanisms. This framework has been used to interpret experimental findings (Gu and Cang, 2016; Sarnaik et al., 2014; Tan et al., 2020; Wang et al., 2010), and additional support comes from models that recapitulate experimental findings by simulating interactions between monocular input streams (Bhaumik and Shah, 2014; Bienenstock et al., 1982; Erwin and Miller, 1998; Xu et al., 2020). Thus, the expectation has been that monocular input populations would exhibit a high degree of match in orientation preference. In contrast, our results from visually experienced ferrets do not support this prediction.

Our study does not rule out a monocular convergence hypothesis entirely. The layer 2/3 neurons we targeted primarily receive intracortical input and little or no thalamocortical

CellPress

Neuron
Article

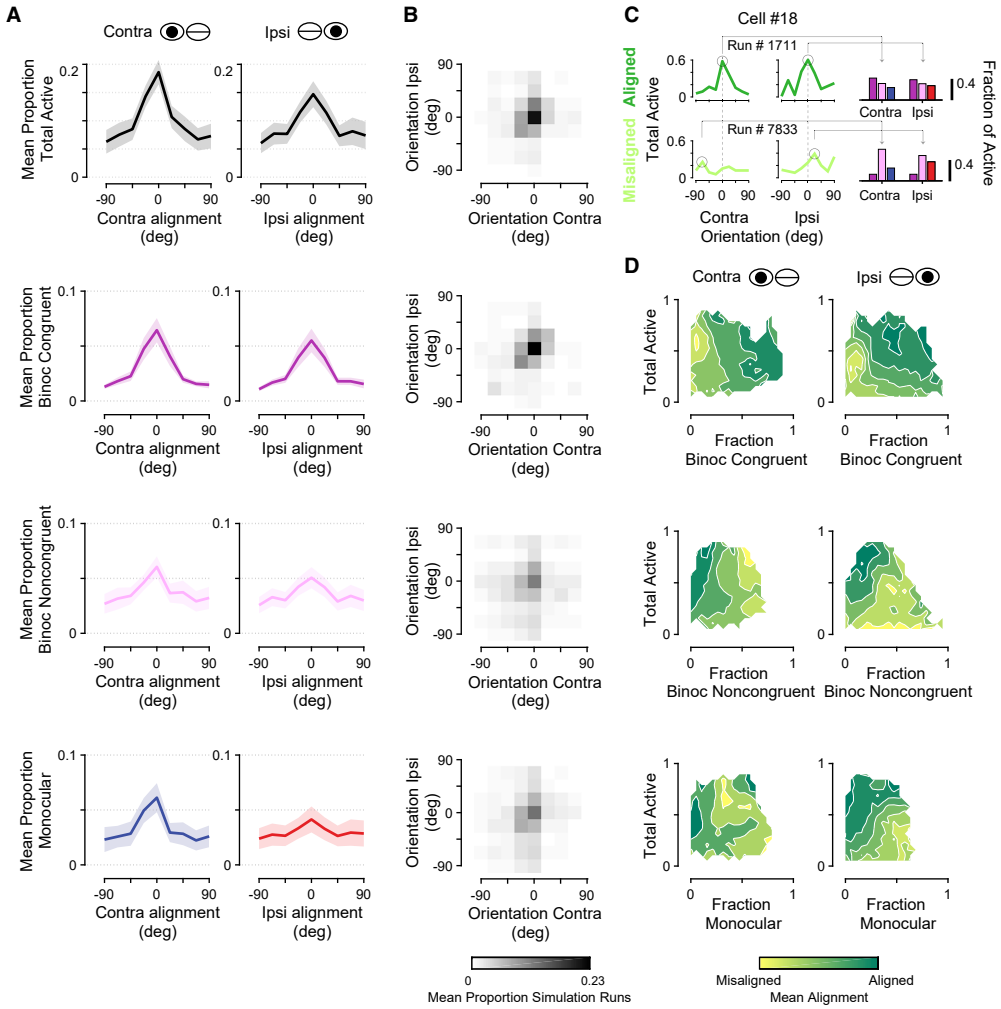

Figure 6. Interocular alignment of total synaptic aggregates strongly depends on activation of binocular congruent synapses

(A) Simulated aggregate tuning for contra and ipsi stimulation across 14 binocular congruent cells. From top to bottom: total aggregate, binocular congruent populations, binocular noncongruent populations, and monocular populations. Tuning is with respect to the soma preferred orientation; data are mean and standard error. See also Figure S5 for the nonlinear model.

(B) Interocular distributions of trial-to-trial alignment of aggregates to the somatic preferred orientation in contra and ipsi stimulation conditions. Each bin is frequency across simulation iterations.

(C) Measurement of active synapses with respect to the total aggregate interocular alignment. Left: Shown is the proportion of spines active for each orientation (with respect to somatic orientation preference) and eye condition for two example simulation runs: one aligned (dark green) and one misaligned (light green). Circles denote maximum number of active synapses and orientations used to calculate alignment. Right: the fractions of spines from each ocular class contributing to the maximum values. Same color scheme as in (A).

(D) Mean alignment conditioned on the proportion of total synapses active (ordinate, normalized by the maximum number active observed) and fraction of those from each ocular class (abscissa). Data are mean across all simulation runs from all congruent cells.

innervation (Binzegger et al., 2004). It is possible that populations of thalamocortical inputs, which converge onto stellate cells in layer 4, are more in line with a model of monocular convergence. Thalamocortical synapses are almost entirely monocular (in carnivores and primates) and may have a greater influence on cortical cells, as their synapses tend to be larger and have a greater number of presynaptic release sites (Ahmed et al., 1994; Kharazia and Weinberg, 1994). In addition, thalamocortical inputs could provide an initial bias in interocular alignment before requisite binocular visual experience (Chang et al., 2020; Gu and Cang, 2016), which could be amplified by layer 2/3 cortical circuits, as they receive input from layer 4.

Neuron
Article

CellPress

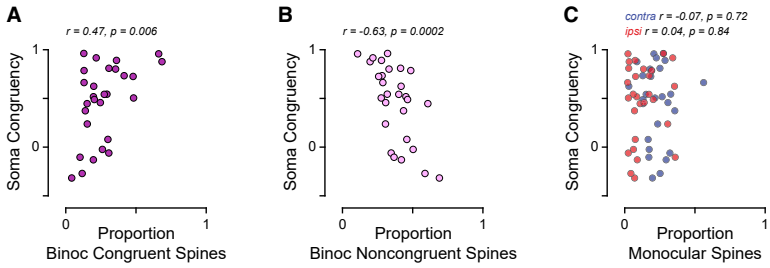

Figure 7. Somatic congruency correlates with synaptic input population properties

(A) Relationship between the proportion of binocular congruent synapses and somatic congruency. Each data point is from a single cell.

(B) Same as in (A) for binocular noncongruent synapses.

(C) Same as in (A) for monocular contra (blue) and monocular ipsi (red) synapses.

Indeed, even in visually experienced animals, layer 2/3 amplification continues to be important: individual cells generate an aligned response from a population of heterogeneous inputs, consistent with binocular alignment being a multistage process. Future studies will be necessary to map synaptic populations onto layer 4 neurons and compare thalamic and cortical contributions to interocular response alignment.

Structural properties of binocular synapses

In this study we do not find systematic differences in the ultrastructural anatomy between different ocular classes. Instead, we observe strength in numbers of synapses (Scholl et al., 2021): binocular synapses were most numerous overall, followed by monocular contra and ipsi inputs, and each ocular class draws from the same synaptic strength distributions. Thus, the aggregate strength of a synaptic network is largely determined by numbers of active synapses (Figure 6). We do, however, observe some curious structure-function relationships. Binocular synapses, as a whole, have shorter necks than monocular synapses (Table S1). As spine neck length can regulate synaptic strength (Araya et al., 2006), this might indicate a predominate role of binocular synaptic networks in shaping layer 2/3 neuron response properties. These spines may also have more energetic demands, as binocular viewing may drive them more frequently than monocular synapses, and shorter necks place the synaptic contact closer to dendritic molecular machinery.

A potential role of "noncongruent" binocular inputs

Subcellular imaging continues to reveal the complicated and diverse nature of synaptic networks underlying cortical neuron selectivity (Scholl and Fitzpatrick, 2020). In this study, we observed diversity in ocular properties. While we focused on binocular congruent inputs, we acknowledge that there is likely a role for those classified here as "noncongruent." One interesting possibility is that these inputs drive neurons under binocular viewing conditions where the left and right eyes are not receiving exactly the same visual information. For example, these inputs might be responsible for signaling motion in depth (Cormack et al., 2017) or signaling features during occlusion of one eye (Anderson and Nakayama, 1994). They might also provide signals to convey a horizontal disparity (i.e., surface slant) (Blakemore et al., 1972; Greenwald and Knill, 2009), and neural models of horizontal disparity predict that the input filters would differ in orientation and be noncongruent by our measure.

Another interesting possibility is that these inputs generate invariant binocular response properties across binocular viewing conditions. For example, head tilt can cause torsional eye movements, so visual features falling on the retina would no longer be matched along the horopter. Under these conditions, synapses we defined as noncongruent might actually be congruent in their responses to visual features. In this way, the somatic output of the cell would be invariant to different binocular viewing conditions and could provide information under a variety of situations. Thereby, diversity may reflect the ability of visual neurons and the network as a whole to encode information invariant of viewing conditions. This could provide an explanation for our observation that binocular noncongruent inputs exhibit synaptic strengths comparable to binocular congruent inputs, as we assessed congruency in just one condition and categorized inputs for this specific situation, neglecting conditions where the noncongruent inputs provide the strongest and most relevant input.

There is always a possibility that our limited stimulus set inaccurately characterized synapsesas noncongruent. However, a number of studies of V1 neurons report fairly large interocular orientation preference differences (which are directly related to congruency) (Blakemore et al., 1972) from a sizeable fraction of cells. Given that an orientation preference difference of ~20 degrees corresponds to our congruency cut-off ($r_{c\text{-}l}$ = 0.5), about 25%–30% of neurons in visually experienced ferrets (Chang et al., 2020) and ~10% of neurons in adult primates (Bridge and Cumming, 2001) are classified as noncongruent. This suggests that noncongruent populations reflect more than a mere measurement error.

One final possibility is that our measurements capture a "snapshot" during synaptic development. The ferret critical period of visual development stretches weeks after eye opening, beyond the age of animals studied here. This period might instruct continued binocular maturation and, thus, noncongruent synapses we observed would be sculpted away or become congruent by the time animals possess a mature visual system.

Development of a binocular synaptic network supporting interocular response alignment

We propose that binocular visual experience, in coordination with the structural development of cortical circuits, gives rise to the binocular congruent synaptic network. Prior to visual experience or the critical period of development, cells exhibit a higher degree of interocular mismatch in orientation preference (Chang et al., 2020; Tan et al., 2020; Wang et al., 2010), but initial biases could facilitate later development. Initial biases could result from (1) thalamocortical inputs (Gu and Cang, 2016), (2) spontaneous cortical activity patterns structuring receptive field

properties (Smith et al., 2018), (3) random connectivity (Ko et al., 2013), or any combination of these possibilities. Gu and Cang (2016) found evidence that, before the critical period in mice, an initial bias is provided by thalamocortical input to layer 4 neurons, while intracortical input exhibits greater mismatch. After maturation, intracortical and thalamocortical input are equivalently matched, suggesting that intracortical connectivity develops, either through instruction from thalamocortical input or *de novo*. However, as the authors were unable to record from the same cells over time, these two possibilities are indistinguishable.

In comparing mouse and ferret studies, it is important to point out that the critical period of development in mice begins almost 2 weeks after eye opening, and it is unknown whether this initial binocular experience shapes cortical circuits. In contrast, Chang et al. (2020) observed a dramatic shift in binocular response alignment in ferret immediately after eye opening and found a considerable amount of congruency in binocular cells, *prior* to binocular visual experience. Thus, at least in ferret, this initial network, which could form through Hebbian modification of horizontal connections without thalamic innervation (Bartsch and van Hemmen, 2001), might instruct the maturation of a binocular congruent synaptic network.

So far, we considered only the functional maturation of cellular and synaptic networks early in development, neglecting concomitant changes in structure. Prior to and following eye opening in the developing visual cortex, dendritic arborization of pyramidal cells increases in size and complexity (Callaway and Borrell, 2011). After the onset of visual experience, long-range horizontal connections between layer 2/3 cells are established and stabilized (Durack and Katz, 1996) and synaptic density increases dramatically (Cragg, 1975; Yuste and Bonhoeffer, 2004). Increased synaptic connections lead to increased dynamics, as synaptic remodeling and elimination continues throughout development (Bhatt et al., 2009). In addition, early in development, the size (strength) of synaptic contacts increases dramatically (Cizeron et al., 2020). As structural development of cortical circuitry coincides with the onset of binocular vision, it stands to reason that binocular synaptic networks emerge and consolidate around this time. In one way, this process can be thought of as ‘‘structural recurrent amplification’’; addition and stabilization of binocular intracortical inputs boosts the excitatory drive underlying interocular response selectivity and alignment. We believe this view, of a dynamic and stabilizing recurrent circuit emerging through development, will provide insight into the nature of binocular synaptic networks and development of binocular vision.

STAR★METHODS

Detailed methods are provided in the online version of this paper and include the following:

- KEY RESOURCES TABLE
- RESOURCE AVAILABILITY
  - Lead contact
  - Materials availability
  - Data and code availability
- EXPERIMENTAL MODEL AND SUBJECT DETAILS
- METHOD DETAILS
  - Viral injections
  - Cranial window
  - Visual stimuli
  - Two-photon imaging
  - Two-photon imaging analysis
  - Serial block-face scanning electron microscopy
  - NEURON modeling
  - Simulation of synaptic population aggregates
- QUANTIFICATION AND STATISTICAL ANALYSIS

SUPPLEMENTAL INFORMATION

Supplemental information can be found online at https://doi.org/10.1016/j.neuron.2022.01.023.

ACKNOWLEDGMENTS

The authors thank the Fitzpatrick lab for helpful scientific discussion, the GENIE project for access to GCaMP6s, and the Max Planck Florida Institute ARC for animal care. This work was supported by funding from NIH grants R01 EY011488 (D.F.) and K99 EY031137 (B.S.), the Max Planck Florida Institute for Neuroscience, and the Max Planck Society.

AUTHOR CONTRIBUTIONS

Conceptualization, B.S.; methodology, B.S.; investigation (biological), B.S. and C.T.; investigation (electron microscopy), C.I.T. and M.A.R.; formal analysis, B.S., C.T., C.I.T., and M.A.R.; writing – original draft, B.S., C.T., D.F.; writing – review & editing, B.S., C.T., C.I.T., M.A.R., N.K., and D.F.; supervision, N.K. and D.F.

DECLARATION OF INTERESTS

The authors declare no competing financial interests.

Received: June 17, 2021
Revised: October 13, 2021
Accepted: January 19, 2022
Published: February 4, 2022

REFERENCES

Ahmadian, Y., Rubin, D.B., and Miller, K.D. (2013). Analysis of the stabilized supralinear network. Neural Comput. *25*, 1994–2037.

Ahmed, B., Anderson, J.C., Douglas, R.J., Martin, K.A., and Nelson, J.C. (1994). Polyneuronal innervation of spiny stellate neurons in cat visual cortex. J. Comp. Neurol. *341*, 39–49.

Anderson, B.L., and Nakayama, K. (1994). Toward a general theory of stereopsis: binocular matching, occluding contours, and fusion. Psychol. Rev. *101*, 414–445.

Anzai, A., Ohzawa, I., and Freeman, R.D. (1999). Neural mechanisms for processing binocular information II. Complex cells. J. Neurophysiol. *82*, 909–924.

Araya, R., Jiang, J., Eisenthal, K.B., and Yuste, R. (2006). The spine neck filters membrane potentials. Proc. Natl. Acad. Sci. USA *103*, 17961–17966.

Barendregt, M., Harvey, B.M., Rokers, B., and Dumoulin, S.O. (2015). Transformation from a retinal to a cyclopean representation in human visual cortex. Curr. Biol. *25*, 1982–1987.

Bartsch, A.P., and van Hemmen, J.L. (2001). Combined Hebbian development of geniculocortical and lateral connectivity in a model of primary visual cortex. Biol. Cybern. *84*, 41–55.

Belevich, I., Joensuu, M., Kumar, D., Vihinen, H., and Jokitalo, E. (2016). Microscopy image browser: A platform for segmentation and analysis of multidimensional datasets. PLoS Biol. *14*, e1002340.

Ben-Yishai, R., Bar-Or, R.L., and Sompolinsky, H. (1995). Theory of orientation tuning in visual cortex. Proc. Natl. Acad. Sci. USA *92*, 3844–3848.

Bhatt, D.H., Zhang, S., and Gan, W.-B. (2009). Dendritic spine dynamics. Annu. Rev. Physiol. *71*, 261–282.

Bhaumik, B., and Shah, N.P. (2014). Development and matching of binocular orientation preference in mouse V1. Front. Syst. Neurosci. *8*, 128.

Bienenstock, E.L., Cooper, L.N., and Munro, P.W. (1982). Theory for the development of neuron selectivity: orientation specificity and binocular interaction in visual cortex. J. Neurosci. *2*, 32–48.

Binzegger, T., Douglas, R.J., and Martin, K.A.C. (2004). A quantitative map of the circuit of cat primary visual cortex. J. Neurosci. *24*, 8441–8453.

Blakemore, C., Fiorentini, A., and Maffei, L. (1972). A second neural mechanism of binocular depth discrimination. J. Physiol. *226*, 725–749.

Bourne, J.N., and Harris, K.M. (2011). Coordination of size and number of excitatory and inhibitory synapses results in a balanced structural plasticity along mature hippocampal CA1 dendrites during LTP. Hippocampus *21*, 354–373.

Bridge, H., and Cumming, B.G. (2001). Responses of macaque V1 neurons to binocular orientation differences. J. Neurosci. *21*, 7293–7302.

Callaway, E.M., and Borrell, V. (2011). Developmental sculpting of dendritic morphology of layer 4 neurons in visual cortex: influence of retinal input. J. Neurosci. *31*, 7456–7470.

Cardona, A., Saalfeld, S., Schindelin, J., Arganda-Carreras, I., Preibisch, S., Longair, M., Tomancak, P., Hartenstein, V., and Douglas, R.J. (2012). TrakEM2 software for neural circuit reconstruction. PLoS ONE *7*, e38011.

Casagrande, V.A., and Boyd, J.D. (1996). The neural architecture of binocular vision. Eye (Lond.) *10*, 153–160.

Chang, J.T., Whitney, D., and Fitzpatrick, D. (2020). Experience-Dependent Reorganization Drives Development of a Binocularly Unified Cortical Representation of Orientation. Neuron *107*, 338–350.e5.

Cizeron, M., Qiu, Z., Koniaris, B., Gokhale, R., Komiyama, N.H., Fransén, E., and Grant, S.G.N. (2020). A brainwide atlas of synapses across the mouse life span. Science *369*, 270–275.

Cormack, L.K., Czuba, T.B., Knöll, J., and Huk, A.C. (2017). Binocular mechanisms of 3D motion processing. Annu. Rev. Vis. Sci. *3*, 297–318.

Cragg, B.G. (1975). The development of synapses in the visual system of the cat. J. Comp. Neurol. *160*, 147–166.

Durack, J.C., and Katz, L.C. (1996). Development of horizontal projections in layer 2/3 of ferret visual cortex. Cereb. Cortex *6*, 178–183.

Erwin, E., and Miller, K.D. (1998). Correlation-based development of ocularly matched orientation and ocular dominance maps: determination of required input activities. J. Neurosci. *18*, 9870–9895.

Ferster, D. (1981). A comparison of binocular depth mechanisms in areas 17 and 18 of the cat visual cortex. J. Physiol. *311*, 623–655.

Greenwald, H.S., and Knill, D.C. (2009). Orientation disparity: a cue for 3D orientation? Neural Comput. *21*, 2581–2604.

Gu, Y., and Cang, J. (2016). Binocular matching of thalamocortical and intracortical circuits in the mouse visual cortex. eLife *5*, 5.

Hofer, S.B., Mrsic-Flogel, T.D., Bonhoeffer, T., and Hübener, M. (2009). Experience leaves a lasting structural trace in cortical circuits. Nature *457*, 313–317.

Holler, S., Köstinger, G., Martin, K.A.C., Schuhknecht, G.F.P., and Stratford, K.J. (2021). Structure and function of a neocortical synapse. Nature *591*, 111–116.

Hubel, D.H., and Wiesel, T.N. (1962). Receptive fields, binocular interaction and functional architecture in the cat's visual cortex. J. Physiol. *160*, 106–154.

Hubel, D.H., and Wiesel, T.N. (1965). Binocular interaction in striate cortex of kittens reared with artificial squint. J. Neurophysiol. *28*, 1041–1059.

Kharazia, V.N., and Weinberg, R.J. (1994). Glutamate in thalamic fibers terminating in layer IV of primary sensory cortex. J. Neurosci. *14*, 6021–6032.

Ko, H., Cossell, L., Baragli, C., Antolik, J., Clopath, C., Hofer, S.B., and Mrsic-Flogel, T.D. (2013). The emergence of functional microcircuits in visual cortex. Nature *496*, 96–100.

Lee, W.-C.A., Bonin, V., Reed, M., Graham, B.J., Hood, G., Glattfelder, K., and Reid, R.C. (2016). Anatomy and function of an excitatory network in the visual cortex. Nature *532*, 370–374.

Longordo, F., To, M.-S., Ikeda, K., and Stuart, G.J. (2013). Sublinear integration underlies binocular processing in primary visual cortex. Nat. Neurosci. *16*, 714–723.

Lowe, G. (2004). SIFT-the scale invariant feature transform. Int. J.

Marr, D., and Poggio, T. (1979). A computational theory of human stereo vision. Proc. R. Soc. Lond. B Biol. Sci. *204*, 301–328.

Mrsic-Flogel, T.D., Hofer, S.B., Ohki, K., Reid, R.C., Bonhoeffer, T., and Hübener, M. (2007). Homeostatic regulation of eye-specific responses in visual cortex during ocular dominance plasticity. Neuron *54*, 961–972.

Nelson, J.I., Kato, H., and Bishop, P.O. (1977). Discrimination of orientation and position disparities by binocularly activated neurons in cat striate cortex. J. Neurophysiol. *40*, 260–283.

Ohzawa, I., and Freeman, R.D. (1986a). The binocular organization of simple cells in the cat's visual cortex. J. Neurophysiol. *56*, 221–242.

Ohzawa, I., and Freeman, R.D. (1986b). The binocular organization of complex cells in the cat's visual cortex. J. Neurophysiol. *56*, 243–259.

Parker, A.J. (2007). Binocular depth perception and the cerebral cortex. Nat. Rev. Neurosci. *8*, 379–391.

Peirce, J.W. (2007). PsychoPy–Psychophysics software in Python. J. Neurosci. Methods *162*, 8–13.

Pnevmatikakis, E.A., and Giovannucci, A. (2017). NoRMCorre: An online algorithm for piecewise rigid motion correction of calcium imaging data. J. Neurosci. Methods *291*, 83–94.

Pologruto, T.A., Sabatini, B.L., and Svoboda, K. (2003). ScanImage: flexible software for operating laser scanning microscopes. Biomed. Eng. Online *2*, 13.

Priebe, N.J. (2008). The relationship between subthreshold and suprathreshold ocular dominance in cat primary visual cortex. J. Neurosci. *28*, 8553–8559.

Priebe, N.J., and Ferster, D. (2012). Mechanisms of neuronal computation in mammalian visual cortex. Neuron *75*, 194–208.

Sage, D., Prodanov, D., and Tinevez, J.Y. (2012). MIJ: making interoperability between ImageJ and Matlab possible (Big). www.Epfl.Ch.

Sarnaik, R., Wang, B.-S., and Cang, J. (2014). Experience-dependent and independent binocular correspondence of receptive field subregions in mouse visual cortex. Cereb. Cortex *24*, 1658–1670.

Scholl, B., and Fitzpatrick, D. (2020). Cortical synaptic architecture supports flexible sensory computations. Curr. Opin. Neurobiol. *64*, 41–45.

Scholl, B., Burge, J., and Priebe, N.J. (2013a). Binocular integration and disparity selectivity in mouse primary visual cortex. J. Neurophysiol. *109*, 3013–3024.

Scholl, B., Tan, A.Y.Y., and Priebe, N.J. (2013b). Strabismus disrupts binocular synaptic integration in primary visual cortex. J. Neurosci. *33*, 17108–17122.

Scholl, B., Thomas, C.I., Ryan, M.A., Kamasawa, N., and Fitzpatrick, D. (2021). Cortical response selectivity derives from strength in numbers of synapses. Nature *590*, 111–114.

Skottun, B.C., and Freeman, R.D. (1984). Stimulus specificity of binocular cells in the cat's visual cortex: ocular dominance and the matching of left and right eyes. Exp. Brain Res. *56*, 206–216.

Smith, S.L., and Trachtenberg, J.T. (2007). Experience-dependent binocular competition in the visual cortex begins at eye opening. Nat. Neurosci. *10*, 370–375.

Smith, G.B., Hein, B., Whitney, D.E., Fitzpatrick, D., and Kaschube, M. (2018). Distributed network interactions and their emergence in developing neocortex. Nat. Neurosci. *21*, 1600–1608.

Takumi, Y., Ramírez-León, V., Laake, P., Rinvik, E., and Ottersen, O.P. (1999). Different modes of expression of AMPA and NMDA receptors in hippocampal synapses. Nat. Neurosci. *2*, 618–624.

Tan, L., Tring, E., Ringach, D.L., Zipursky, S.L., and Trachtenberg, J.T. (2020). Vision Changes the Cellular Composition of Binocular Circuitry during the Critical Period. Neuron *108*, 735–747.e6.

Thomas, C.I., Ryan, M.A., Scholl, B., Guerrero-Given, D., Fitzpatrick, D., and Kamasawa, N. (2021). Targeting functionally characterized synaptic architecture using inherent fiducials and 3D correlative microscopy. Microsc. Microanal. *27*, 156–169.

Toni, N., Buchs, P.A., Nikonenko, I., Bron, C.R., and Muller, D. (1999). LTP promotes formation of multiple spine synapses between a single axon terminal and a dendrite. Nature *402*, 421–425.

Wang, B.-S., Sarnaik, R., and Cang, J. (2010). Critical period plasticity matches binocular orientation preference in the visual cortex. Neuron *65*, 246–256.

Wilson, D.E., Whitney, D.E., Scholl, B., and Fitzpatrick, D. (2016). Orientation selectivity and the functional clustering of synaptic inputs in primary visual cortex. Nat. Neurosci. *19*, 1003–1009.

Xu, X., Cang, J., and Riecke, H. (2020). Development and binocular matching of orientation selectivity in visual cortex: a computational model. J. Neurophysiol. *123*, 1305–1319.

Yuste, R., and Bonhoeffer, T. (2004). Genesis of dendritic spines: insights from ultrastructural and imaging studies. Nat. Rev. Neurosci. *5*, 24–34.

Zhao, X., Liu, M., and Cang, J. (2013). Sublinear binocular integration preserves orientation selectivity in mouse visual cortex. Nat. Commun. *4*, 2088.

Neuron
Article

CellPress

STAR★METHODS

KEY RESOURCES TABLE

REAGENT or RESOURCE	SOURCE	IDENTIFIER
Bacterial and virus strains		
AAV1.Syn.FLEX.GCaMP6s	Custom Preparation, UPenn	Addgene plasmid # 100845
AAV1.hSyn.Cre	Addgene	Addgene plasmids # 105553
Biological samples		
Ferret	Marshall Farms	N/A
Experimental models: Organisms/strains		
Ferret	Marshall Farms	N/A
Software and algorithms		
Cell Magic Wand Tool	MIT License, Wilson et al., 2016 https://doi.org/10.1016/j.neuron.2017.02.035	https://www.mpfi.org/cell-magic-wand/
MATLAB	Mathworks	https://ch.mathworks.com/products/matlab.html
FIJI/ImageJ	NIH	https://fiji.sc
Miji	Sage et al., 2012	https://imagej.net/plugins/miji
PsychoPy	Peirce 2007	https://www.psychopy.org
NEURON Spine Simulation Code	Scholl et al., 2021 https://doi.org/10.1038/s41586-020-03044-3	https://github.com/schollben/StructFuncEM2020

RESOURCE AVAILABILITY

Lead contact

Further information and requests for resources and reagents should be directed to and will be fulfilled by the lead contact: benjamin.scholl@pennmedicine.upenn.edu.

Materials availability

This study did not generate unreported reagents. All reagents used are available upon reasonable request.

Data and code availability

Because of the large size of the imaging dataset, the raw data have not been deposited in a public repository but will be made available upon reasonable request. Cell Magic Wand tool and NEURON modeling scripts have been deposited on GitHub and are publicly available. DOIs are listed in the key resources table. All other processing and analysis routines were written in MATLAB and will be shared upon reasonable request.

EXPERIMENTAL MODEL AND SUBJECT DETAILS

All procedures were performed according to NIH guidelines and approved by the Institutional Animal Care and Use Committee at Max Planck Florida Institute for Neuroscience. Female ferrets (*Mustelidae Furo*, Marshall Farms) were used in this study.

Animals underwent survival injections at ages P18-P23, followed by acute experiments preformed at ages 36-P60. Animals were housed in a vivarium under 12 h light / 8 h dark cycle. No *a priori* sample size estimation was preformed, but sample sizes are similar to other studies which performed *in vivo* two-photon imaging.

METHOD DETAILS

Viral injections

Female ferrets (n = 15) aged P18-23 were anesthetized with isoflurane (delivered in O_2). Atropine was administered and a 1:1 mixture of lidocaine and bupivacaine was administered SQ. Animals were maintained at an internal temperature of 37°C. Under sterile surgical conditions, a small craniotomy (0.8 mm diameter) was made over the visual cortex (7-8 mm lateral and 2-3 mm anterior to lambda). A mixture of diluted AAV1.hSyn.Cre (1:25000 to 1:50000) and AAV1.Syn.FLEX.GCaMP6s (UPenn) was injected (125 - 202.5 nL) through beveled

glass micropipettes (10-15 μm outer diameter) at 600, 400, and 200 μm below the pia. Finally, the craniotomy was filled with sterile agarose (Type IIIa, Sigma-Aldrich) and the incision site was sutured.

Cranial window

After 3-5 weeks of expression, ferrets were anesthetized with 12.5mg/kg ketamine and isoflurane. Atropine and bupivacaine were administered, animals were placed on a feedback-controlled heating pad to maintain an internal temperature of 37°C, and intubated to be artificially respirated. Isoflurane was delivered throughout the surgical procedure to maintain a surgical plane of anesthesia. An intravenous cannula was placed to deliver fluids. Tidal CO_2, external temperature, and internal temperature were continuously monitored. The scalp was retracted and a custom titanium headplate adhered to the skull (Metabond, Parkell). A craniotomy was performed and the dura retracted to reveal the cortex. One piece of custom coverglass (5 mm diameter, 0.7 mm thickness, Warner Instruments) attached to a custom insert using optical adhesive (71, Norland Products) was placed onto the brain to dampen biological motion during imaging. A 1:1 mixture of tropicamide ophthalmic solution (Akorn) and phenylephrine hydrochloride ophthalmic solution (Akorn) was applied to both eyes to dilate the pupils and retract the nictitating membranes. Contact lenses were inserted to protect the eyes. Upon completion of the surgical procedure, isoflurane was gradually reduced and pancuronium (0.2 mg/kg/h) was delivered IV.

Visual stimuli

Visual stimuli were generated using Psychopy (Peirce, 2007). The monitor was placed 25 cm from the animal. Receptive field locations for each cell were hand mapped and the spatial frequency optimized (range: 0.04 to 0.20 cpd). For each soma and dendritic segment, square-wave or sine-wave drifting gratings were presented at 22.5 degree increments to each eye independently (2-3 s duration, 1-2 s ISI, 8-10 trials for each field of view). Drifting gratings of different directions (0 – 337.5°) were presented independently to both eyes. Visual stimulation of either eye was achieved by using a shutter controlled by Arduino which allowed switching between contralateral or ipsilateral view of the monitor at the visuotopic location targeted.

Two-photon imaging

Two-photon imaging was performed on a Bergamo II microscope (Thorlabs) running Scanimage (Pologruto et al., 2003) (Vidrio Technologies) with 940 nm dispersion-compensated excitation provided by an Insight DS+ (Spectraphysics). For spine imaging, power after the objective was limited to < 50 mW. Cells were selected for imaging on the basis of their position relative to large blood vessels, responsiveness to visual stimulation, and lack of prolonged calcium transients resulting from overexpression of GCaMP6s. Images were collected at 30 Hz using bidirectional scanning with 512x512 pixel resolution or with custom ROIs (region of interest; framerate range: 22 - 50 Hz). Somatic imaging was performed with a resolution of 2.05 - 10.24 pixels/ μm. Dendritic spine imaging was performed with a resolution of 6.10 −15.36 pixels/μm.

Two-photon imaging analysis

Imaging data were excluded from analysis if motion along the z axis was detected. Dendrite images were corrected for in-plane motion via a 2D cross-correlation based approach in MATLAB or using a piecewise non-rigid motion correction algorithm (Pnevmatikakis and Giovannucci, 2017). ROIs were drawn in ImageJ; dendritic ROIs spanned contiguous dendritic segments and spine ROIs were fit with custom software. Mean pixel values for ROIs were computed over the imaging time series and imported into MATLAB (Sage et al., 2012). $\Delta F/F_o$ was computed by computing F_o with time-averaged median or percentile filter (10th percentile). For a subset of cells (n = 5/36, n = 1/16 binocular congruent cells), the tuning of the soma was unreliable and an ROI placed on the dendrite apical trunk was used. $\Delta F/F_o$ traces were synchronized to stimulus triggers sent from Psychopy and collected by Spike2. For spine signals, we subtracted a scaled version of the dendritic signal to remove back-propagating action potentials as performed previously (Wilson et al., 2016). Spine ultrastructure and functional response properties were unrelated to the degree of subtraction or residual correlation with dendritic signals.

Peak $\Delta F/F_o$ responses to bars and gratings were computed using the Fourier analysis to calculate mean and modulation amplitudes for each stimulus presentation, which were summed together. Spines were included for analysis if the mean peak $\Delta F/F_o$ for the preferred stimulus was > 20% $\Delta F/F_o$, the SNR at the preferred stimulus was > 1, and spines were weakly correlated with the dendritic signal (Spearman's correlation, r < 0.4). This set of criteria was used to determine the ocular dominance class of each spine and soma. Specifically, if these criteria were passed for stimuli presented only to the contralateral eye (monocular contra), stimuli presented only to the ipsilateral eye (monocular ipsi), or for both (binocular). Binocular congruency was computed as the Pearson's correlation (MATLAB) between mean responses driven by contralateral and ipsilateral stimulation.

Some spine traces contained negative events after subtraction, so response properties were computed ignoring negative $\Delta F/F_o$ values. Preferred orientation for each spine was calculated by fitting responses in orientation space with a Gaussian tuning curve (Wilson et al., 2016) using lsqcurvefit (MATLAB). Orientation selectivity was computed by calculating the vector strength of mean responses. To identify spine or dendritic calcium events (as used in the model shown in Figures 5 and 6), DF/F traces were smoothed with an exponentially weighted moving average filter (MATLAB) and the peaks of calcium events were located. Peak amplitude of calcium events was compared to the standard deviation of baseline spine fluorescence values prior to subtraction.

Neuron
Article

CellPress

Serial block-face scanning electron microscopy

Five layer 2/3 pyramidal neurons from 3 animals previously imaged with *in vivo* two-photon microscopy were imaged with a scanning electron microscope. A total of 23 segments of proximal basal dendrites and 155 spines were reconstructed and analyzed. To facilitate anatomical reconstruction, we limited imaging to proximal basal dendrites. A detailed description of these methods and the data are reported in Scholl et al., 2021; Scholl and Fitzpatrick, 2020, and Thomas et al. (2021).

Fixed (2% paraformaldehyde and 2% glutaraldehyde in a 0.1 mM sodium cacodylate) brain slices of 80 μm thickness were trimmed to approximately 2 × 2 mm to contain the cell of interest at the center. This was accomplished by using blood vessels and slice edges, visible in a 20x epifluorescence image of the slice, as landmarks. The tissue pieces were incubated in an aqueous solution of 2% osmium tetroxide buffered in 0.1 mM sodium cacodylate for 45 min at room temperature (RT). Tissue was not rinsed and the osmium solution was replaced with cacodylate buffered 2.5% potassium ferrocyanide for 45 min at RT in the dark. Tissue was rinsed with water 2 × 10 min, which was repeated between consecutive steps. Tissue was incubated in warm (60þC) aqueous 1% thiocarbohydrizide for 20 min, aqueous 1% osmium tetroxide for 45 min, and then 1% uranyl acetate in 25% ethanol for 20 min. Tissue was rinsed then left in water overnight at 4þC. The following day, tissue was stained with Walton's lead aspartate for 30 min at 60þC. Tissue was then dehydrated in a graded ethanol series (30, 50, 70, 90, 100%), 1:1 ethanol to acetone, then 100% acetone. Tissue was infiltrated using 3:1 acetone to Durcupan resin (Sigma Aldrich) for 2 h, 1:1 acetone to resin for 2 h, and 1:3 acetone to resin overnight, then flat embedded in 100% resin on a glass slide and covered with an Aclar sheet at 60þC for 2 days. Since SBF-SEM requires conductive samples to minimize charging during imaging, the tissue was trimmed to less than 1 × 1 mm and one side was exposed using an ultramicrotome (UC7, Leica), then turned downward to be remounted to a metal pin with conductive silver epoxy (CircuitWorks, CHEMTRONICS).

Tissue was sectioned and imaged using 3View and Digital Micrograph (Gatan Microscopy Suite) installed on a Gemini SEM300 (Carl Zeiss Microscopy LLC.) equipped with an OnPoint BSE detector (Gatan, Inc.). The detector magnification was calibrated within SmartSEM imaging software (Carl Zeiss Microscopy LLC.) and Digital Micrograph with a 500 nm cross line grating standard. Final imaging was performed at 2.0-2.2 kV accelerating voltage, 20 or 30 μm aperture, working distance of ~5 mm, 0.5-1.2 μs pixel dwell time, 5.7-7 nm per pixel, knife speed of 0.1 mm/sec with oscillation, and 56 - 84 nm section thickness. Imaged volumes ranged from 125x125x36 μm to 280x170x52 μm. Serial images were exported as TIFFs to TrakEM2 (Cardona et al., 2012) and aligned using Scale-Invariant Feature Transform image alignment with linear feature correspondences and rigid transformation (Lowe, 2004). Once aligned, each dendrite of interest was cropped from the full volume to reduce computational overhead in subsequent analyses. Aligned images were exported to Microscopy Image Browser (Belevich et al., 2016) for segmentation of dendrites, spines, PSDs, and boutons. Binary labels files were then imported to Amira (versions 6.7, 2019.1) which was used to create 3D surface models of each dendrite, spine, PSD, and bouton. Each reconstructed dendrite was overlaid onto its corresponding two-photon image using Adobe Photoshop for re-identification of individual spines. Amira was used to measure the volume of spine heads and boutons, surface area of PSDs, and spine neck length. Blender (versions 2.79, 2.8) was used to create 3D renderings.

NEURON modeling

For each synapse reconstructed, we simulated the change in membrane potential at the soma due to a single action potential arriving at the synapse (on the spine head). Simulations of anatomical features allow generation of a single metric (voltage attenuation between spine head and soma) accounting for a variety of synapse features. We modeled a somatic compartment (radius = 13 μm, g_{Na} = 0 S/cm^2, g_k = 0.036 S/cm^2, g_{leak} = 0.003 S/cm^2, E_{leak} = −50 mV, R_a = 105 Ωcm, C_m = 1 μF/cm^2) connected to a 400 μm long dendrite (diameter = 1 μm, R_a = 105 Ωcm, C_m = 1 μF/cm^2). Each spine was placed on the dendrite at the distance from soma as measured with EM and connected via a 'neck' to a 'spine head' where a synapse was placed. Synapse compartments had the same basic properties (R_a = 250 Ωcm, C_m = 1 μF/cm^2) and passive conductances. Spine neck diameter was fixed to 200 nm, matching widths measured in serial EM sections (data not shown) and the length was set to measured values. Spine head length was set to 1 μm so the diameter could be determined from volume measurements (assigning spine heads to be a cylindrical compartment):

$$D = \sqrt{V/4\pi}$$

Next, we converted measured PSD area into a value describing the max synaptic conductance. Here we made several assumptions. Based on the linear correlation between the number of receptors and PSD size, we approximated ~0.87 receptors and ~2.0 receptors per 100 nm for AMPA and NMDA, respectively (Takumi et al., 1999). As a simplification, we extract PSD diameter as if our PSDs were circular (as above). Then an AMPA conductance is

$$g_{AMPA} = D_{spine} \cdot (0.87 \,/\, 0.100) \cdot g_R$$

where g_R is 15 pS per channel. In this way, measured PSD area is linearly related to the synaptic conductance used in each model. For each simulation, parameters were set and the maximum depolarization from V_{rest} (−67.5 mV) was measured in the somatic and spine head compartment.

Simulation of synaptic population aggregates

To examine the contribution of synapses of different ocular classes we used a simple linear model combining binary visually evoked calcium events. For each binocular congruent cell (n = 14), a random set of synapses were drawn (80% of the total population) and a

random set of stimulus trials were drawn for each group of synapses imaged simultaneously on each simulation run (10,000 iterations). The number of active spines was tabulated for each stimulus. Total numbers (or aggregates) were separated by ocular class for comparison. Orientation preference of aggregates was defined as the stimulus evoking the largest response. Multivariate linear regression was used to determine how well total aggregate alignment was predicted by total number of active spines (normalized by the maximum number of active spines observed for each cell) and the fraction of different ocular classes contributing. We used predictor matrices without interaction terms:

$$X = [\beta_1 x_a + \beta_2 x_f + \beta_3 n + \beta_4],$$

where x_a is the proportion of active synapses at the preferred orientation, x_f is the fraction of spines contributing from a single ocular class, n is random noise, and β are the linear coefficients. We also used predictor matrices with an interaction term:

$$X = [\beta_1 x_a + \beta_2 x_f + \beta_3 (x_a \times x_f) + \beta_4 n + \beta_5].$$

The function fitlm (MATLAB) was used to obtain coefficient weights and their significance (see Table S2).

QUANTIFICATION AND STATISTICAL ANALYSIS

Statistical analyses are described in the main text. We used non-parametric statistical analyses (Wilcoxon signrank test, Wilcoxon rank-sum test, circular Kruskal-Wallis test) or permutation tests to avoid assumptions about the distributions of the data. All statistical analysis was performed in MATLAB. Correlation coefficients computed with circular-linear correlation or Spearman's correlation. All correlation significance tests were one-sided unless specified otherwise. Quantitative approaches were not used to determine if the data met the assumptions of the parametric tests.

Neuron, Volume *110*

Supplemental information

A binocular synaptic network supports interocular response alignment in visual cortical neurons

Benjamin Scholl, Clara Tepohl, Melissa A. Ryan, Connon I. Thomas, Naomi Kamasawa, and David Fitzpatrick

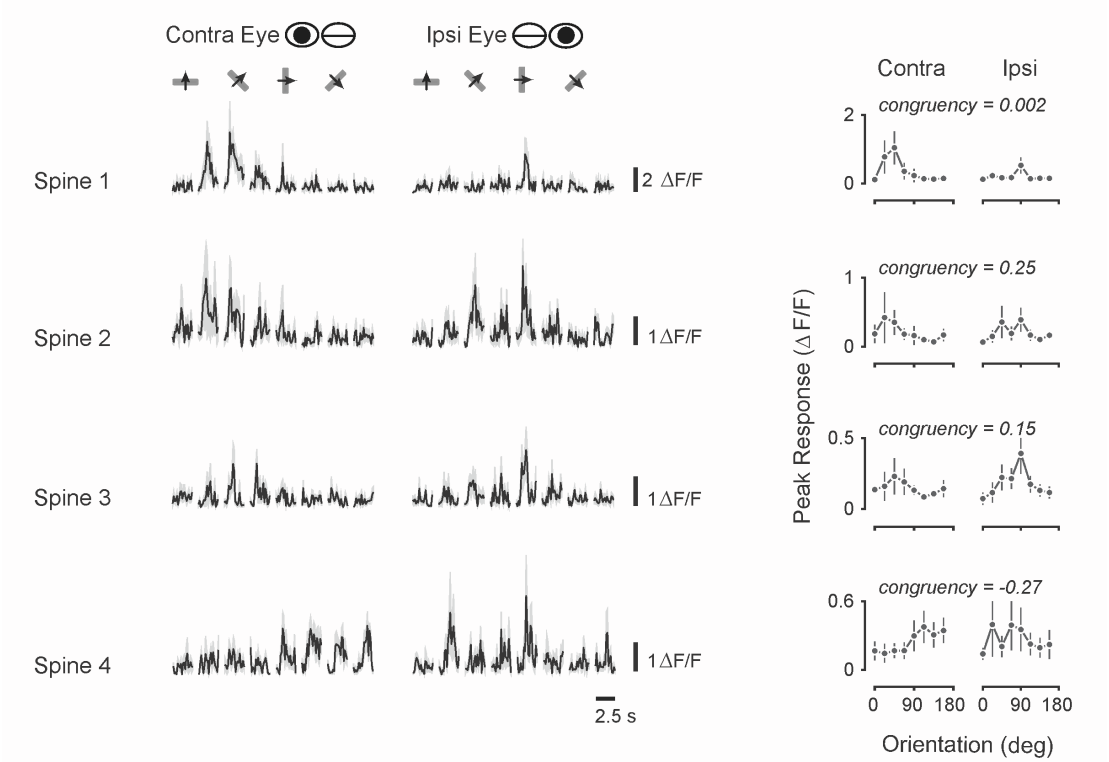

Supplemental Figure 1: Examples of binocular noncongruent spines
Related to and same as in Figure 1b: Left column: Responses of four binocular noncongruent example spines to drifting gratings presented to the contra and ipsi eye. Shown are mean (black) and standard deviation (gray) ΔF/F responses to each stimulus (n = 8 trials) presented to the contra (left) and ipsi (right) eyes. Right column: peak amplitude response mean (black dots) and standard deviation (lines). The respective congruency value is displayed above each trace.

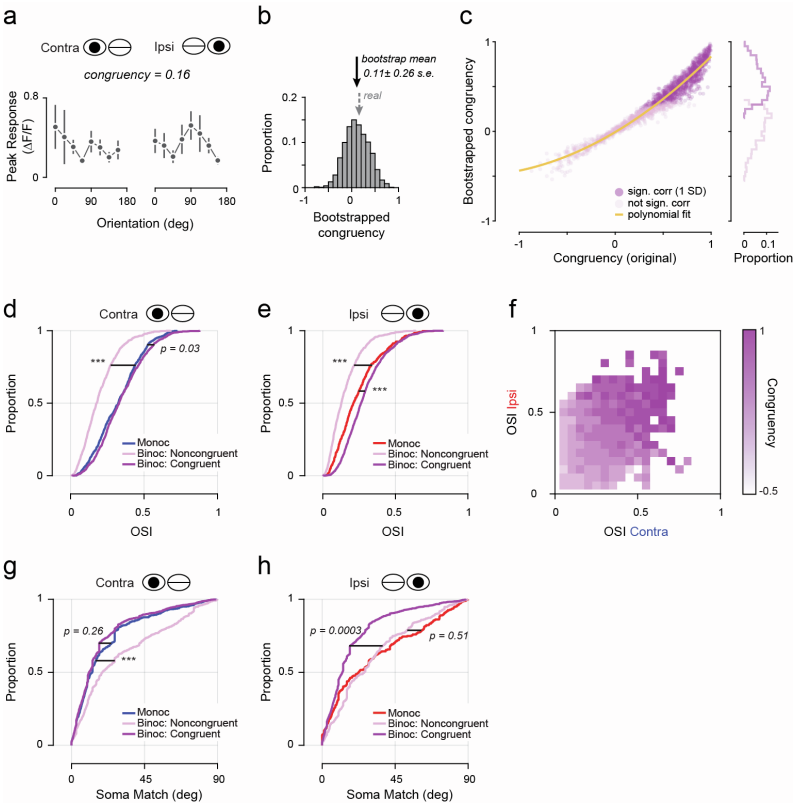

Supplemental Figure 2: A bootstrapped measure of binocular congruency
Related to Figure 2 and 3. **(a)** Peak amplitude response mean (black dots) and standard deviation (lines) of example spine 3 (see Figure 1b). Congruency of the mean response to contra and ipsi stimulation was 0.16. **(b)** Distribution of bootstrapped congruency values for the responses shown in (a). **(c)** Left: Measured congruency and mean bootstrapped congruency are strongly correlated (Spearman's r = 0.98, p < 0.0001) and was well fit by a second order polynomial (yellow line, $y = (0.2)x^2 + (0.64)x - 0.01$, $r^2 = 0.95$). Spines whose response was significantly correlated between the eyes (bootstrapped mean > 1 s.d.) were classified as binocular congruent (dark purple). Right: Histograms of significant and nonsignificant spines. (d-h) Repetition of results shown in Figures 2 and 3 using the bootstrap analysis to define binocular congruent and noncongruent spines (***, p<0.0001). **(d-f)** Same as in Figure 2 b-d: Cumulative distribution of orientation selectivity index (OSI) of contra (d) and ipsi (e) responses for each ocular class. (f) Heatmap of mean bootstrapped congruency of binocular inputs with respect to contra and ipsi OSI. **(g-h)** Same as in Figure 3 b-c: Cumulative distribution of functional specificity (mismatch in orientation preference between individual spines and the soma) for responses during contra (g) and ipsi (h) stimulation for each ocular class.

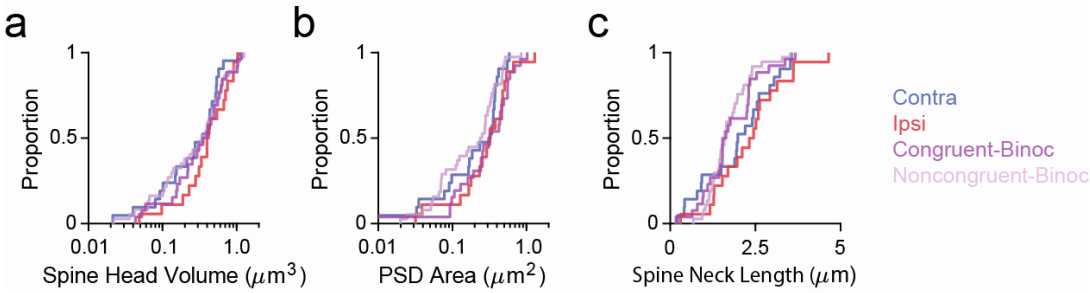

Supplemental Figure 3: Ultrastructural properties are comparable across ocular classes

Related to Figure 4 and Table 3. **(a-c)** Cumulative distribution of ultrastructural features of spines as measured by EM reconstruction for each ocular class. **(a)** Spine Head Volume, **(b)** Postsynaptic Density (PSD) Area (shown in red in Figure 4 c), **(c)** Spine Neck Length.

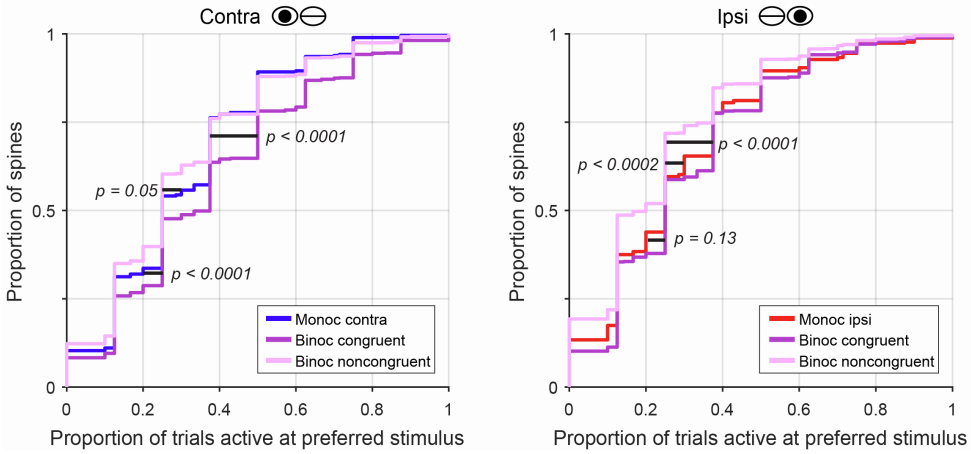

Supplemental Figure 4: Binocular congruent inputs are most reliable
Related to Figure 5 and 6. Cumulative distribution of reliability measured as proportion of trials active (see Methods) at the spine's preferred stimulus for monocular, binocular noncongruent, and binocular congruent inputs for contra (left) and ipsi (right) stimulation. Binocular congruent spines are more reliable than binocular noncongruent and monocular contra spines ($p < 0.001$, two-sided Wilcoxon's ranksum test). Monocular ipsi spines are slightly less reliable than binocular congruent, but this trend is not significant ($p = 0.13$, two-sided Wilcoxon's ranksum test). In addition, the congruency of binocular spines is positively correlated with increased reliability (Spearman's r: contra: $r = 0.20$, $p < 0.0001$; ipsi: $r = 0.22$, $p < 0.0001$).

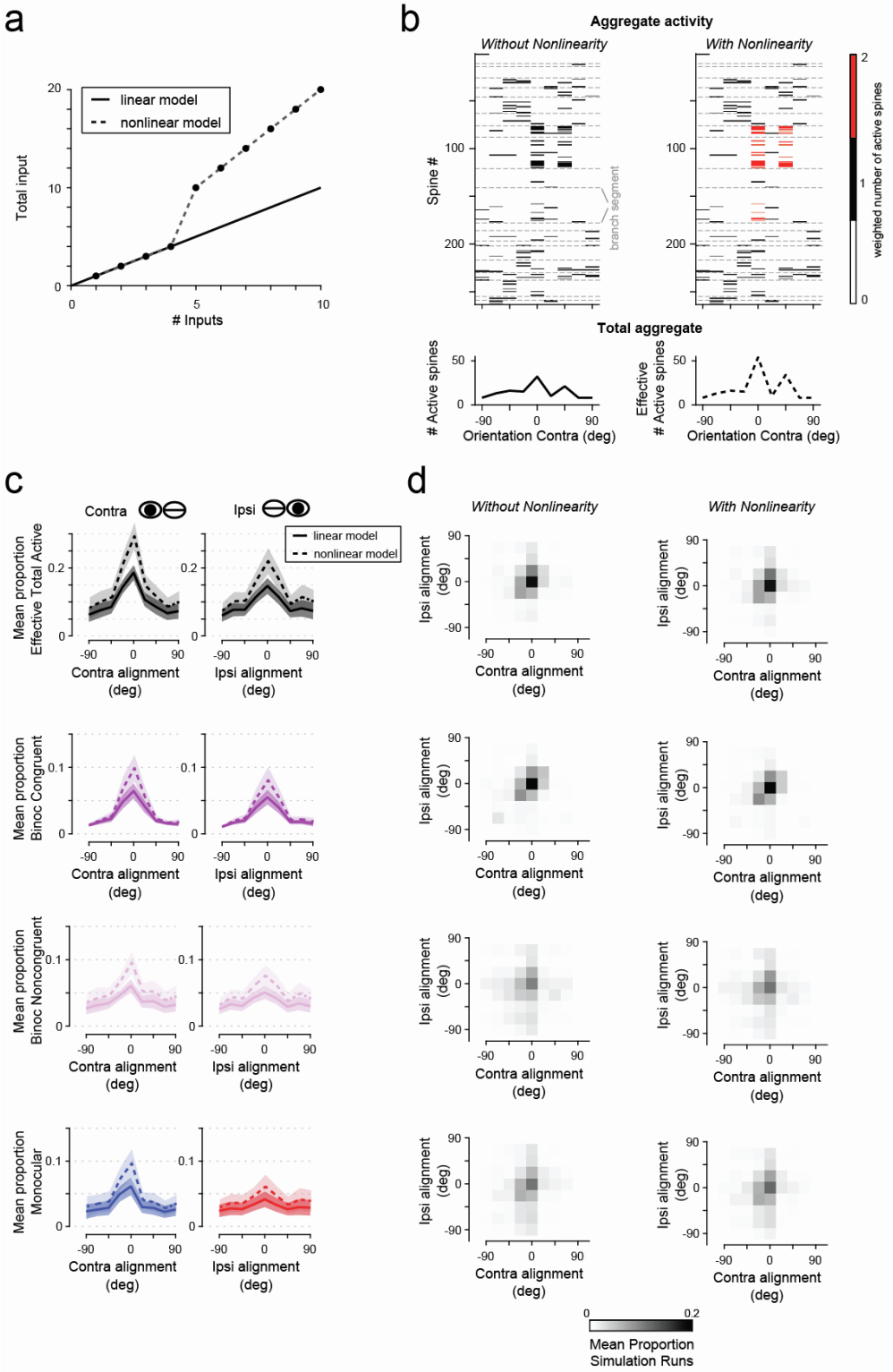
a
linear model
nonlinear model
Total input
Inputs
b
Aggregate activity
Without Nonlinearity
With Nonlinearity
Spine #
branch segment
weighted number of active spines
Total aggregate
Active spines
Effective # Active spines
Orientation Contra (deg)
c
Contra
Ipsi
linear model
nonlinear model
Mean proportion Effective Total Active
Mean proportion Binoc Congruent
Mean proportion Binoc Noncongruent
Mean proportion Monocular
Contra alignment (deg)
Ipsi alignment (deg)
d
Without Nonlinearity
With Nonlinearity
Ipsi alignment (deg)
Contra alignment (deg)
Mean Proportion Simulation Runs

Supplemental Figure 5: Implementing a nonlinearity does not alter aggregate alignment

Related to Figure 5 and 6. **(a)** Comparison of the linear and nonlinear model implemented in the simulation. With the nonlinearity, co-activity of five or more inputs within the same dendritic segment got weighted more heavily (Losonczy and Magee, 2006). **(b)** Similar to Figure 5. Synaptic activity (top, discrete calcium events, shown in black) and the resulting effective total aggregate (bottom) for one simulation run in the linear (left) and nonlinear (right) model. Shown is activity driven by contra stimulation, with respect to the somatic preferred orientation. In the nonlinear model, in 5 conditions across 3 branch segments the synaptic activity got weighed more strongly (red instead of black). **(c)** Linear (solid line) and nonlinear (dashed line) simulated aggregate tuning for contra and ipsi stimulation across 14 binocular congruent cells. From top to bottom: total aggregate, binocular congruent populations, binocular noncongruent populations, and monocular populations. Tuning is with respect to the soma preferred orientation; data are mean and standard error. **(d)** Interocular distributions of trial-to-trial alignment of aggregates to the somatic preferred orientation in contra and ipsi stimulation conditions for linear (left) and nonlinear (right) model. Each bin is frequency across simulation iterations (n = 1000). Aggregate orientation preference was changed by the nonlinearity in about 25% of cases but did not result in stark changes of aggregate specificity overall.

Supplemental Table 1: Ultrastructural properties of synapses of each ocular class. Related to Fig. 4 and Fig S3. Values reported are mean and standard deviation for each ocular class and anatomical feature or metric of strength.

Class	Spine Head Volume (μm^3)	Spine PSD Area (μm^2)	Spine Neck Length (μm)	Simulated Soma Input (mV)
Monocular Contra *(n = 21)*	0.35 ± 0.26	0.26 ± 0.17	1.97 ± 1.04	1.02 ± 0.42
Monocular Ipsi *(n = 18)*	0.48 ± 0.29	0.38 ± 0.29	2.32 ± 1.05	1.25 ± 0.52
Binocular congruent *(n = 26)*	0.42 ± 0.31	0.37 ± 0.25	1.78 ± 0.82	1.12 ± 0.44
Binocular noncongruent *(n = 38)*	0.40 ± 0.32	0.24 ± 0.19	1.72 ± 0.62	1.04 ± 0.40

Supplemental Table 2: Linear regression model with and without interaction term predicting simulated total aggregate interocular alignment.
Related to Fig. 6. Shown are coefficients from model fits. All coefficients were statistically significant ($p < 0.05$) unless stated otherwise. Coefficients for noise model and constant terms (see Methods) were not significant.

		Total Active	Binocular congruent	Binocular noncongruent	Monocular	Interaction
Contralateral Responses	*Linear Model 1*	+0.015	+0.37			n/a
		- 0.079	+ 0.233			+ 0.29
	Linear Model 2	- 0.02		- 0.43		n/a
		+ 0.26		- 0.036		- 0.86
	Linear Model 3	- 0.058			- 0.22	n/a
		- 0.064			- 0.23	0.017 *(n.s.)*
Ipsilateral Responses	*Linear Model 1*	+0.33	+0.34			n/a
		+ 0.10	+ 0.14			+ 0.59
	Linear Model 2	+0.27		- 0.22		n/a
		+ 0.65		+ 0.10		- 1.12
	Linear Model 3	+0 .36			- 0.44	n/a
		+ 0.48			- 0.29	- 0.47

A.2. Orientation selectivity of synaptic inputs and input populations

For somatic orientation preference as well as congruency, previous work has shown that the sheer numbers of inputs carrying the feature of interest are a powerful predictor of somatic output in experienced animals [46, 287, 288, 291]. Nevertheless, there are additional properties of synaptic inputs and input populations that could affect their impact on somatic output.

For instance, a broadly tuned or even unselective input provides a similar drive to the postsynaptic neuron for all stimuli. In contrast, a highly selective input provides strong drive for only a specific subset of stimuli and not others, thus more strongly impacting the stimulus preference of the postsynaptic neuron. The concept of exerted modulation can also be extended to the level of input populations, since depolarization of the soma is a reflection of the sum of all synaptic inputs. Consider a group of highly selective inputs, yet all preferring different orientations. As a population, they will convey similar drive for stimuli of all orientations. In contrast, a group of inputs all preferring the same orientation can as a population more strongly modulate responses and thereby affect somatic tuning, even when this group is rather small in numbers or individual spines not as selective.

We measured orientation selectivity and preference similarity within subpopulations of synaptic inputs. Both these features may vary between monocular and binocular spines and could reveal differential contributions of these subpopulations to somatic output. Moreover, this may change over development and reveal changes in the synaptic make up of somatic responses that improve binocular alignment.

Orientation selectivity of dendritic spines increases after eye opening but exhibits consistent biases between ocular classes over development

To assess to which degree excitatory inputs at eye opening convey orientation modulated signal to the postsynaptic neuron, we measured the orientation selectivity (OS, see methods) of individual spines for each eye. Regardless of the ocular class of a given dendritic spine, responses display lower degrees of orientation selectivity than that found in experienced animals (Fig.A.1c-d; rank sum test naïve-experienced, $p < 0.0001$ for all ocular classes). The median OS for inputs from each ocular class is below 0.2, which amounts to about 50-75% of the respective median value in experienced animals (see Table A.1); A.1). Despite low OS, differences between inputs across ocular classes are apparent. Binocular congruent spines are more selective than monocular contra and monocular ipsi spines whereas noncongruent spines are consistently the least selective group of inputs (see Table A.1; Fig.A.1a-b). Accordingly, congruency of binocular inputs is significantly correlated with their orientation selectivity for contra and ipsi responses (two-sided Spearman's correlation: contra: $r = 0.31$; ipsi: $r = 0.30$, $p < 0.0001$ for both). As in the adult, responses of binocular spines to contra stimulation are more selective than their responses to ipsi stimulation (paired signed rank test: binocular congruent: $p < 0.0001$; binocular noncongruent: $p = 0.0008$) and even

monocular spines exhibit the same difference across eyes (rank sum test: contra vs. ipsi: $p = 0.0009$).

In sum, the synaptic inputs appear to generally mirror the properties of the immature somatic responses seen in V1 at this age ([4]; and Fig.3.2): not only do they display lower congruency, but they also show lower orientation selectivity and their ipsi responses tend to be even less selective than contra. Despite these signatures of an immature response, the relative differences across inputs from distinct ocular classes already resemble those seen in the experienced state. And already in naïve animals, the comparably stronger orientation selectivity of the binocular congruent network could give it an advantage in affecting the somatic response despite its small input proportion.

	Median (IQR)	Binocular congruent	Binocular noncongruent	Monocular
	Contralateral responses			
Binocular congruent	0.18 (0.15)	-	$p < 0.0001$	$p = 0.006$
Binocular noncongruent	0.12 (0.12)	-	-	$p < 0.0001$
Monocular	0.16 (0.13)	-	-	-
	Ipsilateral responses			
Binocular congruent	0.16 (0.11)	-	$p < 0.0001$	$p = 0.001$
Binocular noncongruent	0.10 (0.10)	-	-	$p = 0.024$
Monocular	0.12 (0.12)	-	-	-

Table A.1.: Comparison of orientation selectivity across ocular classes of dendritic spines.
All statistical tests are Wilcoxon's rank sum test.

Populations of binocular congruent inputs display the least orientation preference variance

Next, we examined the similarity in orientation preference of inputs from the same ocular class for a given cell. High similarity of orientation preference within an ocular class population can boost their joint influence on somatic tuning, whereas larger diversity in orientation preference could weaken the population's impact (see Fig.A.2a). By exhibiting strong preference similarity, monocular and binocular noncongruent inputs could still strongly contribute to the somatic response to a certain orientation despite overall low orientation selectivity of these inputs. Binocular congruent inputs in turn, may employ this to further boost their modulating impact and compensate their low numbers.

The diversity of orientation preference was measured via the variance of preferred orientations within a subpopulation of inputs. For each cell, we computed the respective population variance of binocular congruent, binocular noncongruent, and monocular spine populations for responses to the contra and ipsi eye separately. We only extracted the orientation preference for spines with OS > 0.1, and input populations

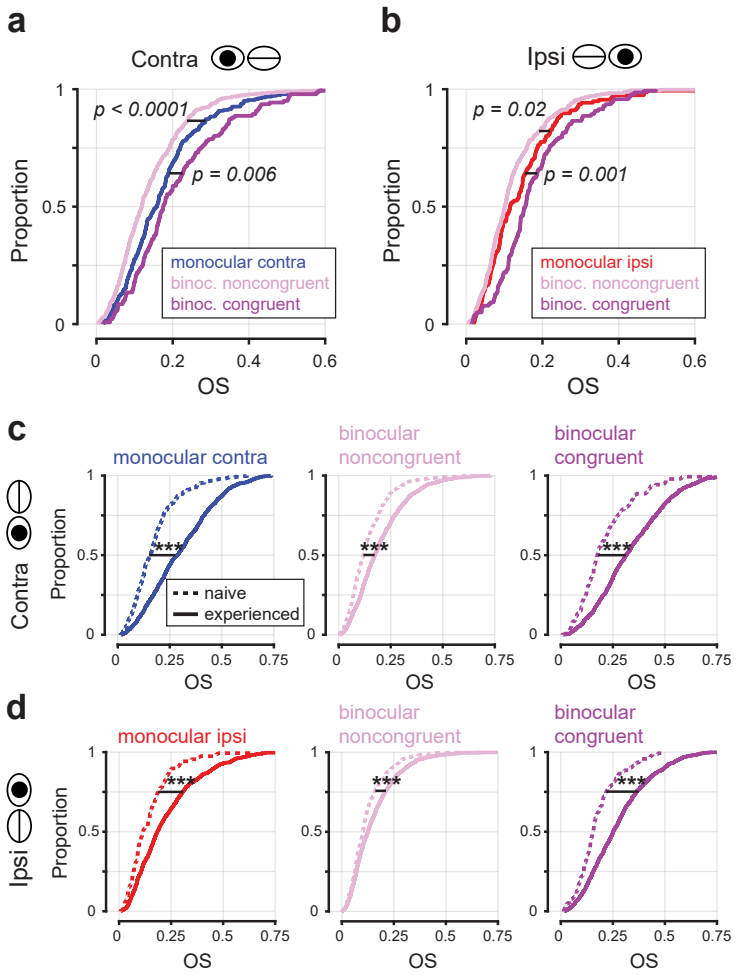

Figure A.1.: Orientation selectivity increases for all synaptic inputs after eye opening
(a-b) Cumulative distribution plots of orientation selectivity (OS) of somatic responses to contra (a) and ipsi (b) eye stimulation of binocular neurons in visually naïve and experienced animals. **(c-d)** Cumulative distribution plots of OS for spines from different ocular classes in naïve and experienced animals for the contra (c) and ipsi (d) eye. All statistical tests are Wilcoxon's rank sum test. *** $p < 0.0001$

for each ocular class had to encompass at least 3 selective spines. For aggregates in experienced animals, we randomly subsampled spines for each aggregate to match aggregate sizes from the naïve state and took the average for each aggregate across 20 iterations of subsampling.

First, we wanted to test whether population similarity is exploited by binocular congruent spines in the experienced state. In experienced animals, for contra stimulation, binocular congruent input populations demonstrate the lowest variance, indicative of low orientation preference diversity (see Fig.A.2b). Binocular noncongruent aggregates tend to exhibit the highest variance and monocular contra aggregates are in between (rank sum test: binocular congruent vs. monocular contra: $p = 0.06$; binocular congruent vs. noncongruent: $p = 0.003$). As binocular congruent inputs are per definition well aligned between eyes, a similar degree of variance is expected for the ipsi response as for the contra response. This is indeed the case. Monocular ipsi and binocular noncongruent populations are more diverse in their inputs' orientation preference, with binocular noncongruent inputs displaying the largest variance (rank sum test: binocular congruent vs. monocular ipsi: $p = 0.02$; binocular congruent vs. binocular noncongruent: $p = 0.0001$; monocular ipsi vs. binocular noncongruent: $p = 0.02$).

This highlights that, in the experienced state, binocular congruent inputs are not only the most selective, but also as a population are best coordinated in their orientation preference. Thereby, they can enhance their impact on somatic tuning compared to that of other input populations, and disproportionately contribute for select stimuli and thereby drive somatic alignment.

These results prompted us to ask: Do binocular congruent inputs to a cell develop to exhibit highly similar orientation preferences, thereby boosting their impact not only by an increase in numbers, or does also the naïve population exhibit such a tight coordination among its binocular, congruent inputs? To answer this question, we next measured population variance in the naïve animals.

Remarkably, binocular congruent inputs are biased to display similar orientation preferences, even prior to eye opening. In short, we find the similar biases across input subpopulations from different ocular classes in the naïve as in experienced animals: binocular congruent aggregates show the least variance overall and binocular noncongruent aggregates the most (Fig.A.2c). In the naïve, monocular contra aggregates show similar variance as binocular congruent aggregates for contra while monocular ipsi aggregates show similar to binocular noncongruent aggregates for ipsi. There are trends for monocular contra aggregates to become more diverse in their tuning over development (naïve vs. experienced: rank sum test: $p = 0.13$) and monocular ipsi aggregates to become less diverse (naïve vs. experienced: rank sum test: $p = 0.10$). Yet, for all types of subpopulations, the naïve levels of population variance are not significantly different from those observed in the experienced (rank sum test, $p \geq 0.1$ for all comparisons naïve vs. experienced).

In sum, while orientation selectivity of all inputs amplifies after eye opening, the relative modulatory impact that inputs from ocular classes may exert, seems comparable across development. Consistently, binocular congruent inputs are best positioned to influence somatic orientation preference, especially for the ipsi eye. Notably, for contra stimulation in the naïve, monocular contra inputs as a population display similar

properties as binocular congruent inputs and could therefore also have a substantial impact on somatic tuning.

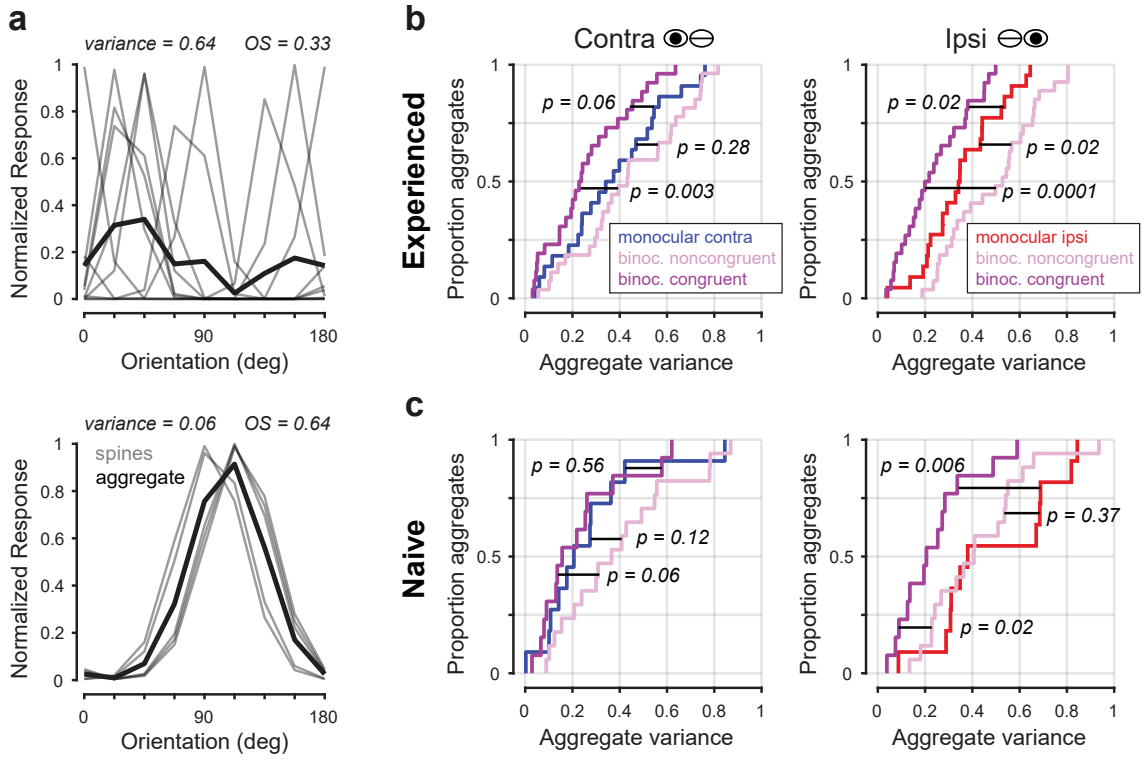

Figure A.2.: Binocular congruent input aggregates display lowest orientation preference variance throughout development
(a) Examples on how population variance in orientation preference can affect aggregate orientation selectivity (OS). Top: population of 10 highly orientation selective spines with high orientation preference variance resulting in an aggregate response with OS = 0.33. Spine response (gray) and aggregate mean response (black). bottom: population of 5 moderately orientation selective spines but low orientation preference variance resulting in an aggregate response with OS = 0.64. **(b)** Cumulative distribution plots of aggregate variance for contra (left) and ipsi (right) responses. Aggregates for spines from each ocular class were randomly subsampled to match aggregate size in the naïve. **(c)** same as in (b) but for aggregate formed by spine responses in visually naïve animals. All statistical tests are Wilcoxon's rank sum test.